UNIVERSITÀ POLITECNICA DELLE MARCHE

Scuola di Dottorato di Ricerca della Facoltà di Medicina e Chirurgia
Curriculum Salute dell'Uomo
XXXI Ciclo

The regulation of haematopoietic niche: is there a role for Bone Marrow Adipocytes?

PhD Student: Domenico Mattiucci

Supervisor: Prof. Antonella Poloni

Table of Contents

Summary

The bone marrow (BM) niche is a highly specialised microenvironment that provides structural and trophic support through its stromal components for Haematopoietic Stem Cells (HSC). Besides the haematopoietic element, the BM contains stromal constituents such as adipocytes (BM-A), osteoblasts and mesenchymal stromal cells (BM-MSC), which play an active role in regulating haematopoiesis through cell-cell contact and secretion of growth factors and cytokines.

BM-A are the most abundant stromal components in the BM niche and during various human conditions, including bone disease, haematological malignancies, diabetes, and dietary intake, the BM niche can modulate the amount of adipocytes within the marrow. Indeed, it has been demonstrated that during caloric restriction (CR) there is an expansion of bone marrow adipose tissue and this contributes to increased circulating levels of adiponectin, a hormone potentially involved in haematopoiesis regulation.

Changes induced by CR might reflect evolutionary functions that are essential to survival. Indeed, CR is also of great interest as a strategy to treat chronic diseases.

Surprisingly the role of BM-A in haematopoiesis regulation remains unclear, therefore the aims of our work were to molecularly and functionally characterise BM-A, and to determine if adiponectin contributes to the regulation of the HSC during CR.

To address these aims, human BM-A were isolated from hip surgery patients, analysed through microarray analysis and compared to adipose tissue adipocytes (AT-A) and BM-MSC, while their relationship with primary human HSC was assessed *in vitro* using long-term co-culture assay with HSC. The role of Adiponectin was studied using a mouse model of Adiponectin$^{-/-}$ mice (KO) fed ad libitum (AL) or with 70% of AL food intake

(CR) from 9 to 13 weeks of age. Blood was sampled weekly and white blood cell populations were analysed by flow cytometry. Following 4 weeks of CR, animals were sacrificed; HSCs from the femur and lumbar vertebrae were isolated and characterised by Colony Forming Unit (CFU) assays and flow cytometry.

Molecular data suggested that BM-A displayed a different gene expression profile compared with subcutaneous AT-A collected from abdominal surgery patients, especially in terms of regulation of lipid metabolism, stemness genes and white-to-brown differentiation pathways. Accordingly, analysis of the gene pathways involved in haematopoiesis regulation showed that BM-A are more closely related to BM-MSC than to AT-A. Also, we demonstrated that BM-A are capable of supporting HSC survival in the co-culture assay, since after 5 weeks of co-culture, HSC were still able to proliferate and differentiate.

Adiponectin KO mouse models showed that KO had a reduced number of white blood cells which turned into an increased proportion of Granulocytes in the whole CD45 population and to a significantly reduced number of B cells especially after the first week of CR. Characterisation of HSC however didn't reveal any significant diet or genotype-induced difference among samples, as a similar number of CFU and a similar HSC phenotype was observed.

These results suggested that BM-A are not the main HSC supporting population in BM, but may contribute to the survival of HSC together with other stromal cells.

Furthermore, data suggested that even if not directly acting on BM-HSC, adiponectin contributes to the regulation of immune cells during CR, highlighting a potential evolutionary role of adiponectin in the regulation of the immune system.

Introduction

1. Haematopoiesis and Haematopoietic Stem Cells (HSCs)

Haematopoiesis is a dynamic process that ensures the continuous regeneration of circulating blood cells. The production of blood cells occurs in the Bone Marrow (BM) and is regulated by a small population of Haematopoietic Stem Cells (HSC). The HSCs are rare multipotent cells with self-renewal capacity and are able to produce between eight to ten distinct lineages (Bonnet D et al, 2002) (Figure 1).

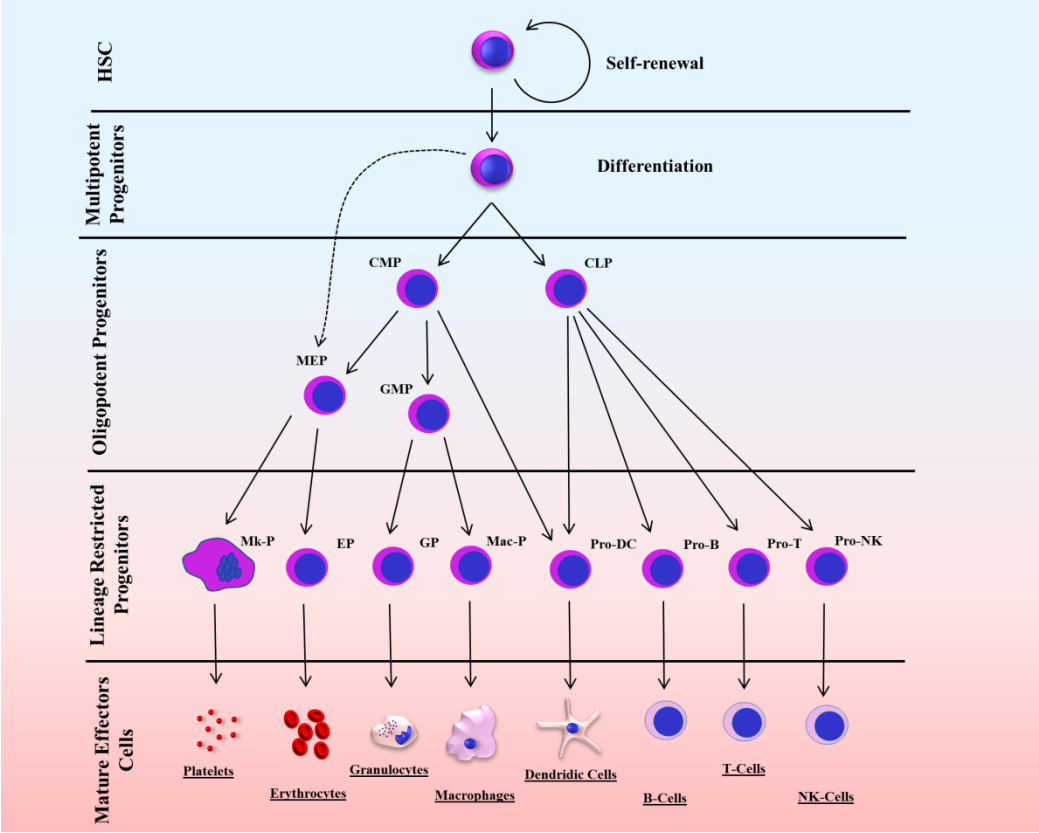

Figure 1 Model of the hematopoietic hierarchy
The HSC resides at the top of the hierarchy, and harbor both the self-renewal capacity and the potential to differentiate into all hematopoietic cell types (multi-potency). Throughout differentiation, a HSC commits to become a mature functional cell of a certain lineage.
Multi-potent can directly give rise to megakaryocyte/erythrocyte progenitors (MEP) without passing through CMP (dashed arrow). HSC: hematopoietic stem cell, CLP: common lymphoid progenitor, CMP: common myeloid progenitor, GMP: granulocyte/macrophage progenitor, MkP: Megakaryocyte progenitor, EP: erythrocyte progenitor, GP: granulocyte progenitor, MacP: macrophage progenitor, DC: dendritic cell, NK: natural killer, Lin: lineage markers (From Seita J et al., 2010).

The term “stem cell” can be found in earlier publications of the hematopoietic field. In 1896, Pappenheim used stem cell to describe a precursor cell capable of giving rise to both red and white blood cells (Pappenheim A, 1896; Ramalho-Santos M et al, 2007). The debate about the existence of a common hematopoietic stem cell continued for several decades until definitive evidence was provided by the work of James Till, Ernest McCulloch, and others in the 1960s (Becker AJ et al, 1963; Siminovitch L et al, 1963) following their studies of blood system regeneration *in vivo*. Ten days after transplanting syngenic BM cells into recipient mice, Till and McCulloch observed that the donor cells were able to reconstitute the BM and formed nodules in the spleen of the recipient mice named colony-forming units-spleen cells (CFU-S). The analysis of these colonies showed that these cells were derived from donor BM cells and that they had self-renewal capacity and the ability to generate multiple types of myeloerythroid cells (Rossi DJ et al, 2007; Becker AJ et al, 1963; Siminovitch L et al 1963; Till JE et al, 1961; Wu AM et al, 1968; Seita J et al, 2010). They proposed therefore that these “self-renewing units” must be the primitive cell source that were capable of giving rise to multiple lineages and regenerated the whole hematopoietic system, and therefore they hypothesised these cells to be stem cells (Yu V.W.C. et al, 2016; Worton RG et al, 1969).

These findings allowed the introduction of two main criteria to define Stem Cells: the **Multi-lineage potential,** which for haematopoietic stem cells specifically represents the ability to differentiate into all the mature circulating blood cells; and **Self-renewal potential** that consists in the capacity of cells to give rise to identical daughter HSCs without differentiation (Seita J et al, 2010). This phenomenon is defined as “symmetrical division” and leads to increased number of the same cell type and occurs mainly during organogenesis and embryogenesis. In adults and under homeostatic conditions the

number of cells within a tissue remains substantially constant because stem cells not only self-renew but are also capable to give rise to a differentiated progeny, therefore it is commonly accepted that a single HSC can asymmetrically divide giving rise to two different daughter cells, one maintaining the stem cell identity and the other becoming a differentiated cell.

The asymmetry can be achieved by cells pre- or post-division and can be therefore identified as divisional asymmetry, or environmental asymmetry. In the divisional asymmetry, the cell fate is determined by the distribution of mRNA and protein within the cytoplasm at the time of cell division. In the model of the environmental asymmetry the HSC divides generating two identical daughter cells one remaining in the haematopoietic niche and maintaining the features of stem cell, the other moving to a different microenvironment which will determine the fate of the cell providing extrinsic signals. (Figure 2) (Wilson A et al, 2006).

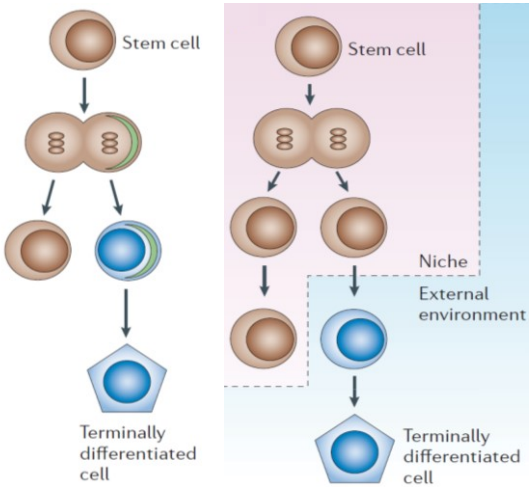

Figure 2: HSC division models.
(a) Divisional asymmetry: cell-fate determinants are localized to one of the two daughter cells. After division, one cell retains stem-cell fate, while the second daughter cell differentiates. (b) Environmental asymmetry, after division, one of two identical daughter cells remain in the self-renewing niche while the other relocates into a differentiation-promoting microenvironment (Modified from Wilson A et al., 2006)

1.1 HSC Phenotype and characterisation

Representing a rare population within the BM, HSCs are difficult to study, however flow cytometry, cell sorting techniques and serial transplantation studies allowed to identify different HSC populations with different self-renewal potential. Spangrude and colleagues characterised for the first time murine HSCs, showing that only 0.05% of cells are capable of long-term reconstitution in serial transplantation and they present a surface marker phenotype of Thy-1^{low} Lin (Lineage-markers^{-}) and Sca-1^{+} (Spangrude JG et al, 1988). Since this study, murine HSC have been intensively studied and in 1994 Morrison and colleagues (Morrison SJ et al, 1994) demonstrated that the population originally isolated by Spangrude can be further dived in 3 sub-populations: the **Long-Term HSCs**, ($CD150^{+}$ $CD244^{-}$ $CD48^{-}$), **the multipotent hematopoietic progenitors** (MPP) ($CD244^{+}$ $CD150^{-}$ $CD48^{-}$) which only showed transient multilineage reconstitution capability, and the more restricted **haematopoietic progenitor cells** (HPC) (CD48+ CD244+ CD150-) who didn't present any reconstitution capability. (Oguro H et al, 2013).

In the human, the first marker used to identify HSCs population was CD34 and it represented only the 0.05-5% of adult BM cells. In vitro assays revealed that almost all CD34+ cells showed multi-potency differentiation capability, but also that this population is very heterogeneous (Seita J et al, 2010). The characterisation of human HSCs has been improved combining CD34 expression together with Lineage-specific markers and CD90. The work of Baum and colleagues showed that CD34+ cells can be further subdivided in two populations: $CD90^{+}$ $Lineage^{-}$ and $CD90^{+}$ $Lineage^{+}$ cells. In vitro assays and xenoptransplantation models allowed to identify the $CD34^{+}$ $CD90^{+}$ $Lineage^{-}$ population as the only one capable of generating clones containing both myeloid and lymphoid cell types (Baum CM, et al, 1992). The purification strategy of human HSCs

has been further refined by the use of CD38 marker. It has been shown that even if most of CD34+ cells co-express CD38, only the fraction which is CD34+ $CD38^{low\text{-}to\text{-}negative}$ can produce multilineage colonies (Hao QL et al., 1996; Huang S et al., 1994; Miller JS et al., 1999). These studies concluded that human HSC are enriched in the Lin− CD34+ CD38− CD90+ population of human sources of hematopoietic cells (Seita J et al., 2010).

2. ***The haematopoietic niche***

One of the first demonstrations of the importance of a specific microenvironment was obtained by Dexter and colleagues who demonstrated in an ex vivo experiment the requirement of a BM stromal feeder layer to maintain stemness properties and sustain primitive haematopoiesis (Dexter, TM et al, 1977). Following this work, in 1978 Schofield developed the concept of the **haematopoietic niche**, (Schofield R, 1978) which was described as a defined limited anatomical space where HSCs can be maintained and where the differentiation processes are inhibited. (Yu VW et al., 2016). Schofield proposed that HSCs are in intimate contact with bone and that this bone-cell interaction is responsible for the inhibition of differentiation and for the maintenance of the self-renewal capacity (Wilson A, et al, 2006). In 2003 Calvi *et al.* (Calvi, LM et al. 2003) used an *in vivo* murine model which constitutively expressed parathyroid hormone (PTH) in osteoblastic cells to study the relationship between bone and HSC's. In this model the total number of osteoblasts was increased and determined an increment in the levels of haematopoietic cells partially, confirming the Schofield hypothesis and demonstrating a direct correlation between bone and HSCs.

Further experimental data obtained by both *in vivo* and *in vitro* models, (Taichman RS et al., 1998; Taichman RS et al., 2005; Oostendorp RA et al., 2002) demonstrated that cells involved in bone formation represented an important source of cytokines and growth factors that can both promote the proliferation and support the survival of HSCs. Also, transplantation experiments showed that HSCs preferentially localize from blood vessels to endosteal regions retaining a quiescence status (Morrison SJ et al., 2014; Ellis SL et al., 2011; Lo Celso C et al., 2009). These observations supported the concept of a specific **endosteal BM niche** responsible for the maintenance of HSCs quiescence and for their stemness properties. It has also been demonstrated that an important proportion of HSCs can reside in the perivascular regions in direct contact with endothelial cells away from the endosteum, originating also the hypothesis that a **perivascular BM niche** might exist and play an important role in the regulation of HSCs (Sugiyama T et al., 2006; Kiel MJ et al., 2008; Kiel MJ et al., 2007; Lévesque JP et al., 2010).

2.1 The endosteal niche:

The endosteal surface of bone is constituted of all cells that line the interface between bone and marrow, from the most immature precursors to the most mature cell type. Within this heterogeneous microenvironment a peculiar extracellular matrix rich in glycoproteins and with a high-density calcium salt concentration has been shown to work together with osteoblasts to regulate the homing, maintenance and differentiation of HSCs (Adams GB et al., 2006; Calvi LM et al., 2003; Park D et al., 2012; Zhang J et al., 2003)

The high mineral content present in the bone make the endosteal niche a microenvironment whose Ca^{2+} concentration can substantially increase in condition of

injury, inflammation and bone remodelling (Adams GB et al., 2006). Interestingly, it has been shown that HSCs express a calcium ion receptor (CaR) on their cell surface which is responsible for an intracellular G protein-coupled response (Chattopadhyay N et al., 1997). It has been shown that CaR-depleted mice normally develop HSCs in the fetal liver, but they are not able to engraft the endosteal surface of the marrow. These mice present a hypocellular BM and increased number of HSPC in peripheral blood demonstrating that the ability of HSCs to respond to calcium concentration is involved in the establishment of a specific endosteal niche. (Adams GB et al., 2006 B).

Twenty years after that Dexter and colleagues demonstrated the requirement of a stromal BM feeder layer for the long-term survival of HSCs a series of scientific reports showed that these stromal cells expressed alkaline phosphatase and were able to mineralise in culture, demonstrating their osteoblastic origin (Askmyr M et al., 2009).

Molecular studies on osteoblasts led to the discovery that they are able to produce soluble factors and transmembrane receptors involved in the regulation of HSCs. One of the first key molecules identified was N-cadherin, a trans-membrane protein involved in the HSCs-osteoblast interaction. It has been shown that N-cadherin is expressed by both osteoblasts and a subset of HSCs (Wilson A, et al., 2006) and is responsible for the anchorage of HSCs to the endosteal niche. The role of this molecule, however, has been controversial as conditional deletion from HSCs or from osteoblast lineage cells had no effect on HSC frequency, HSC function, or haematopoiesis (Zhang J, et al. 2003; Xie Y et al., 2008; Hosokawa K et al. 2010, 2009; Wilson A et al., 2004; Morrison SJ 2009; Bromberg O et al. 2012)

Primary murine osteoblasts have also been studied to characterise their cytokines secretion profile *in vitro* and it has been shown that they are able to produce several stimulating cytokine of crucial importance for haematopoietic maintenance such as Granulocyte-Colony Stimulating Factor (G-CSF), Macrophage-CSF (M-CSF), Granlocyte-Macrophage-CSF (GM-CSF), Interleukin 1 (IL-1) and interleukin 6 (IL-6). (Taichman RS et al., 1998). These data further confirm that osteoblasts represent a cell population involved in the support and the maintenance of HSCs

Furthermore osteoblasts can produce haematopoietic inhibitory factors such as Tumor Growth Factor β, (TGF- β), Leukemia Inhibitory Factor (LIF), and Tumor Necrosis Factor α and β (TNF-α, TNF- β) (Taichman RS et al., 1998). This simultaneous presence of both inhibitory and stimulatory signals is not surprising, as within the endosteal niche both long term quiescent HSCs and more proliferating haematopoietic progenitor cells can be found. A balanced proportion of stimulatory and inhibitory signals would therefore allow both to maintain the pool of long-term HSCs throughout aging and guarantee to the organism a continuous production of all the mature blood cell elements.

Another important molecule secreted in the endosteal niche is Osteopontin (OPN), a protein whose expression is highly restricted at the endosteal surface of the niche. It has been shown that OPN-deficient mice present an increased number of cycling HSC *in vivo*, suggesting a crucial role for this protein in the maintenance of quiescence status of HSCs, providing a mechanism to restrict excess stem cell expansion under conditions of niche stimulation. (Nilsson SK et al., 2005; Stier S et al., 2005)

2.2 The perivascular niche:

It has been demonstrated that BM sinusoidal vessels could serve as alternative cellular scaffolds where HSCs can reside and mature. To delineate the BM sinusoidal network as a separate anatomic and functional entity from the endosteal zone, the name "vascular niche" was employed (Kopp HG et al., 2005). Considering the complex three-dimensional structure of BM, and the tight association between the trabecular bone and the microvascular network, the identification of two separate niches has been challenging. The ultrastructural characterization of the BM niche showed that the more committed haematopoietic progenitors rather than long-term HSCs have a close association with the bone marrow microvasculature (Walkley CR et al., 2007). These findings demonstrated the interaction between HSCs and the vascular niche is a crucial step for haematopoietic differentiation processes (Park D et al., 2012). Avecilla and colleagues in 2004 demonstrated that the exposure of megakaryocytes progenitor to sinusoidal BM endothelial cells (EC) promoted thrombopoiesis, supporting the idea that the translocation of non-differentiated progenitors toward the perivascular niche promote the maturation and differentiation of HSCs. The authors demonstrated that this process was mainly dependent on Stromal Derived Factor 1 (SDF-1/CXCL-12) and Fibroblast Growth Factor 4 (FGF-4), that enhanced the expression of Vascular Cell Adhesion molecule 1 (VCAM-1) and of Very Late Antigen 4 (VLA-4) on megakaryocytes, promoting their maturation and platelet release (Avecilla ST et al., 2004). Endothelial cells form the inner cellular lining of blood vessels are essential for haematopoietic recovery after irradiation and BM transplantation, (Hooper AT et al., 2009; Kobayashi H et al., 2010; Salter AB et al., 2009) and have been shown to support haematopoiesis *in vitro* (Butler JM et al., 2010; Li N et al., 2006; Yildirim S et al., 2005; Chute JP et al., 2002, 2004).

Unsurprisingly, HSCs and EC are able to establish a close interaction as both lineages arise from the same embryonic progenitor: the haemoangioblast. (Huber TL et al., 2004). Furthermore, at any time point during development, HSCs can be found in close contact with EC; (Lu LS et al., 1996) and that in the human embryo they can be detected within the aorta (Tavian M et al., 1996) and in perivascular location of the foetal liver (Oberlin E et al., 2002). Together, these developmental findings support a strong interdependence of HSCs and EC during ontogenesis and this concept can be extended to the adult where haematopoiesis can develop in the BM only in specific structures organised by vascular cells (Kopp HG et al., 2005).

The dynamic and circulating nature of the HSCs still raises the possibility that the accumulation of HSCs near sinusoids is due to normal HSC trafficking. Hooper and colleagues (Hooper AT et al., 2009) demonstrated that the deletion of Vascular Endothelial Growth Factor 2 and 3 (VEGF2; VEGF3) did not result in heamatopoietic defects for several weeks but could inhibit HSC engraftment and reconstitution. This may suggest that sinusoidal endothelial cells function in the homing and engraftment of HSCs, rather than for the maintenance of endogenous HSCs under homeostatic conditions (Park D et al., 2012).

3. ***Mesenchymal Stromal Cells***

Mesenchymal Stromal Cells (MSCs) or Pericytes were originally identified as a non-haematopoietic cellular population of the BM niche with osteogenic differentiation potential. (Friedenstein et al., 1968, 1970, 1976). Heterotopic transplantation experiments demonstrated that these cells had osteogenic differentiation potential and that a cell population deriving from a single stromal cell could originate also cartilage and adipocytes. In consideration of these results, it was hypothesized that in the post-natal BM stroma reside a second type of non-haematopoietic multipotent progenitor able to differentiate in different connective tissues (cartilage bone and fat) which are all part of a multilineage system downstream this common progenitor (Bianco P, 2014).

MSC were also identified as Adventitial Reticular Cells (ARC) for their morphology and for their localization (Weiss 1976, 1980). Pericytes are distributed both in the perivascular niche over the sinusoid surface and in the endosteal niche. They contact maturing blood cells and express high level of C-X-C motif chemokine ligand 12 (CXCL-12), Nestin, and Leptin Receptor (LepR) (Omatsu Y et al., 2010; Méndez-Ferrer S et al., 2010; Ding L et al., 2012). In 2006 Sugiyama and colleagues (Sugiyama T et al., 2006) defined these cells as CXCl-12 Abundant reticular cells (CAR) and demonstrated the importance of its interaction with C-X-C motif chemokine receptor type 4 (CXCR4), a receptor expressed on the surface of HSCs. It has been demonstrated that deletion of CXCl-12 from osteoblast do not affect frequency of HSCs while when this chemokine was deleted in EC, HSCs were depleted from the BM. Notably, only a conditional deletion of CXCL-12 from perivascular MSC caused both a depletion and mobilization of HSC underlining the importance of this cellular population (Greenbaum A et al., 2013; Ding L et al., 2013).

The expression of this chemokine is induced in response to haematopoietic loss and HSCs are able to specifically migrate toward the production source. CXCL-12 indeed is a chemotactic molecule that induces motility of cells expressing its receptor (Wilson A et al., 2006) and is essential for retention and maintenance of adult HSCs in the BM. Further confirmation of MSC-supporting role in the BM niche comes from human clinical data and experimental animal models which suggested that contransplantion of HSCs and MSCs results in increased chimerism and haematopoietic recovery (Koç ON et al., 2000; Devine SM et al., 2001; In 't Anker PS et al., 2003; Bensidhoum M et al., 2004). MSC are able to support haematopoiesis supplying to haematopoietic cells signals for survival proliferation and differentiation through cell-contact-mediated mechanisms or by secreting cytokines and growth factors (Pontikoglou C et al., 2011). Indeed, it has been shown that MSCs can secrete Stem Cell Factor (SCF), thrombopoietin, leukemia-inhibitory factor (LIF), TGF- β, interleukins (IL-6, 8, 11, 12, 14, 15), GM-CSF, M-CFS and can also synthetize adhesion molecules and extracellular matrix proteins (Dazzi, F et al., 2006; Majumdar MK et al., 2000; Di Nicola M et al., 2002; Prockop DJ, 1997).

Because of the low frequency of MSC in the BM (0.01-0.001% of total BM cells), (Caplan AI, 1991) and because of the lack of specific markers to identify them, little is known about the features of MSC in vivo. Most data come therefore from ex vivo studies where the high proliferative potential and the plastic adherence properties were used to isolate and expand MSC. So far many surface markers have been used to identify a specific immunophenotype of MSC, applying both positive (Stro-1, CD271, CD146, CD106, CD73, CD105, FZD9, SUSD2, LEPR, CD90) and negative selection markers (CD44, CD31, CD34, CD45). However, none of the markers are specific for MSCs, and

the precise in vivo identity and phenotypic signature of adult BM-MSCs have therefore remained elusive (Li H et al., 2016).

Considering the different properties and roles played by Osteoblast and Adipocytes, a proper balance between adipogenic and osteogenic differentiation of MSC is required for healthy and sustainable haematopoiesis. The differentiation of MSCs is a two-step process, lineage commitment (from MSCs to lineage-specific progenitors) and maturation (from progenitors to specific cell types). Many signaling pathways are involved in the regulation of lineage commitment of MSCs, including TGFβ/bone morphogenic protein (BMP) signaling, wingless-type MMTV integration site (Wnt) signaling, Hedgehogs (Hh), Notch, and fibroblast growth factors (FGFs) (Chen Q et al., 2016).

PPARγ and C/EBPs represent two of the main factors responsible for adipogenic commitment and differentiation (Lefterova MI et al., 2008; Cao Z et al., 1991; Kushwaha P et al., 2014; Kim J et al., 2014) while Runx2 and Osterix are crucial for osteogenic differentiation (Augello A., 2001). However, upstream molecular processes, biological and metabolic conditions are likely to be responsible for the activation of these two alternative differentiation pathways. It has been demonstrated that aging (Meunier P et al., 1971; Justesen J et al., 2001; Moerman EJ et al., 2004), mitochondrial metabolism (Zhang Y et al., 2013), oxidative stress (Atashi F et al., 2015), glucose uptake (Wei J et al., 2015), osteoporosis and haematological malignancies might be responsible for a skewed balance in the osteo/adipogenic differentiation.

4. ***Bone Marrow Adipocytes***

At birth, bone cavities are mainly constituted by red hematopoietic marrow, then during childhood the red marrow which is gradually replaced by yellow, fatty marrow (Hardouin P et al., 2014). The conversion of red to yellow marrow begins in distal skeleton regions after birth, then goes forward in a centripetal manner, to the axial skeleton (Vande Berg BC et al., 199). The yellow marrow is composed by BM adipocytes (BM-A), which represent the most abundant stromal component of the BM niche. In adults, BM adipose tissue (BMAT) volume is estimated at 7% of total fat (Shen W et al., 2012) and progressively increases during ageing, replacing the haematopoietic elements and occupying up to 50% of the cavity of long bones. (Mattiucci D et al., 2017). BM-A are morphologically similar to AT-A: they have a single, large cytoplasmic lipid droplet which account for ca. 90% of the cellular volume, they originate from mesenchymal like progenitor cells and are able to release and store fatty acids (Hardouin P et al. 2016; Sanchez-Gurmaches, J et al., 2014).

BM-A were historically considered as space-filling, inert cells and only in recent times the scientific attention on this cell population has increased focusing on the relationship between BM-A, bones, HSCs and metabolism. One of the first authors who tried to characterise BM-A was Tavassoli in 1976 (Tavassoli M 1976). Using histochemical techniques he was able to identify two different BM-A populations: one interspersed in the red haematopoietic marrow which was positively stained with performic acid-Schiff (PFAS), and a second population represented by BM-A, located in the yellow marrow that did not stain with this technique highlighting a difference in lipid composition of BM-A. Tavassoli noticed that when haemopoietic tissue expanded in response to

experimentally induced hemolysis, PFAS-positive BM-A of red marrow disappeared whereas the PFAS-negative BM-A of yellow marrow remained stable. (Tavasoli M 1976). This concept has been further developed in 2015 by Scheller *et al.* (Scheller EL et al., 2015) who classified the BM-A according to their anatomical localisation, lipid composition, morphology and metabolic responsiveness. The authors identified two different subtypes of marrow adipose tissue (MAT) named respectively constitutive (cMAT) and regulated (rMAT) (Figure 3).

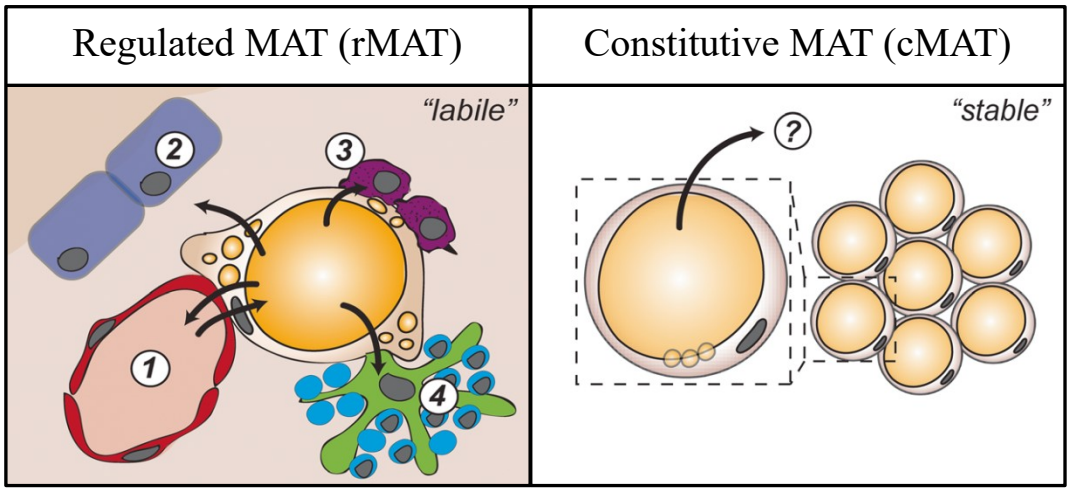

Figure 3: Regulated and constitutive bone marrow adipose tissue
Regulated bone marrow adipocytes (rBMA) are located generally in the haematopoietic perivascular niche and are in close contact with a diversity of populations including (1) endothelial cells and perivascular progenitors, (2) osteoblasts and bone-lining cells, (3) granulocyte/macrophage lineage cells, and (4) erythroblast islands. These population might represent possible utilizers of rBMA energy reserves (arrows outward). By contrast, constitutive BMAs are located in a homogeneous niche that is packed with adipocytes and relatively inaccessible to hematopoietic and osteogenic cell populations. It remains unclear when and where the lipid from the cBMAs is utilized, however, evidence to date suggests that these cells may serve as a last-resort energy reserve in times of tertiary starvation (Modified from Craft CF et al., 2018).

The cMAT represents the early developmental stage forming MAT, mainly located in the distal skeletal regions with low haematopoitic activity. Cells that constitute cMAT are bigger and densely packed adipocytes that resemble peripheral white adipose tissue (WAT). This fat depot is stable and does not seem to be responsive to dietary intake, haematological malignancies or cold exposure. The term rMAT on the contrary is used

to refer to the MAT population that accumulate in late developmental stage in areas of red haematopoietic marrow as smaller single interspersed cells (Mattiucci et al., 2018; Craft CS et al., 2018). rMAT is more susceptible to metabolic changes and conditions as obesity, caloric restriction, diabetes, osteoporosis and aging can determine an increase in the amount of rMAT (Ambrosi TH et al., 2017; Yeung DK Yeung DK et al., 2005; Mattiucci et al., 2018). The data suggest that BM-A function varies depending on anatomical location, and that rMAT may be more closely related to the regulation of active hematopoiesis (Mattiucci et al., 2018).

5. ***Bone Marrow Adipocytes and Haematopoiesis***

The proximity of BM-A to haematopoietic elements likely contributes to the behaviour of surrounding HSCs. A recent work characterised the ultrastructural features of the BM, reconstructing the three-dimensional architecture of the niche and focusing also on the existing physical interaction between adipocytes and HSCs. It was observed that BM-A are spatially positioned to influence both erythropoiesis and myelopoiesis. They can interact with up to 20 maturing hematopoietic cells and with further maturing hematopoietic elements such as erythroblast islands. Due to the high rate of mature blood element production occurring in the BM it would not be surprising if BM-A represented an energy reserve into the hematopoietic niche (Robles H et al., 2018). This hypothesis would be in agreement with previous studies by Tavassoli which showed a decreased BM-A size after induced anaemia or severe blood loss (Tavassoli M 1976 B; Bathija et al., 1978) and also with data showing that erythropoietin treatment a potent stimulant of erythrocyte maturation, markedly reduced BMAT in chow and high-fat diet fed mice, and inhibited the increase in BMAT with high-fat feeding (Suresh S et al. 2017).

However, it would be simplistic to believe the BM-A only represent a source of energy for the production of mature blood cells. Indeed, several *in vitro* and *in vivo* studies have been conducted to evaluate a potential regulatory role of BM-A toward haematopoietic compartment but results obtained are still controversial and it is not yet clear whether the presence of these cells is detrimental or beneficial for haematopoiesis.

One of first evidences of BM-A influencing the haematopoietic compartment has been provided by Naveiras and colleagues in 2009. (Naveiras et al., 2009). The authors

compared the hematopoietic activity of distinct regions of the mouse skeleton that differ in adiposity using flow cytometry, colony forming activity, and competitive repopulation assay. They showed that the frequency of HSCs is reduced in MAT-enriched bones and that lipoatrophic mice (genetically incapable of producing adipocytes) or mice treated with a PPARγ inhibitor had an accelerated marrow engraftment post irradiation. Similar results were obtained by Ambrosi and colleagues (Ambrosi TH et al., 2017) who showed that in high-fat diet mice, adipocyte accumulation in the BM impairs haematopoietic regeneration. However, whether these results can be considered valid for all the human conditions which presents increased BM adiposity is still controversial. Considering that adipocyte accumulation occurs both in high fat diet and during caloric restriction, (Cawthorn WP et al., 2014) it can be hypothesised that subtypes of healthy and pathological MAT exist and that they might regulate the haematopoietic compartment in different ways.

A paper from Zhou *et al.* (Zhou BO et al., 2017) has recently challenged the notion that BM-A act mainly as negative regulator of the BM niche. The authors showed that adipogenesis in the BM happens as a response to cytopenia as BM-A are able to produce haematopoietic growth factors and contribute to stimulate the expansion of HSC. The construction of new perivascular niches to provide support to HSCs would indeed involve the generation of new blood vessels, a slower and more complex process which in emergency condition would be less effective. Furthermore, the authors proved that after irradiation in mice, BM-A represent the main source of Stem Cell Factor (SCF) and ablation of SCF in adipocytes resulted in decreased blood cell count, reduced LSK and diminished total BM cells. However, context-dependent differences in adipocyte function between BM compartments (long bones versus caudal vertebrae) were detected. The

authors found that while BM-A presence is crucial in long bones for haematopoietic recovery, an excess of adiposity in caudal vertebrae is detrimental to vascularization and has negative effect on HSCs and haematopoiesis (Zhou BO et al., 2017).

Other results have been obtained employing in vitro co-culture assay with BM-MSC-derived adipocytes obtained by in vitro differentiation and haematopoietic cells. These data are quite heterogeneous probably because of different sources used to obtain BM-MSC, diverse differentiation protocols and also different co-culture conditions (Corre J et al., 2004; Spindler TJ et al., 2014; Belaid-Choucair Z et al., 2008; Naveiras et al., 2009). Therefore more studies are required to fully understand the role that these cells play within the BM microenvironment.

6. Bone Marrow Adipocytes, Adiponectin and Haematopoiesis

Adipocytes are cells able to secrete a large number of molecules named **adipokines,** the concentration of these molecules within target tissues can be highly variable. First discovered in 1995, adiponectin (APN) is the most abundant adipokine in the circulation, where it exists in distinct multimeric forms (Scheller EL et al., 2016). Its plasmatic concentration (μg/ml) is extremely high if compared to that of other conventional hormones like insulin and leptin (ng/ml) (Pajvani UB et al., 2003). APN is a hormone involved in the regulation of glucose metabolism and it has been demonstrated that when injected in mice it is able to suppress glucose production and stimulate glucose assimilation independently by insulin levels (Berg AH et al., 2001; Yamauchi T et al., 2001; Wang ZV et al., 2016). APN has therefore been intensively studied for its involvement in obesity, metabolic syndrome, cardiovascular disease and type 2 diabetes, and it has been shown that even if mainly produced by adipocytes, it is paradoxically decreased in obese subjects reflecting an obesity-induced adipocyte dysfunction (Ye R et al., 2013; Fantuzzi G. 2013). Surprisingly, circulating levels of APN increases in lean, insulin-sensitive state and in anorexia nervosa (Cawthorn WP et al., 2014; Combs TP et al., 2003; Dolezalova R et al., 2007; Pannaciulli et al., 2003) despite its expression in WAT remain unchanged. (Behre CJ et al., 2007; Combs TP et al., 2003; Kovacova Z et al., 2009; Wang Z et al., 2006). Interestingly a study conducted in 2014 by Cawthorn *et al.* (Cawthorn WP et al., 2014) demonstrated that in anorexic patients the MAT composes 31.5% of total adipose mass. Also, it has been demonstrated that, in mice, MAT specifically contributes to increased level of serum adiponectin during CR and perhaps in other adverse states. Beyond a potential effect on glucose metabolism, it is not yet clear

if APN might also exert a role in vascular function, cancer risk or immune response. One of the first evidence obtained about a potential role of APN in the regulation of immune system was obtained by Yokota in 2000 (Yokota T et al., 2000) who demonstrated that APN could suppress the formation of granulocyte (CFU-G) macrophage (CFU-M) and granulocyte/macrophage (CFU-GM) colonies in vitro. As the same inhibitory role was also exerted toward the Lymphoid lineage, the author hypothesized that APN might be involved in ending inflammatory processes within the BM (Yokota et al., 2003).

Opposite results were obtained by Di Mascio and colleagues in 2007. The authors showed that HSC express Adiponectin Receptor 1 (AdipoR1) and 2 (ADipoR2) and that AdipoR1 is overexpressed in HSC when cells are stimulated with recombinant APN. The specific activation of more primitive HSCs was further demonstrated by the increased number of CFU-GM (representative of a more immature progenitor cell type) in *in vitro* colony assays. (Di Mascio et al., 2007). Nonetheless, HSCs treated with APN showed an increased engraftment capacity in transplantation experiment performed in mice demonstrating for the first time a regulatory effect of this hormone in *in vivo* animal model. A similar stimulatory effect was observed by Masamoto who demonstrated that APN is crucial for the cell cycle regulation of HSCs as it promotes haematopoietic recovery enhancing quiescence exit of HSCs. The same author has also shown that loss of APN impairs granulopoiesis and antibacterial response in obese mice (Masamoto et al., 2016. 2017).

Altogether these data suggest that BM-A by secreting APN might be able to regulate the survival and the differentiation of HSCs.

Aims

Despite the fact that BM-A represent the most abundant stromal cell population within the marrow, their characterization is still far from being exhaustive. Their role in the haematopoietic niche has been investigated in several animal models, however only few studies on primary human cells have been published and results are still controversial and didn't entirely clarify the relationship between BM-A and HSCs.

Furthermore, it has been demonstrated that BM-A are able to secrete a large number of molecules named adipokines whose role in metabolic processes is still debated. APN represents one of most intensively studied adipokines, its concentration in the blood is extremely high and it has been demonstrated that it plays a role in the regulation of glucose metabolism and might exert a protective role in cardiovascular diseases. Several authors also reported on a potential role of APN in the regulation of the immune system however further studies are required to fully understand the specific relationship between HSC and APN.

The aims of this work were to molecularly and functionally characterize BM-A, and to determine if APN contributes to the regulation of the HSC in conditions of increased BM adiposity. In the study presented here, primary human BM-A were isolated and microarray analysis was performed comparing them to BM-MSC, a crucial population involved in the maintenance and functional support of HSC, and to subcutaneous AT-A. Long Term Culture-Initiating Cell (LTC-IC) assay, developed in 1988 By Eaves and colleagues (Eaves et al., 1998), was optimized and used to establish an in vitro co-culture model between primary human BM-A and HSCs which allowed to study the interaction between these cellular populations and how the survival and the differentiation potential of HSCs is influenced by BM-A.

It has been demonstrated that Caloric Restriction (CR) causes an expansion of BM fat that contributes to increased level of circulating APN. Therefore to study the role of APN in haematopoiesis regulation in vivo, Adiponectin$^{-/-}$ (KO) mice were placed under CR (70% of AL food intake) to cause an expansion of BMAT and compared to AL and Wild Type (WT) littermate controls. Peripheral white blood cells and HSCs were studied by Flow Cytometry analysis to evaluate any potential APN-induced change. HSCs were also characterized by Colony Forming Unit (CFU) assays to evaluate their proliferation and differentiation potential.

Methods

1. Isolation and culture of BM-A, AT-A, and BM-MSC

All Samples were collected in accordance with local ethics committee guidelines (300/DG), and all participants provided their written informed consent to take part in the study. The donors' characteristics are listed in Table 1. BM-A were harvested from the femoral head of male and female patients (median age: 78 years, range 63–90) undergoing hip surgery and cut in four pieces. Subcutaneous fat (5–10 g) was obtained from non-obese male and female patients undergoing abdominal surgery (median age: 67 years, range 53–81) for localized abdominal diseases that did not involve omental or subcutaneous fat (Table 1). After prompt washing in DMEM (Biological Industries, cat. no. L0064- 500, Milano, Italy), any visible blood vessels were removed and the tissue was minced into smaller pieces. Bone and subcutaneous WAT were treated with a solution containing 1 mg/ml of type I collagenase (Gibco, Invitrogen, Milan, Italy) and 1% human albumin (Albital, Kedrion, Lucca, Italy) at 37°C for 90 min. After collagenase digestion, samples were filtered through a 200 μm nylon sieve to remove stromal elements. Cells were then washed four times with DMEM and centrifuged at 250 g for 5 min. Collection of the floating layer after each centrifugation provided a pure fraction of floating adipocytes and a pellet containing stromal cells. The floating adipocytes were seeded for ceiling culture in 12.5 cm^2 cell culture flasks completely filled with DMEM supplemented with 20% fetal bovine serum (FBS, Stem Cell Technologies, Vancouver, Canada) in a 5% CO2 incubator (37°C).

The pellets from the femoral heads containing stromal cells were used for BM-MSC generation and expansion. After collagenase digestion and centrifugation, the pellet was washed twice with PBS, and BM-MSC were seeded at a density of 2,000 cells/cm2 in

DMEM supplemented with 20% FBS. Flasks were incubated at 37°C in a fully humidified atmosphere of 5% CO2 in air. When cells reached 70–80% confluence, they were treated with trypsin for 3 min and seeded in culture flasks for subculture

Tissue	Age	Gender
Femoral Head	63	Male
Femoral Head	68	Female
Femoral Head	71	Female
Femoral Head	55	Female
Femoral Head	83	Female
Femoral Head	90	Female
Femoral Head	80	Female
Femoral Head	82	Male
Femoral Head	87	Female
Femoral Head	76	Female
Subcutaneous Adipose Tissue	67	Male
Subcutaneous Adipose Tissue	56	Male
Subcutaneous Adipose Tissue	70	Male
Subcutaneous Adipose Tissue	77	Female
Subcutaneous Adipose Tissue	57	Female
Subcutaneous Adipose Tissue	62	Male
Subcutaneous Adipose Tissue	53	Male
Subcutaneous Adipose Tissue	81	Female
Subcutaneous Adipose Tissue	71	Male
Subcutaneous Adipose Tissue	62	Female
Subcutaneous Adipose Tissue	80	Male

Table 1: Samples and patients included in the study.
Table shows tissues age and gender of the subjects who provided bone and adipose tissue for BM-A and AT-A isolation.

2. Immunofluorescence of isolated adipocytes

Isolated adipocytes were incubated for 10 min with 1 μg/ml Nile Red solution (Sigma–Aldrich) at room temperature and washed with PBS; the nucleus was counterstained with Hoechst 33342 solution (5 μg/ml; Sigma–Aldrich). Cells were visualized in the blue and red channel. At least 100 adipocytes from each suspension were examined. The brightness and contrast of the final images were adjusted using Photoshop 6 software (Adobe Systems; Mountain View, CA).

3. BM-MSC immunophenotyping

BM-MSC were analyzed for purity by flow cytometry after the third passage. They were stained with FITC- (BD Biosciences, Franklin Lakes, NJ), phycoerythrin (PE-; Dako, Glostrup, Denmark), or peridin chlorophyll protein (PerCP-; BD PharMingen, Milan, Italy) conjugated antibodies against CD90 (BD Pharmingen, San Diego, CA), CD44, CD29, CD73, CD34, CD45, CD14 (all from BD Biosciences), CD105 (Immunostep, Salamanca, Spain), and CD31 (Dako). FITC-, PE-, and PerCP-negative isotypes were used as control antibodies. Cells were incubated with the antibody at 4°C for 30 min, then cell fluorescence was examined by flow cytometry using a FACS Calibur apparatus (BD Biosciences). Data were analyzed using Cell Quest software (Milano, Italy).

4. Long-term culture-initiating cell assay (LTC-IC)

For the LTC-IC assay, 3 ml of BM-A suspension was seeded for ceiling culture in a final volume of 25 ml DMEM supplemented with 20% FBS in a 9 cm^2 surface flask. BM-MSC (used as a positive control) were seeded at a density of 2×10^5 cells per 9 cm^2 in a final volume of 3 ml DMEM supplemented with 20% FBS. The experiment was also performed on a mixed feeder layer of BM-A and BM-MSC. In brief, BM-MSC were seeded at a density of 1×10^5 cells per 9 cm^2; after 24 hr a suspension of 1.5 ml BM-A was seeded in the same flask for ceiling culture. After 48 hr, cells were irradiated (80 Gy) for 20 min to inhibit BM-MSC proliferation and BM-A de-differentiation throughout the co-culture period. When BM-A adhered to the ceiling, the flask was re-inverted and the medium removed and replaced with 3 ml MyeloCult H5100 (Stem Cell Technologies, Milano, Italy) supplemented with 1% hydrocortisone. Only flasks where more than 70% of the surface was covered with cells were used for the assay. No cell feeder layer was used in the negative control. CD34+ HSC were isolated from healthy BM by immunomagnetic separation (CD34+ Progenitor Cell Isolation kit, Miltenyi Biotech, Bologna, Italy). CD34+ HSC were seeded at a density of 50,000 cells/flask. Cultures were performed in quadruplicate and incubated at 33°C in a fully humidified atmosphere of 5% CO2. They were fed weekly by replacing half of the medium. The supernatant removed in the first 4 weeks was centrifuged and the pellets containing floating cells were seeded in methylcellulose medium HSC-CFU Lite (Miltenyi Biotech) in 35 mm tissue culture dishes for myeloid and erythroid progenitor proliferation and differentiation assay. Cultures were incubated at 37°C in a fully humidified atmosphere of 5% CO2 and

after 14 days colony-forming unit-granulocyte/macrophage (CFU-GM) and burst-forming unit-erythroid, (BFU-E) were examined and counted.

After the fifth week of co-culture the medium was removed, the wells were trypsinized, and all cells were seeded in HSC-CFU Lite medium. After 14 days of incubation CFU GM and BFU-E were examined and counted (Figure 4).

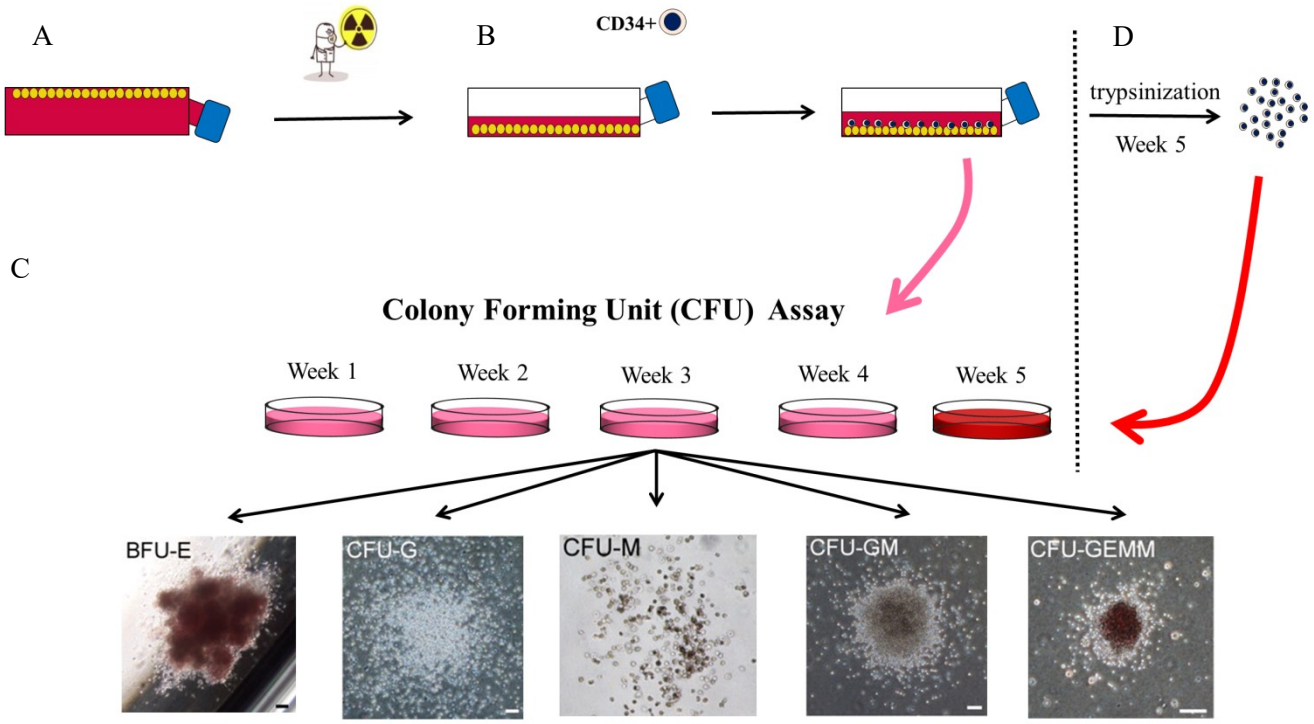

Figure 4: LTC-IC assay.
(A) BM-A were seeded for ceiling culture and irradiated to avoid dedifferentiation processes. (B) CD34+ cells were added to the BM-A culture. (C) Medium is replaced and seeded for CFU assay. (D) After the fifth week all the cells are trypsinized and seeded for CFU assay.

5. Immunocytochemical procedures

CFU obtained from methylcellulose assay were washed four times with PBS and attached to slides by centrifugation. Cell morphology was evaluated by Giemsa staining.

6. Quantitative cytokine assay

Supernatants from 7 day BM-A, AT-A, and BM-MSC cultures were collected and frozen at −20°C. Production of IL-1β, IL-3, IL-6, IL-8, IL-10, IL-17, leukaemia inhibitory factor (LIF), stromal-derived factor 1 (CXCL12), CSF2, CSF3, macrophage inflammatory protein 1α (CCL3), tumor necrosis factor (TNF)-α, SCF, and hepatocyte growth factor (HGF) was measured in the supernatants by multiplex detection of human cytokines, chemokines, and growth factors (BioPlex, BioRad, Milano, Italy) using three independent samples per cell type (BM-A, AT-A, and BM-MSC).

7. Sample preparation and hybridization

RNA was extracted from freshly isolated adipocytes and from BM-MSC after three culture passages (RNeasy mini kit, Qiagen, Milano, Italy). Single-strand biotinylated cDNA was obtained as follows: 100 ng of total RNA was subjected to two cycles of cDNA synthesis with the Ambion®WTPLUS Expression Kit (Affymetrix, Santa Clara, CA). Firstcycle, first-strand synthesis involved using an engineered set of random primers that exclude rRNA-matching sequences and include T7 promoter sequences. cDNA

resulting from second-strand synthesis was transcribed in vitro with T7 RNA polymerase to generate cRNA, which was subjected to second-cycle, first-strand synthesis in presence of dUTP at a fixed ratio relative to dTTP. Single-strand cDNA was then purified and fragmented with a mixture of uracil DNA glycosylase and apurinic/apirimidinic endonuclease 1 (Affymetrix) in correspondence of incorporated dUTP. DNA fragments were terminally labeled with biotin by terminal deoxynucleotidyl transferase (Affymetrix). The biotinylated DNA was then hybridized to Human GeneChip® HTA 2.0 Arrays (Affymetrix), containing more than 285,000 full-length transcripts covering 44,700 coding genes and 22,800 non-coding genes selected from the Homo sapiens genome databases RefSeq, ENSEMBL, and GenBank. Chips were washed and scanned on the Affymetrix Complete GeneChip® Instrument System, generating digitized image data (DAT) files. Three biological samples for each cell type (BM-A, AT-A, and BMMSC) were used.

8. Microarray data analysis

The DAT files were analyzed with the Affymetrix Expression Console software. The full dataset was normalized using the Robust Multialignment Algorithm (RMA). The expression values thus obtained were tested with R software. Further normalization steps included per chip normalization to the 50th percentile and per gene normalization to the median. Filtering the results for fold changes >1.5 yielded a total of number of 4047 probe sets differentially expressed in at least one experimental condition. Statistical analysis was performed with ANOVA using a cut-off of 0.01 as the p-value. Pathway analysis was

performed with Ingenuity Pathway Analysis (IPA) software (Qiagen). Principal component analysis (PCA), clustering using Ward's method and Pearson correlation analysis were performed with IBM SPSS Statistics 21. Gene-set enrichment analysis (GSEA) was performed using Broad Institute's GenePattern tools (https://genepattern.broadinstitute.org/). Protein network analysis and gene ontology were performed in String (http://string-db.org/).

9. Caloric Restriction Time Course, blood sampling and APN quantification.

WT and Adiponectin KO C57BL/6NCrl mice were single housed from 8-9 week of age and fed ad libitum to determine average daily food intake. Four-week CR (week 9-12) were performed administering 70% of AL food intake. Mice weight was daily monitored for the first two weeks of CR. For flow cytometry analysis and cell count blood was taken every week from the tail vein using Microvette CB 300 capillary tubes (Sarstedt, Newton, NC). The number and the characteristics of the mice used are shown in table 2.

Circulating APN was quantified using Adiponectin ELISA (R&D, MRP300). Plasma was diluted with assay diluent (RD1W) 4000-fold to obtain signal within the range of the standard curve. The provided adiponectin standard was prepared and serially diluted according to manufacturer's instructions. 50µl assay diluent was added to each well of the provided 96 well anti-adiponectin coated plate followed by 50µl of sample or standard. The plate was then incubated for 3 hours at room temperature. Wells were

aspirated and washed 5 times with 400µl wash buffer. 100µl mouse APN conjugate antibody was added to each well and the plate incubated for 1 hour at room temperature. All wells were aspirated and washed 5 times again. 100µl of substrate solution was added to each well and the plate was incubated for 30 minutes at room temperature in the dark. 100µl stop solution was added to each well and the optical density of each well measured at 450nm with a correction against 570nm. Sample concentrations were interpolated from standard curve and corrected for initial dilution

Sex	Diet	Genotype	Number of mice
M	AL	WT	5
M	AL	KO	5
M	CR	WT	8
M	CR	KO	6
F	AL	WT	6
F	AL	KO	4
F	CR	WT	5
F	CR	KO	5

Table 2: Characteristics of mice included in the study.
Table shows gender, diet, genotype and number of the mice used for the study.

10. Peripheral blood cell count

PB was collected from the tail vein using Microvette CB 300 capillary tubes (Sarstedt, Newton, NC). 1:5 dilution was performed in a solution of PBS, 2% FBS and 0.04 mM EDTA. Cells were counted on Celltac α MEK-6500K (NIHON KOHDEN) according to the manufacturer's instructions.

11. BM Mononuclear cells (MNC) isolation and CFU assay.

Femoral metaphysis were cut and BM was flushed out using a solution of PBS, 10% FBS, 1%PS and 2mM EDTA. Cells were washed in PBS and centrifuged at 2000 Rpm for 10 minutes. Cells were resuspended in 1 ml of PBS and 300 µl were harvested and centrifuged at 2000 Rpm for 10 minutes. Red blood cell lysis was performed resuspending the pellet in 2 ml of Red Blood Cell Lysing Buffer Hybri-Max (Sigma, Dorset, UK) and incubating cells at room temperature for 12 minutes. After incubation cells were centrifuged at 2000 rpm for 10 minutes and the pellet was resuspended in 200 µl of PBS, 10% FBS, 1%PS and 2mM EDTA. Cells were diluted 1:50 for counting and 25.000 cells were seeded into 2.250 µl of MethoCult (Stem Cell technologies) for CFU assay. A final volume of 2.500 µl of Methocult was reached adding PBS and 1 ml of media was seeded in 35mm tissue culture dishes and incubated at 37°C in a fully humidified atmosphere of 5% CO2 and after 10-12 days CFU-G, CFU-M, CFU-GM, BFU-E and CFU-GMEM (granulocytes, macrophages, erythroid) were examined and counted.

12. Flow Cytometry analysis

PB cells were analyzed with the following antibodies: Alexa Fluor 488 anti-mouse CD3, Alexa Fluor 700 anti-mouse CD45, APC anti-mouse CD4, Brilliant Violet 421 anti-mouse CD19, PE anti-mouse Gr-1, PE/Dazzle 594 anti-mouse CD8a and PE Cy-7 anti-mouse CD11b (all from BioLegend, London, UK).

PB was collected from the tail vein of mice. 40 µl of blood were incubated with 1 ml of Red Blood Cell Lysing Buffer Hybri-Max for 12 minutes at Room Temperature. After lysis, cells were centrifuged at 500 rcf for 10 minutes, resuspended in 100 µl of PB Staining solution Mix (PBS, 2% FBS and antibodies) and incubated for 30 minutes at 4 ºC. Following incubation cells were washed with PBS, centrifuged for at 500 rcf for ten minutes, resuspended in 400 µl of PBS + 2% FBS and acquired with BD LSR Fortessa cell analyzer. Antibodies' dilution is reported in Table 3

PB Staining solution	
Antibody	**Dilution**
CD3 AF488	1:200
CD45 AF700	1:200
CD4 APC	1:200
CD 19 BV421	1:200
GR-1 PE	1:200
CD8 PE DAZZLE 594	1:200
CD 11b PE Cy-7	1:200

Table 3: Antibodies' dilution.
Table shows dilutions used for each antibody to prepare PB staining solution Mix.

Femoral metaphysis were cut and BM was flushed out using a solution of PBS, 10% FBS, 1%PS and 2mM EDTA. Cells were washed in PBS and centrifuged at 2000 Rpm for 10 minutes. Cells were resuspended in 1 ml of PBS and 300 µl were collected for flow cytometry analysis. BM-MNC were analyzed for Lineage$^-$ Sca1$^+$ cKit$^+$ (LSK) expression (Kiel M et al., 2008). Whole BM-MNC cells were incubated for 30 minutes at 4 ºC with 100 µl of HSC Staining Solution 1 containing PBS, 2% FBS, biotinylated anti-mouse unconjugated monoclonal antibodies for lineage markers (CD4, CD5, CD8a, GR-1, TER-119, CD11b and CD45R/B220) and Alexa Fluor 488 anti-mouse CD150, APC anti-

mouse CD117, PE anti-mouse Ly-6A/E (Sca-1) (All from BioLegend, London, UK). Following incubation cells were washed with PBS centrifuged and incubated for 30 minutes at 4 ºC with 100 µl of HSC Staining Solution Two containing PBS, 2% FBS, and Brilliant Violet 421 Streptavidin (BioLegend, London, UK). Following incubation cells were washed with PBS, centrifuged for at 500 rcf for ten minutes, resuspended in 400 µl of PBS + 2% FBS and acquired with BD LSR Fortessa cell analyzer. Antibodies' dilution is reported in Table 4 and 5.

HSC staining solution 1	
Antibody	**Dilution**
CD 4 biotin	1:1600
Cd 5 biotin	1:800
CD 8a biotin	1:800
CD 11b (Mac) biotin	1:200
CD45 R biotin	1:200
Gr 1 biotin	1:100
Ter 119 biotin	1:50
C-kit (CD117) APC	1:200
CD48 PE	1:400
SCA-1 PE Cy7	1:200
CD150 AF 488	1:200

Table 4: Antibodies' dilution for HSC staining solution 1.
Table shows dilutions used for each antibody to prepare HSC staining solution 1.

HSC staining solution 2	
Antibody	**Dilution**
Streptavidine BV 421	1:200

Table 5: Antibodies' dilution for HSC staining solution 2.
Table shows dilutions used for each antibody to prepare HSC staining solution 2.

13. Statistical analysis

Data are presented as mean ± standard deviation. They were analyzed using parametric or non-parametric two-tailed Student's t-test or oneway ANOVA according to data distribution. Differences were considered statistically significant at $p < 0.05$.

Results

1. ***Isolation of adipocytes and BM-MSCs***

Fluorescence microscopy showed that isolated BM-A and AT-A cell represented a pure cell fraction as no other nuclei were present in the cell suspension or attached to the surface of the cells. (Figure 5).

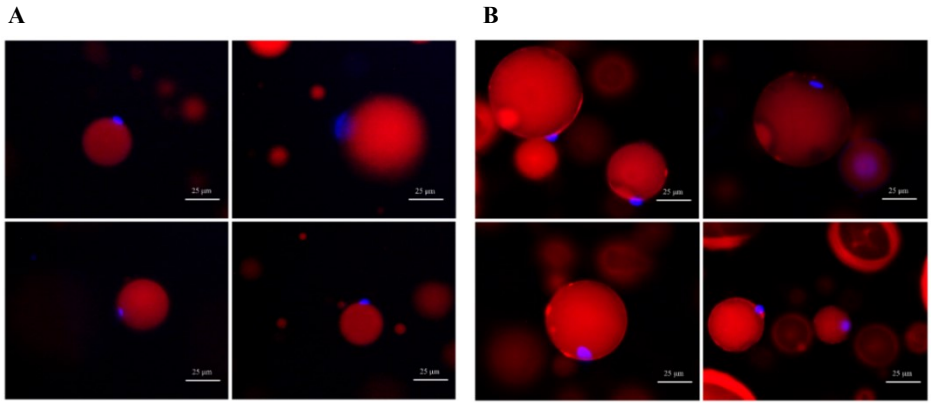

Figure 5: Purity of isolated adipocytes.
The floating (A) Bone marrow adipocyte and (B) subcutaneous adipocyte fractions were stained with Nile Red and the nuclei were counterstained with Hoechst 33342. Scale bar, 25 µm.

Furthermore, adipocytes fractions showed very low expression of osteoblast markers when compared to BM-MSC and higher expression of typical adipogenic markers such as PPARg, ADIPOQ, FABP4, CD36, LEPTIN, and PLIN1 (Figure 6). The higher expression of CD11b and F4/80 (leukocyte and macrophage markers highly expressed in the whole bone marrow) observed in BM-A might partly result from a transcriptomic specific signature left by the BM. BM-A were analysed immediately following the isolation from the BM and, as demonstrated by Sacchetti et al (Sacchetti et al., 2016), cells, depending on their anatomical location, can maintain a tissue-specific gene expression profile.

BM-MSC were analysed by flow cytometry after the third passage. They were positively stained for the common mesenchymal cell markers (CD105, CD73, CD90, CD44, and CD29) and were negative for endothelial and hematopoietic cell markers (CD34, CD45,

CD14, and CD31) (Figure 7). Altogether, these findings demonstrate that the BM-A, AT-A, and BM-MSC were pure cellular fractions free of any contamination from other cells.

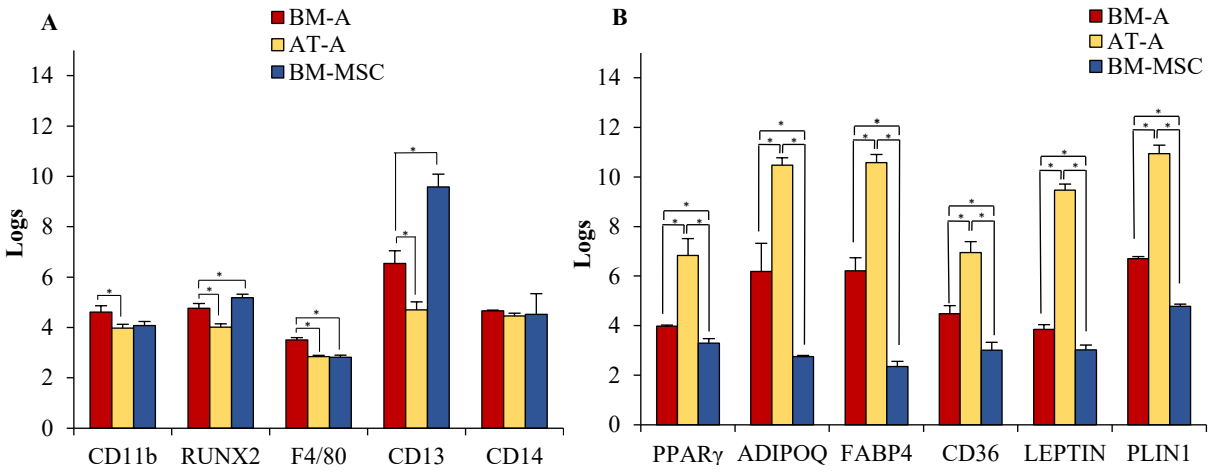

Figure 6: Molecular analysis of the purity of isolated adipocytes and BM-MSC.
Histograms show the expression levels of (A) macrophages, osteoblasts and (B)adipocytes markers in BM-A, AT-A and BM-MSC detected by microarray analysis (=p<0.05).*

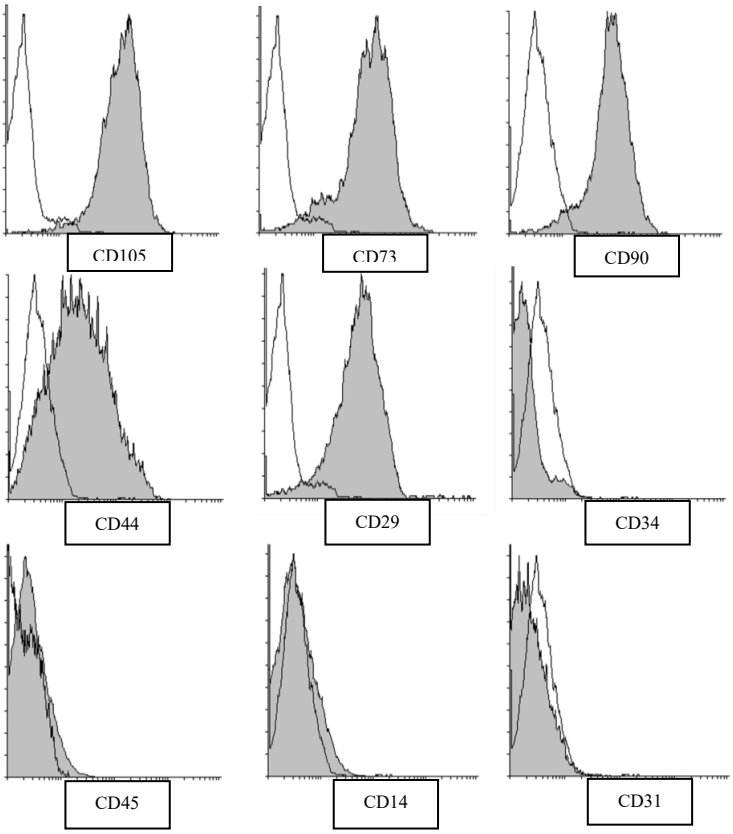

Figure 7: Flow Cytometry analysis of BM-MSC.
Flow cytometry analysis of MB-MSC surface antigens. The open histograms indicate negative controls.

2. ***Long-term culture-initiating cell assay***

LTC-IC assay represents an in vitro co-culture system optimized to assess the capacity of an adherent stromal feeder layer to maintain the survival and the differentiation of HSCs. Scoring of CFU after 5 weeks of co-culture showed that BM-A, even if not at the same level of BM-MSC, were able to support HSC in co-culture. In more detail in presence of BM-MSC 417 ± 35 CFU-GM and 12 ± 4 BFU-E/100,000 CD34+ were counted while in presence of BM-A 45 ± 12 CFU-GM, and 4 ± 2 BFU-E/100,000 CD34+ (Figure 8). No colonies were found in the negative control cultures (data not shown).

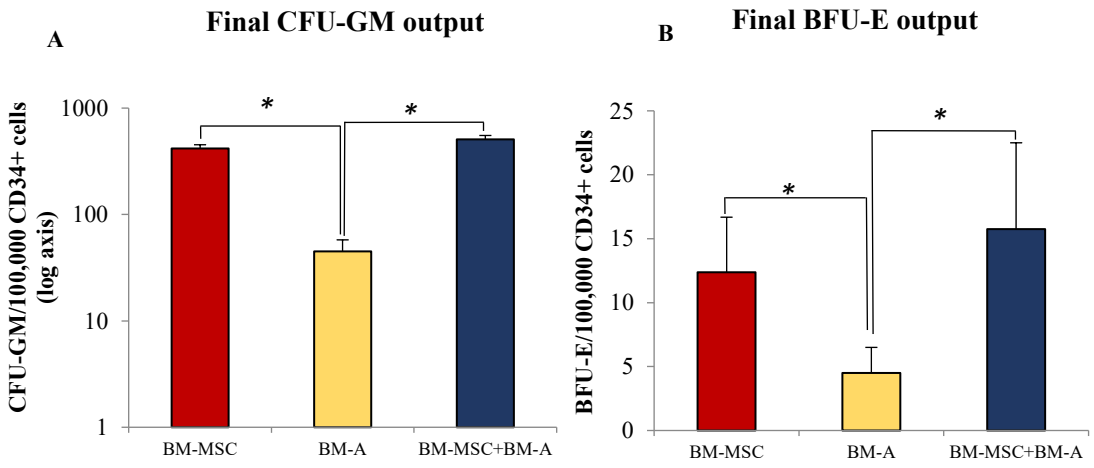

Figure 8: Final CFU output of LTC-IC with BM-A and BM-MSC.
Histograms show the final number of BFU-E and CFU-GM/100,000 CD34+ cells after 5 co-culture weeks with BM-A, BM-MSC and BM-A+BM-MSC feeder layer and 2 culture weeks in methylcellulose (=p<0.05).*

Scoring of CFU was also performed by seeding the floating cells found in the co-culture medium collected every week. Results showed that in the first 4 weeks BM-MSC were able to stimulate the proliferation of haematopoietic progenitor cells (HPC) leading to production of 550 ± 67, 193 ± 45, 130 ± 40, and 75 ± 11 CFU-GM and BFU-E/100,000 CD34+ cells in the 1st, 2nd, 3rd, and 4th week, respectively. In contrast, BM-A did not

appear to be able to stimulate HPC growth in the first 4 weeks (never more than six colonies/100,000 CD34+ cells) (Figure 9), but they ensured HSC survival until the end of the co-culture. Coherently with these observations, the mixed BM-A and BM-MSC feeder layer showed a lower colony output compared with the BM-MSC culture in the first 4 weeks, (218±29, 148±25, 121±13, 67±13 CFU-GM and BFU-E/100,000 CD34+ cells in the 1st, 2nd, 3rd, and 4th week, respectively. Differences between BM-MSC feeder layer and mixed BM-MSC/BM-A feeder layer are statistically significant only in the 1st week) but produced a higher number of colonies at the end of the co-culture (524 ± 51 CFU-GM and BFU-E/ 100,000 CD34+ cells; not significant) (Figure 9). These data suggest that BM-A could play a synergistic role with BM-MSC in the BM niche, supporting the long-term maintenance of HSC.

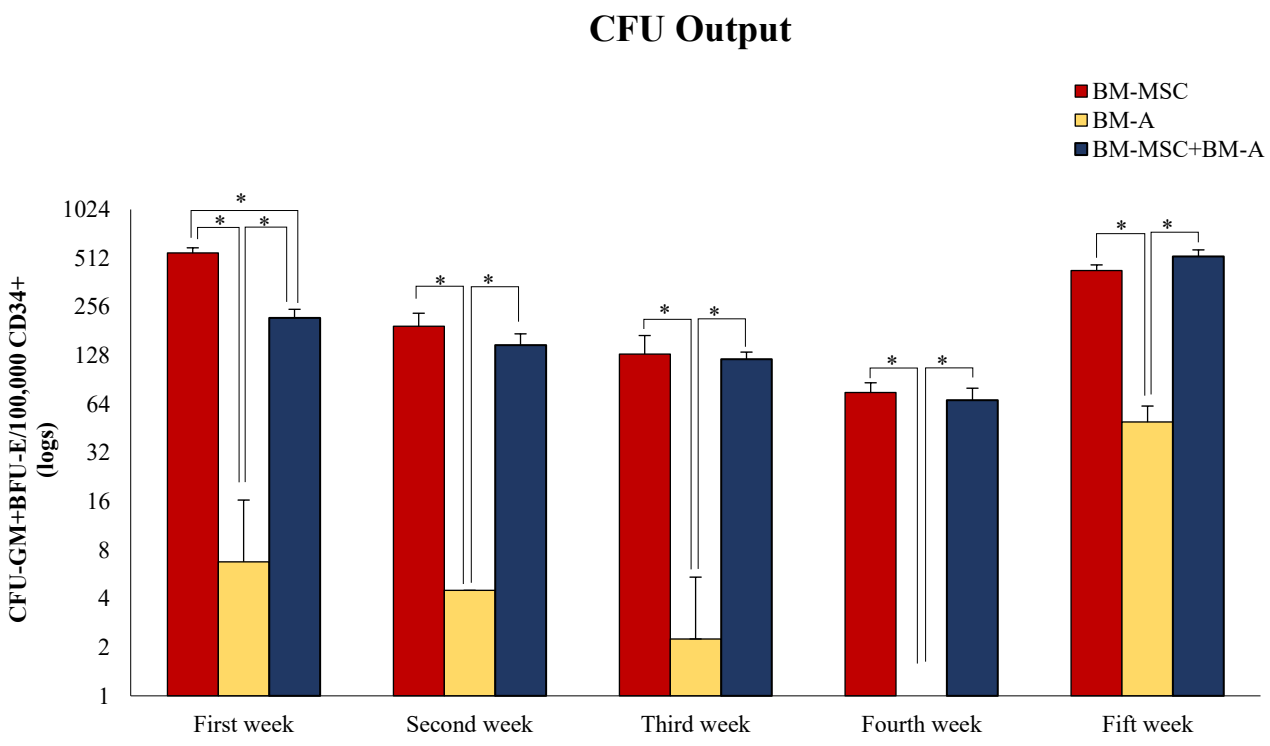

Figure 9: CFU output of the 5 weeks co-culture time course.
Histogram shows the total haematopoietic colony output (CFU-GM + BFU-E) after each week of co-culture with BM-A and BM-MSC and after two culture weeks in methylcellulose (=p<0.05).*

After culture in methylcellulose, CFU were collected, washed, and Giemsa staining was performed. Most cells were macrophages, but granulocytes and erythroid progenitors were also identified (Figure 10). There were no morphological differences between colonies co-cultured with BM-A and those co-cultured with BM-MSC.

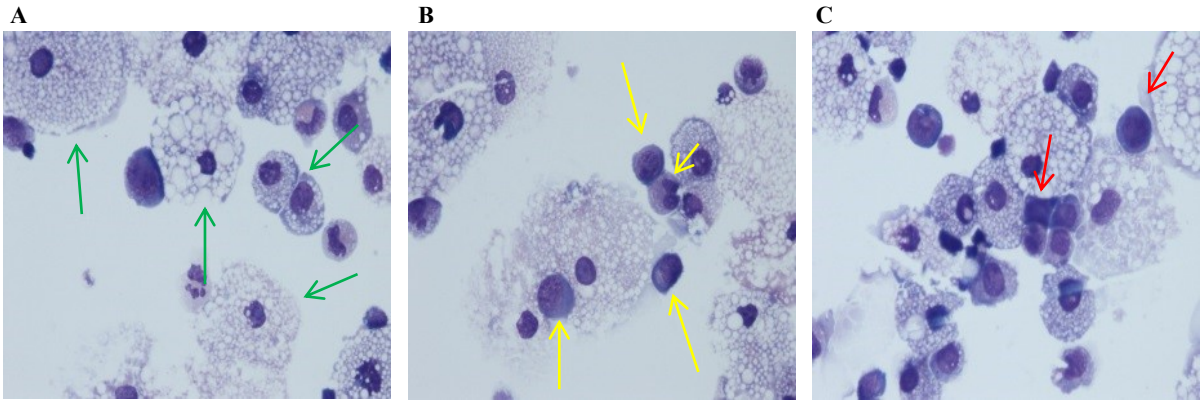

Figure 10: Morphology of haematopoietic colonies after culture in methylcellulose.
The panels show the colonies, collected all together after culture in methylcellulose and after cyto-centrifuge and GIEMSA staining. (A) Most of cells are represented by macrophages (green arrows) but also several (B) granulocytes (yellow arrows) and myelocytes are visible, (C) few erythroid-lineage cells (red arrows) have been observed.

3. Quantitative cytokine assay

Based on the well-established ability of BM-MSC to support hematopoietic cell growth via cytokine secretion (Eastment et al., 1982), BM-A and BM-MSC culture supernatants were examined for cytokines that might positively or negatively affect HSC support. The results documented IL-3 overexpression in BM-A and overexpression of IL-6, CSF2, HGF, and TNF-α in BM-MSC. Interestingly, LIF and CXCL12 levels were lower in AT-A and higher and similar in BM-A and BM-MSC, suggesting a linkage between the latter two populations in hematopoiesis support. The levels of IL-1β, IL-10, IL-17, CCL3, IL-8, CSF3, and SCF were not significantly different in the three cell populations (Table 6).

Cytokines	BM-A	AT-A	BM-MSC
IL-1β	ND	ND	ND
IL-3	47±15	2±3	3±3
IL-6	420±500	347±336	1159±154
IL-8	3700±3860	1108±1058	675±757
IL-10	18±32	ND	34±12
IL-17	9.29±11.9	1±2	10±4
CXCL-12	173±65	40±10	182±102
CSF3	76±139	56±57	10±4
CSF2	20±25	9.51±5.98	48±15
HGF	381±387	9.16±2.05	216.25±93.88
LIF	74±88	ND	48±50
CCL3	11±5	9±6	11±1
SCF	ND	ND	ND
TNF-α	49±67	13±17	73±27

Table 6: Quantitative Cytokines assay.
Table shows level of secreted factors from BM-A, AT-A and BM-MSC. Results, showed in pg/ml, represent the means of four samples for each category.

4. Gene expression profile

BM-A gene expression profile was compared with AT-A and BM-MSC transcriptome. Principal Component Analysis (PCA) and sample clustering using Ward's method or Pearson's correlation analysis showed a clear separation of the BM-A from BM-MSC and AT-A (Figure 11).

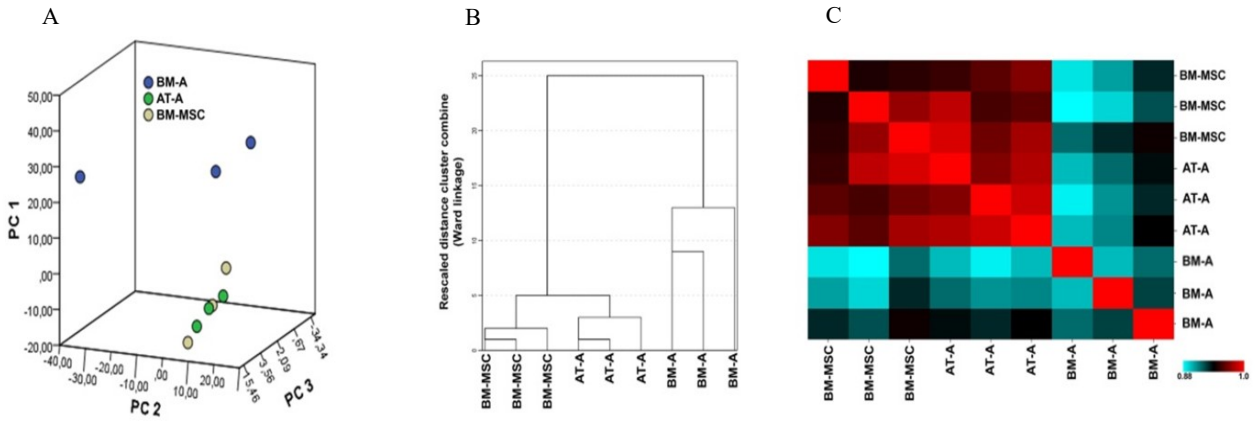

Figure 11: Transcriptional program of BM-A, AT-A and BM-MSC.
The transcriptional profile of microarray data from sorted BM-A is largely different from that of subcutaneous AT-A and of BM-MSC. (A) Unsupervised principal component analysis (PCA) of total microarray data, and (B) clustering of these data using Ward complete linkage and (C)Pearson associated values.

These data demonstrate that the two adipocyte populations, though morphologically similar, play different roles. In particular, of the 2860 genes showing differential expression ($p < 0.01$), 565 were overexpressed in BM-A (Figure 12).

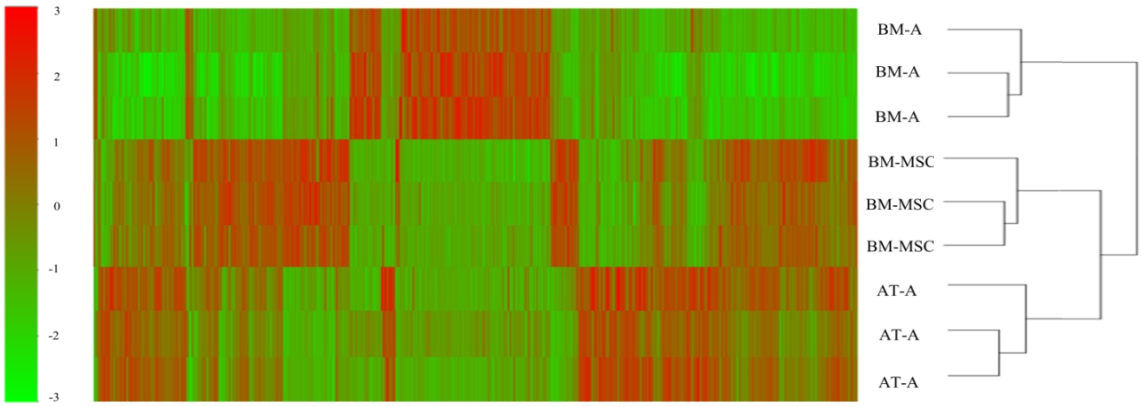

Figure 12: Cluster analysis of global gene expression profile in BM-A, BM-MSC and AT-A.
Heatmap shows the hierarchical clustering of global microarray data obtained from BM-A, BM-MSC and AT-A.

4.1 AT-A-associated pathways

Since adipocytes can accumulate and release fatty acids, contributing to the energy homeostasis, the genes involved in lipid metabolism were examined to evaluate differences between BM-A and AT-A. Five pathways involved in energy balance regulation were identified: lipid synthesis, fatty acid synthesis, fatty acid metabolism, lipid concentration, and polyunsaturated fatty acid biosynthesis. Up-regulated genes ($p < 0.05$) were more numerous in AT-A than in BM-A in all but the last pathway, where BM-A and AT-A presented respectively eight up-regulated and eight down-regulated genes (Figure 13, Table 7).

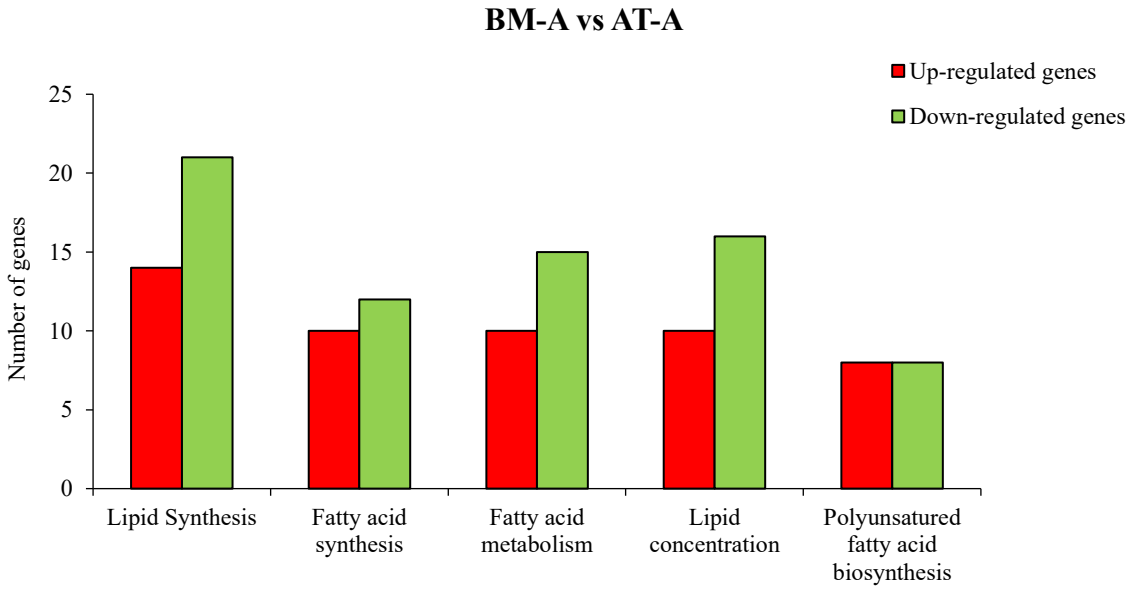

Figure 13. Differentially gene expression of lipid metabolism pathways in BM-A and AT-A.
Pathways and genes involved in lipid metabolism were analysed. (Synthesis of lipid, Synthesis of fatty acid, Fatty acid metabolism, Concentration of lipid, Biosynthesis of polyunsaturated fatty acids). Histogram shows the number of Up and Down-Regulated lipid metabolism genes in BM-A respect to AT-A in the analysed pathways.

	BM-A	AT-A		BM-A	AT-A
ADH5	4.36±0.03	6.19±0.19	LYN	5.87±0.53	4.74±0.13
AKT1	6.37±0.17	7.45±0.09	MAPK14	4.75±0.04	5.82±0.25
ANGPT1	4.70±0.44	6.07±0.06	MMP9	6.60±0.31	5.67±0.22
APP	7.65±0.18	5.94±0.24	MYC	6.45±0.04	7.63±0.31
CAV1	6.12±0.83	8.80±0.14	NR4A2	6.86±0.47	5.74±0.08
CBL	5.57±0.13	6.93±0.03	PIK3R1	4.89±0.12	7.21±0.58
CDKN2C	4.01±0.24	5.07±0.41	PPARG	3.97±0.04	6.82±0.68
CXCL12	7.80±0.48	5.13±0.21	PTGS2	9.14±0.91	3.49±0.63
FGF2	7.06±0.64	8.62±0.13	PTPN11	6.97±0.44	9.18±0.11
FLT1	4.52±0.48	2.96±0.30	RARRES2	6.20±0.11	7.94±0.38
FOXO1	5.25±0.04	8.92±0.57	S1PR3	6.40±0.52	4.00±0.12
HTT	5.48±0.12	6.65±0.10	SIRT1	6.11±0.57	7.64±0.39
IGF1	3.81±0.06	7.04±0.56	SLC1A3	4.87±0.36	6.38±0.55
IL1B	7.31±0.57	3.95±0.68	SOCS3	6.55±0.55	8.86±0.35
IL6	7.29±0.16	4.77±0.68	STAT3	7.38±0.40	8.60±0.08
JAK2	4.14±0.29	5.51±0.66	STAT5A	5.92±0.03	7.80±0.19
JUN	7.08±0.52	9.59±0.04	STAT5B	5.88±0.13	7.71±0.08
KDR	4.60±0.43	3.14±0.34	TGFB1	6.63±0.07	5.61±0.16
KITLG	4.61±0.11	3.23±0.03	THRA	6.31±0.16	7.33±0.19
LIF	6.27±1.78	3.97±0.12			

Table 7: Quantitative microarray data of lipid metabolism gene expression in BM-A and AT-A.
Values are represented as means of the three samples studied for each category and displayed in Logs. All values are statistically significant

Considering the high plasticity of AT-A, which has been demonstrated both in vivo (Barbatelli G et al., 2010; De Matteis R et al., 2009; Maurizi G et al., 2017) and in vitro (Poloni A et al., 2012; 2015; 2015 B), the genes involved in white and brown adipocyte transdifferentiation and stem cell development were also analyzed. Interestingly, 20 of the 23 genes involved in white to brown adipocyte transdifferentiation (all except SNAI2, VASP, and PTGS2) were up-regulated in AT-A compared with BM-A ($p < 0.05$) (Figure 14), whereas of the 110 genes involved in stem cell development pathways 72 were up-regulated in AT-A and 38 in BM-A ($p < 0.05$) (Figure 15). Altogether, these data show completely different gene expression profiles in BM-A and AT-A that is likely to affect their biological properties and their role in the BM microenvironment.

A

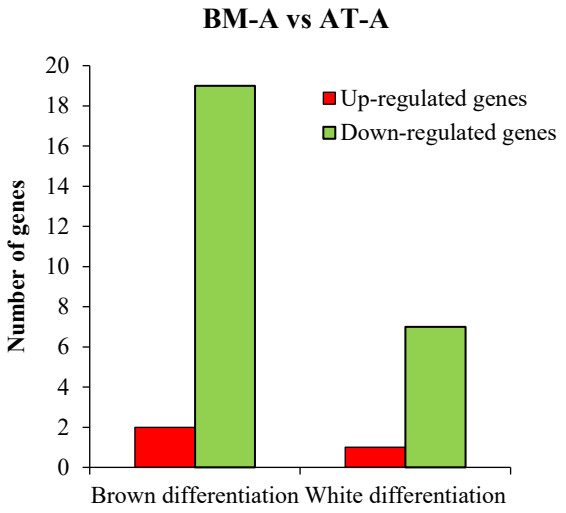

B

Pathway	Up-regulated genes in BM-A	Up-regulated genes in AT-A
Brown differentiation	PTGS2, VASP	RGS2, SELENBP1, PPARG, ADIPOQ, LAMA4, RARRES2, EBF2, FABP4, SCD, ADRB1, BNIP3, LGR4, ERO1L, ALDH6A1, PEX11A, SLC2A4, CEBPA
White differentiation	SNAI2	PPARG, TBLXR1, EBF2, FABP4, SIRT1, SCD, CEBPA

C

Genes	BM-A	AT-A
RGS2	4,86	5,22
SELENBP1	6,28	7,44
PPARG	4,19	6,61
ADIPOQ	7,51	10,91
LAMA4	7,14	9,04
RARRES2	6,31	7,94
EBF2	4,71	4,76
FABP4	6,48	10,58
SCD	7,40	10,76
ADRB1	4,86	6,07
BNIP3	5,04	7,23
LGR4	4,17	6,27
EROIL	5,55	5,87
ALDH6A1	4,25	6,97
PEX11A	4,55	5,55
SLC2A4	4,90	6,1
CEBPA	6,30	8,27
PTGS2	9,02	3,47
VASP	5,88	5,39
TBLXR1	5,81	7,33
SIRT1	6,08	7,52
SNAI2	6,45	6,02

Figure 14: Differentially gene expression of white and brown differentiation in AT-A and BM-A.
Differentially expressed genes in white and brown differentiation were analysed. (A) Histogram shows the number of Up and Down-Regulated genes associated with white and brown differentiation in BM-A and AT-A. (B) Table shows all the up-regulated genes in BM-A and AT-A in white and brown differentiation pathways. (C) Table shows values of microarray analysis represented as means of the three samples studied for each category and displayed in Logs. All values are statistically significant.

A

Genes	*BM-A*	*AT-A*	*BM-MSC*	Genes	*BM-A*	*AT-A*	*BM-MSC*
KDM1A	5.46±0.11	6.27±0.03	6.97±0.19	JAK2	4.20±0.23	5.50±0.65	4.62±0.36
TCEB3	5.23±0.36	6.68±0.09	6.35±0.08	TGFBR1	5.52±0.07	5.99±0.17	7.69±0.32
CDKN2C	4.39±0.30	5.43±0.48	4.73±0.06	NFIB	5.50±0.06	7.99±0.14	5.54±1.37
CYR61	7.07±0.23	8.62±0.70	8.76±0.38	TPM2	5.63±0.19	5.62±0.07	8.24±0.55
MLLT11	3.81±0.00	3.44±0.09	4.47±0.12	TLN1	7.50±0.43	8.93±0.21	8.67±0.27
PRRX1	4.66±0.43	4.07±0.07	6.48±0.93	TNC	7.54±0.65	4.37±0.11	9.82±0.16
PTPRC	3.98±0.55	2.61±0.10	2.65±0.22	ENG	7.24±0.29	6.21±0.37	9.27±0.30
TGFB2	4.02±0.05	3.70±0.28	4.99±0.52	S1PR3	6.80±0.51	4.61±0.18	5.56±0.31
ID3	4.29±0.14	4.06±0.19	5.92±0.49	DKK1	3.02±0.10	2.84±0.14	5.29±1.08
WASF2	6.42±0.30	8.54±0.33	7.79±0.14	SIRT1	6.08±0.56	7.52±0.39	6.21±0.31
JUN	6.96±0.50	9.39±0.04	6.32±0.14	BMPR1A	5.39±0.25	7.77±0.35	7.16±0.20
ADAR	6.00±0.04	6.68±0.36	7.03±0.20	PTEN	5.50±0.04	7.96±0.64	6.57±0.08
PTGS2	9.01±0.90	3.46±0.61	6.33±0.49	CXCL12	7.69±0.45	4.87±0.20	7.94±0.81
ZNF281	5.70±0.20	6.13±0.14	7.27±0.03	CCND1	5.85±0.40	7.88±0.24	8.39±0.52
KDM5B	5.14±0.01	5.35±0.18	6.81±0.16	YAP1	5.43±0.39	8.03±0.11	7.21±0.04
CCL20	4.22±1.04	2.44±0.36	2.38±0.18	ATM	4.15±0.21	4.59±0.09	5.30±0.36
IL1B	7.52±0.52	4.18±0.63	4.46±0.44	CBL	5.50±0.18	6.77±0.04	6.52±0.12
NR4A2	6.75±0.49	5.69±0.09	5.30±0.44	GAB2	5.86±0.12	7.59±0.34	5.56±0.48
FN1	8.57±0.40	4.47±0.11	12.0±0.13	NANOG	4.12±0.22	2.86±0.14	2.77±0.20
PPARG	4.19±0.02	6.61±0.52	3.43±0.14	MDM2	5.62±0.64	5.96±0.18	6.93±0.10
WNT5A	4.23±0.39	3.71±0.07	6.77±0.48	HSP90B1	9.10±1.07	9.18±0.20	10.1±0.10
GSK3B	5.97±0.27	6.99±0.13	7.17±0.23	PTPN11	6.95±0.41	9.13±0.14	7.99±0
HTT	5.49±0.12	6.59±0.11	6.26±0.00	BHLHE41	4.21±0.08	5.97±0.61	3.85±0.18
RBPJ	4.87±0.09	5.39±0.12	6.06±0.21	KITLG	4.17±0.19	3.11±0.06	4.51±0.28
BMP3	4.33±0.11	6.18±0.74	3.97±0.09	IGF1	4.16±0.07	6.97±0.53	3.43±0.55
FGF2	7.15±0.49	8.56±0.10	8.28±0.04	CMKLR1	4.55±0.03	4.11±0.15	5.19±0.88
KDR	4.69±0.44	3.37±0.29	3.04±0.09	CDK2AP1	6.05±0.25	6.55±0.07	7.35±0.08
ADH5	4.28±0.04	6.08±0.15	5.50±0.23	FLT1	4.59±0.46	3.13±0.25	2.92±0.09
SFRP2	3.83±0.21	4.83±1.97	3.43±0.04	FOXO1	5.45±0.10	8.36±0.60	5.09±0.58
NPY1R	3.57±0	6.62±0.25	2.86±0.02	YY1	5.88±0.27	6.98±0.17	6.74±0.19
PDGFRA	5.37±0.09	4.08±0.17	8.13±1.09	AKT1	6.35±0.19	7.41±0.08	7.28±0.00
SLC1A3	4.90±0.31	6.34±0.52	4.67±0.31	HIF1A	7.68±0.42	6.95±0.38	9.61±0.16
PIK3R1	4.93±0.13	6.96±0.61	4.76±0.26	THBS1	9.35±0.06	10.3±1.20	11.5±0.75
RAD50	4.96±0.28	6.77±0.32	6.32±0.25	FGF7	3.36±0.08	2.64±0.10	5.51±0.71
IL6ST	8.20±0.47	9.47±0.38	8.48±0.23	TCF12	6.07±0.27	6.97±0.14	7.21±0.17
ITGA1	4.97±0.32	7.06±0.35	5.77±0.69	SMAD3	6.01±0.60	6.57±0.15	7.24±0.30
MAPK14	4.74±0.04	5.75±0.22	5.52±0.14	RBL2	4.86±0.15	6.81±0.21	5.96±0.29
PIM1	6.81±0.26	8.16±0.54	6.88±0.32	CBFB	5.42±0.43	6.15±0.33	7.02±0.42
RUNX2	4.50±0.08	3.85±0.11	4.90±0.15	SERPINF1	6.79±0.05	9.87±0.31	7.12±0.27
GJA1	6.63±0.20	7.31±0.13	9.21±0.42	PSMD11	5.54±0.59	6.59±0.12	6.51±0.06
MAP3K5	4.60±0.28	6.60±0.84	4.38±0.10	CSF3	6.32±0.41	5.44±0.14	5.31±0.15

IL6	7.36±0.14	4.87±0.69	6.04±0.11	STAT5A	5.98±1.08	7.66±0.18	5.51±0.20
HOXA7	5.08±0.24	6.32±0.25	5.76±0.04	NMT1	5.48±0.66	7.52±0.25	7.11±0.16
IGFBP3	6.67±0.27	6.27±0.13	9.51±0.65	STAT5B	6.05±0.22	7.64±0.11	5.91±0.05
HGF	3.27±0	2.81±0.12	4.19±0.70	STAT3	7.30±0.43	8.49±0.07	7.96±0.29
ERVW-1	5.02±0.62	3.64±0.22	3.61±0.30	SOCS3	6.39±0.64	8.45±0.38	6.07±0.72
CDK6	4.95±0.08	4.91±0.20	5.91±0.11	GATA6	5.18±0.13	5.93±0.06	6.38±0.46
RARRES2	6.30±0.06	7.93±0.31	5.86±0.28	SS18	5.71±0.31	7.01±0.10	7.19±0.12
CAV1	6.00±0.86	8.61±0.17	8.04±0.16	DNMT1	5.76±0.07	5.35±0.08	6.43±0.01
NRG1	4.14±0.04	3.84±0.14	5.95±0.81	TGFB1	6.64±0	5.57±0.22	7.74±0.11
LYN	5.66±0.55	4.61±0.12	5.07±0.45	ID1	4.99±0.35	5.28±0.17	6.50±1.07
MYC	6.63±0.05	7.71±0.34	6.53±0.08	APP	7.33±0.09	5.89±0.23	8.21±0.31
CEBPD	5.72±0.17	7.02±0.24	5.90±0.31	LGALS1	7.05±0.43	9.87±0.04	10.2±0.29
ANGPT1	4.59±0.37	5.87±0.12	4.73±0.36	MAPK1	5.54±0.21	6.42±0	6.98±0.12
EXT1	6.92±0.50	7.16±0.45	9.29±0.22	LIF	5.84±1.87	3.79±0.11	5.05±0.32

B

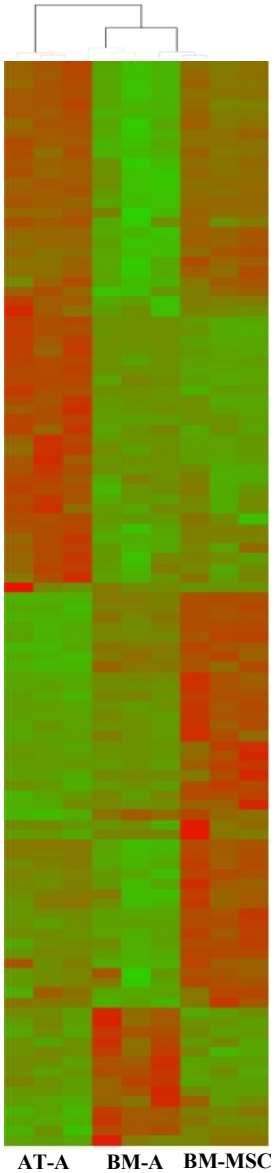

Figure 15: Differentially gene expression of stem cell development pathway in AT-A, BM-A and BM-MSC.

Differentially expressed genes stem cell development were analysed. (A) Table shows values (represented as means of the three samples studied for each category and displayed in Logs) obtained from microarray analysis of each gene involved into stem cell development pathways for AT-A, BM-A and BM-MSC. (B) Heatmap shows hierarchical clustering of stem cell development microarray data obtained from AT-A, BM-A and BM-MSC.

4.2 Hematopoiesis-associated pathways

Since cell-cell signaling is vital for HSC maintenance and activation (Eastment C et al., 1982; Eaves et al., 1988), five key pathways involved in the process were examined: activation of antigen-presenting cells (A), leukocytes (B) blood cells (C), myeloid cells (D) and phagocytes (E). The pathways exhibited differential regulation, and the cluster analysis data demonstrated that BM-A were closer to BM-MSC than to AT-A (Figure 16). In particular, of all the genes studied, only 10 showed a more than twofold up-regulation in BM-MSC compared with BM-A, and four were up-regulated in BM-A (Table 8). In contrast, the BM-A and AT-A signaling pathways demonstrated greater gene expression differences, suggesting widely different roles for the two adipocyte populations.

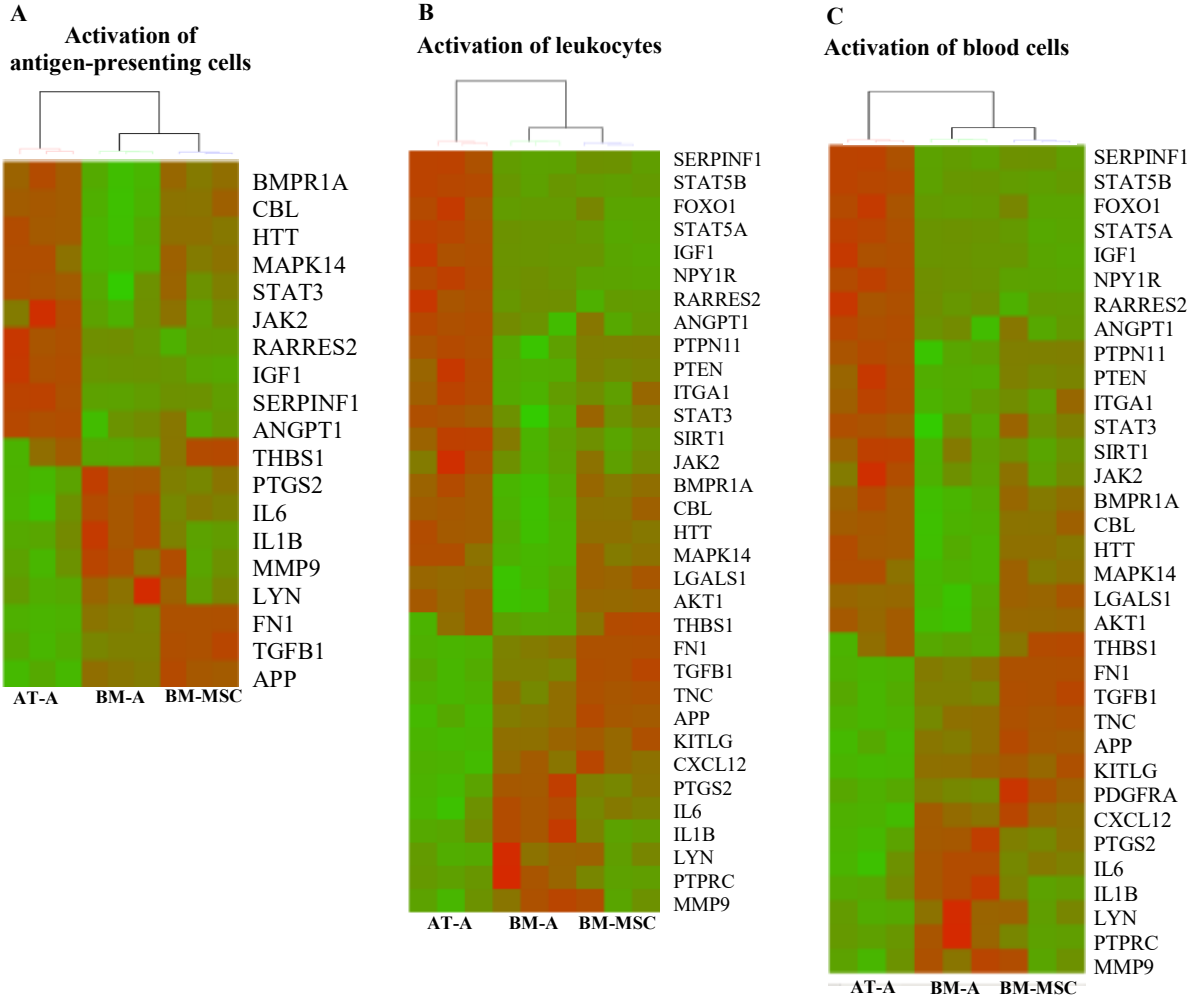

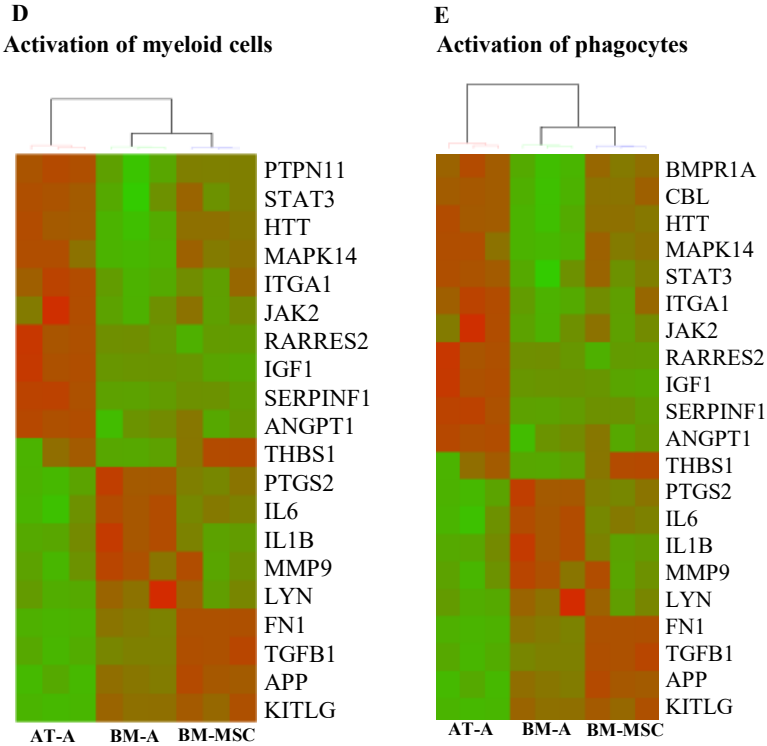

Figure 16: Cluster analysis of cell-to-cell signalling gene expression profile in BM-A, BM-MSC and AT-A.

Differentially expressed genes and pathways involved into cell-to-cell signaling were analyzed. Hierarchical clustering of cell-to-cell signaling microarray data obtained from BM-A, BM-MSC and AT-A in (A) activation of antigen-presenting cells, (B) leukocytes, (C) blood cells, (D) myeloid cells and (E) phagocytes.

CELL-CELL SIGNALLING GENES	BM-A	BM-MSC	AT-A
AKT1	6.38±0.17	7.35±0.02	7.46±0.09
ANGPT1	4.70±0.44	4.90±0.42	6.08±0.06
APP	7.66±0.18	8.58±0.25	5.95±0.24
BMPR1A*	5.43±0.27	7.33±0.27	7.96±0.34
CBL*	5.58±0.13	6.67±0.17	6.94±0.03
CXCL-12	7.81±0.48	8.15±0.81	5.13±0.21
FN1*	9.12±0.54	12.39±0.01	4.89±0.17
FOXO1	5.26±0.04	5.28±0.76	8.93±0.57
HTT	5.48±0.12	6.30±0.05	6.66±0.10
IGF1	3.82±0.06	3.29±0.40	7.05±0.56
IL1B†	7.32±0.57	4.29±0.68	3.96±0.68
IL6†	7.29±0.16	5.97±0.20	4.77±0.68
ITGA1	4.77±0.28	5.63±0.75	7.07±0.36
JAK2	4.14±0.29	4.55±0.41	5.52±0.66
KITLG	4.62±0.11	4.92±0.23	3.23±0.03
LGALS1*	7.00±0.45	10.20±0.28	9.85±0.06
LYN	5.87±0.53	5.25±0.43	4.74±0.13
MAPK14	4.76±0.04	5.57±0.16	5.82±0.25
MMP9	6.61±0.31	6.10±0.57	5.68±0.22
NPY1R	3.41±0.11	2.65±0.06	6.59±0.29
PDGFRA*	5.91±0.33	8.61±1.04	4.24±0.22
PTEN*	5.62±0.04	6.64±0.11	8.08±0.60
PTGS2†	9.15±0.91	6.42±0.56	3.50±0.63
PTPN11*	6.98±0.44	8.06±0.02	9.19±0.11
PTPRC†	4.04±0.57	2.64±0.28	2.58±0.10
RARRES2	6.20±0.11	5.80±0.29	7.94±0.38

SERPINF1	6.95±0.10	7.30±0.25	10.02±.29
SIRT1	6.12±0.57	6.14±0.22	7.65±0.39
STAT3	7.38±0.40	8.05±0.32	8.60±0.08
STAT5A	5.92±0.03	5.55±0.19	7.80±0.19
STAT5B	5.88±0.13	5.83±0.06	7.72±0.08
TGFB1*	6.63±0.07	7.86±0.13	5.61±0.16
THBS1*	9.55±0.10	11.62±0.68	10.60±1.24
TNC*	7.78±0.85	9.95±0.16	4.32±0.18

Table 8: quantitative data of cell-to-cell signalling gene expression profile in BM-A, BM-MSC and AT-A.
Table shows values (represented as means of the three samples studied for each category and displayed in Logs)

The secretion of cytokines and growth factors is crucial for HSC maintenance and differentiation (Eastment C et al., 1982). Remarkably, gene expression analysis showed the highest number of overexpressed cytokines in BM-A, as 26 of the 30 genes studied were upregulated in BM-A compared with AT-A, and 20 were up-regulated in BM-A compared with BM-MSC (Figure 17 A, B). Analysis of the cytokines involved exclusively in hematopoiesis regulation again demonstrated the highest number of up-regulated genes in BM-A; in particular LIF, CCL3, CSF3, CCL4, CCL2, IL-23A, IL-6, CXCL10, CXCL2, PF4, CXCL1, and IL-1β were all up-regulated in BM-A compared with both AT-A and BM-MSC (Figure 16 C).

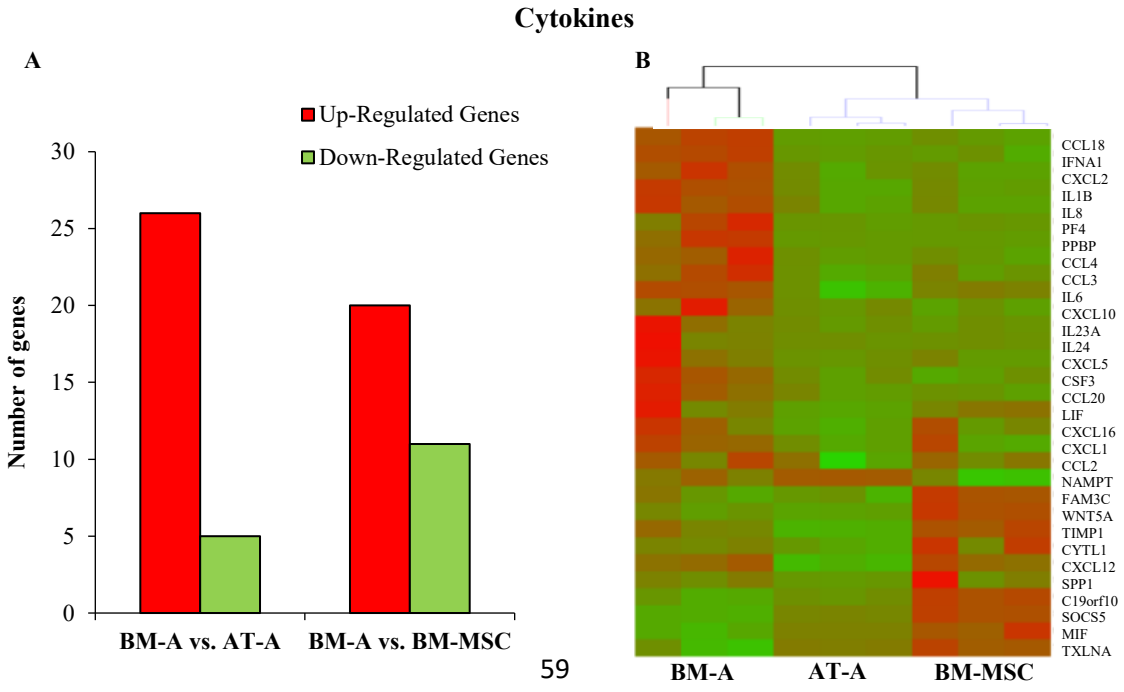

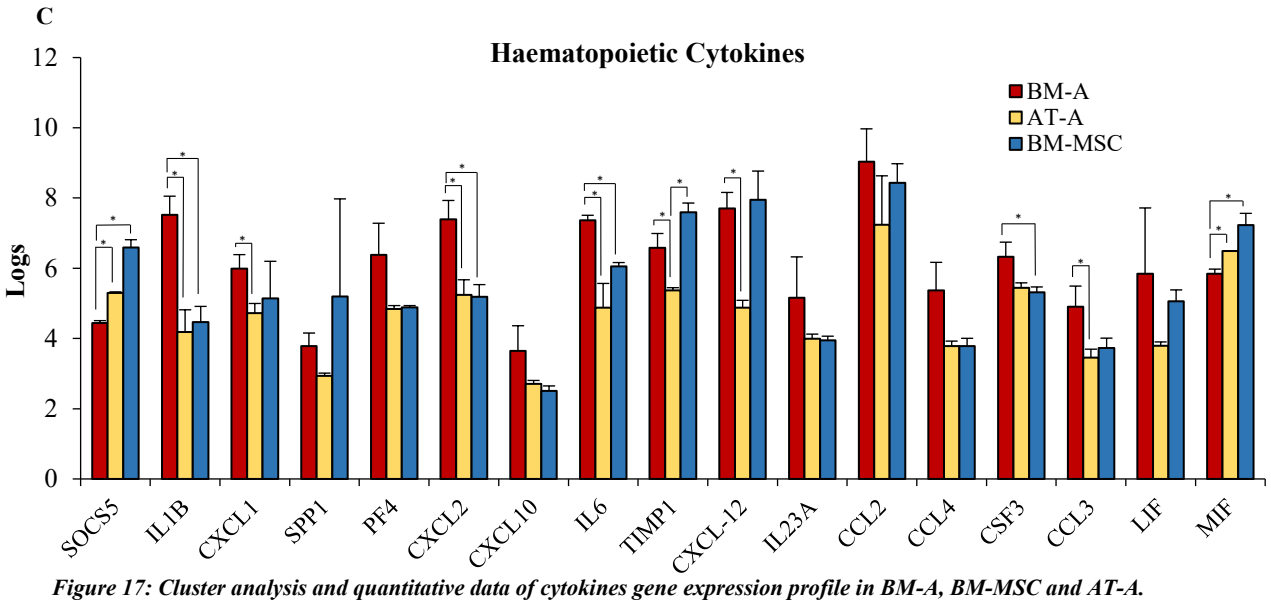

Figure 17: Cluster analysis and quantitative data of cytokines gene expression profile in BM-A, BM-MSC and AT-A.
*Differentially expressed cytokines genes were analysed. (A) Number of Up and Down-Regulated cytokines genes in BM-A respect to AT-A and BM-MSC. (B) Hierarchical clustering of cytokines microarray data obtained from BM-A, BM-MSC and AT-A. (C) Histogram shows data (represented as means of the three samples studied for each category and displayed in Logs) obtained from haematopoietic cytokines microarray analysis in BM-A, AT-A and BM-MSC (*p<0.05).*

Examination of the gene expression profile of the extracellular growth factors not directly involved in hematopoiesis regulation showed that fewer genes were up-regulated in BM-A with respect to AT-A and BM-MSC (Figure 18).

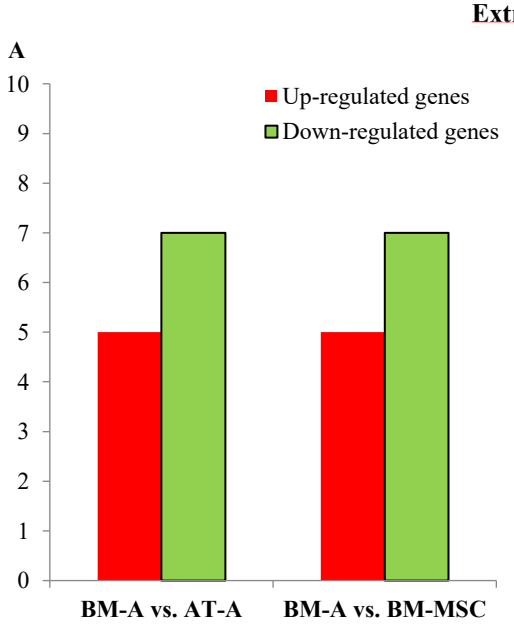

B

Genes	BM-A	AT-A	BM-MSC
INHBB*	4.11±0.40	6.46±0.68	3.73±0.33
EREG*◊	4.09±0.01	2.98±0.09	3.15±0.23
BMP3*◊	4.33±0.11	6.18±0.75	3.98±0.09
PDGFC*	4.58±0.08	5.67±0.14	6.33±0.48
VEGFC◊	4.47±0.22	4.69±0.17	7.57±0.79
BMP5*◊	3.95±0.60	2.47±0.08	2.42±0.07
CTGF◊	7.12±0.33	6.37±1.16	10.43±0.96
LEP*◊	4.11±0.18	9.24±.29	3.10±0.22
NRG1	4.14±0.04	3.84±0.14	5.96±0.82
VEGFB*◊	6.48±0.09	7.93±0.17	6.88±0.04
FGF7*◊	3.36±0.09	2.64±0.10	5.52±0.72
GRN*◊	7.40±0.31	8.20±0.09	8.79±0.49

Figure 18: Differentially gene expression of extracellular growth factor in BM-A, AT-A and BM-MSC.
*Differentially expressed extracellular growth factors genes were analysed. (A) Histogram shows the number of Up and Down-Regulated extracellular growth factors genes in BM-A respect to AT-A and BM-MSC; (B) table shows values (represented as means of the three samples studied for each category and displayed in Logs) obtained from microarray analysis of each extracellular growth factors gene for BM-A, AT-A and BM-MSC. (*p < 0.05; BM-A vs. AT-A; ◊p < 0.05 BM-A vs. BM-MSC)*

In contrast, assessment of the hematopoietic extracellular growth factors highlighted greater differences, since BMA expressed a larger number of up-regulated genes than AT-A. In particular, TGF-β2, INHBA, HGF, ANGPT2, DKK1, RITLG, GAS6, and TGF-β1 were overexpressed in BM-A compared with AT-A, whereas only ANGPT2 and IGF1 were overexpressed in BM-A compared with BM-MSC (Figure 19).

Extracellular haematopoietic growth factors

A

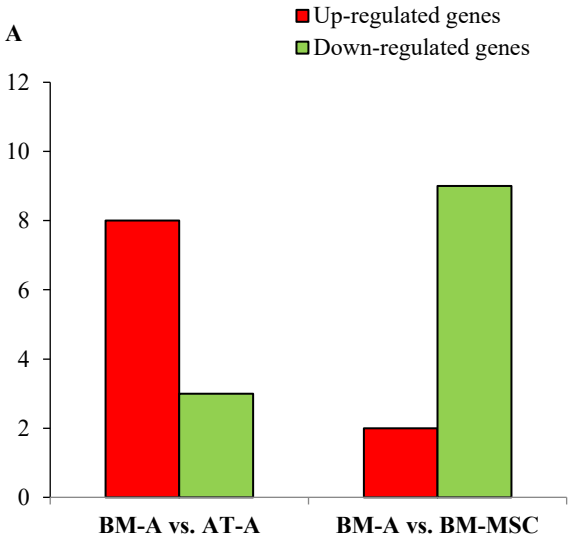

B

Genes	BM-A	AT-A	BM-MSC
TGFB2	4.02±0.05	3.71±0.28	5.00±0.52
FGF2*	7.16±0.50	8.57±0.11	8.29±0.05
INHBA	5.68±1.13	4.10±0.10	7.30±1.01
HGF*	3.27±0.00	2.82±0.12	4.20±0.70
ANGPT2	4.17±1.06	2.98±0.09	2.89±0.03
ANGPT1*	4.60±0.37	5.87±0.13	4.74±0.36
DKK1	3.02±0.10	2.84±0.14	5.30±1.09
KITLG*	4.18±0.20	3.12±0.06	4.52±0.28
IGF1*	4.17±0.07	6.98±0.53	3.43±0.55
GAS6*◊	6.54±0.23	5.93±0.29	8.19±0.41
TGFB1*◊	6.64±0.00	5.57±0.22	7.74±0.12

Figure 19: Differentially gene expression of extracellular hematopoietic growth factor in BM-A, AT-A and BM-MSC. *Differentially expressed extracellular hematopoietic growth factors genes were analysed. (A) Histogram shows the number of Up and Down-Regulated extracellular hematopoietic growth factors genes in BM-A respect to AT-A and BM-MSC; (B) table shows values (represented as means of the three samples studied for each category and displayed in Logs) obtained from microarray analysis of each extracellular hematopoietic growth factors gene for BM-A, AT-A and BM-MSC. (*p < 0.05; BM-A vs. AT-A; ◊p < 0.05 BM-A vs. BM-MSC)*

5. Caloric Restriction Time Course

During the CR time course, AL and CR mouse weights were recorded weekly. Weight loss was statistically significant in both male and female CR mice compared to AL mice during the dietary regimen time course. Interestingly, male mice lost weight until the 3rd week of CR and then started to regain body mass on week 4 (not statistically significant), whereas, females quickly adapted to the dietary regimen and stopped losing weight at week 2.

Interestingly a statistical significance difference was detected between WT and KO AL female mice body mass on week 3, but no genotype differences were found in male mice. (Figure 20; Table 9).

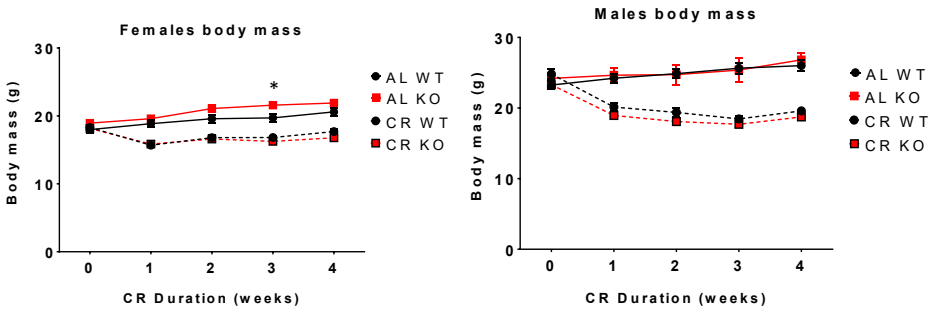

Figure 20: Female and male Body masses of WT and KO mice fed AL or under CR.
Each point represents the body mass of (A) female and (B) male mice during week 1, 2, 3 and 4 of CR
(*=P<0.05)

Body Masses (grams)							
Sex	**Genotype**	**Diet**	**Week 0**	**Week 1**	**Week 2**	**Week 3**	**Week 4**
Female	WT	AL	17,9 ± 1,6	18,8 ± 2,0	19,6 ± 2,1	19,7 ± 2,3	20,6 ± 2,0
Female	WT	CR	18,2 ± 1,6	15,6 ± 1,5	16,9 ± 1,2	16,8 ± 0,9	17,8 ± 1,1
Female	KO	AL	18,9 ± 1,4	19,5 ± 1,0	21,0 ± 1,5	21,5 ± 1,4	21,9 ± 1,6
Female	KO	CR	18,5 ± 1,4	15,7 ± 1,6	16,7 ± 1,3	16,2 ± 1,3	16,8 ± 1,3
Male	WT	AL	24,1 ± 2,7	24,2 ± 2,2	24,8 ± 2,1	25,6 ± 2,6	26,0 ± 2,5
Male	WT	CR	24,1 ± 2,7	20,1 ± 2,3	19,3 ± 2,2	18,4 ± 1,2	19,6 ± 0,4
Male	KO	AL	23,5 ± 1,7	24,6 ± 2,5	24,7 ± 3,7	25,3 ± 4,5	26,8 ± 2,5
Male	KO	CR	23,5 ± 1,7	18,9 ± 1,7	18,0 ± 1,7	17,7 ± 1,3	18,7 ± 1,1

Table 9: Quantitative data of body masses WT and KO mice fed AL or under CR.
Table shows values (expressed in grams) of AL WT, AL KO, CR WT, CR KO male and female mice during the 4 weeks CR time course.

Circulating levels of serum APN, measured by ELISA, were significantly increased ($p<0,05$) in CR male mice during week 3 and 4 and in CR female mice during week 2, 3 and 4. (Figure 21).

Also, using immunoblotting, plasma adiponectin was detectable in the WT mice but not in the KO mice, confirming the genotype (R. Sulston, unpublished observation, data not shown).

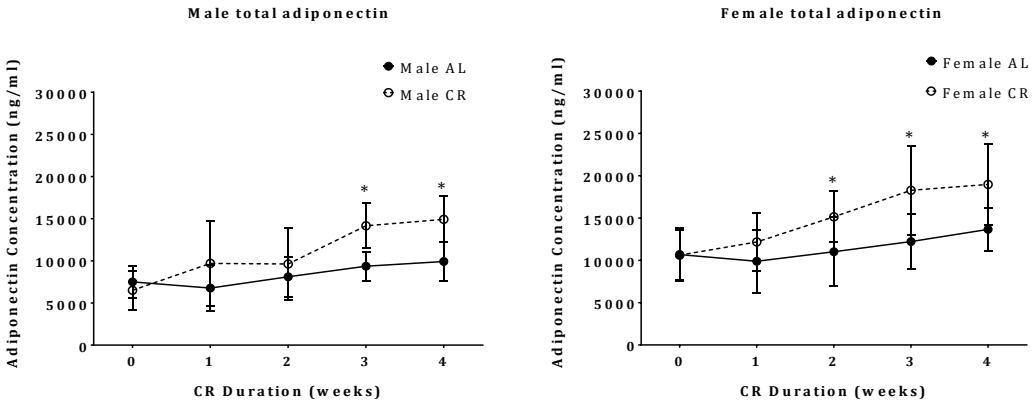

Figure 21: Female and male circulating levels of plasma APN in mice fed AL or under CR.
Each point represents the concentration of (A) female and (B) male circulating APN during week 1, 2, 3 and 4 (*=P<0.05).

6. Peripheral white blood cell count

Peripheral white blood cell count was performed weekly prior to feeding. Caloric restriction caused a global reduction of circulating WBC in both WT and KO animals. Notably, at week 1 and 2, a genotype effect was observed and statistical significant differences in the number of WBC were detected between AL KO and CR KO mice. During week 3 and 4, CR WT mice showed a further decrease in WBC and statistical differences were observed between CR WT and AL WT. (Figure 22; Table 10)

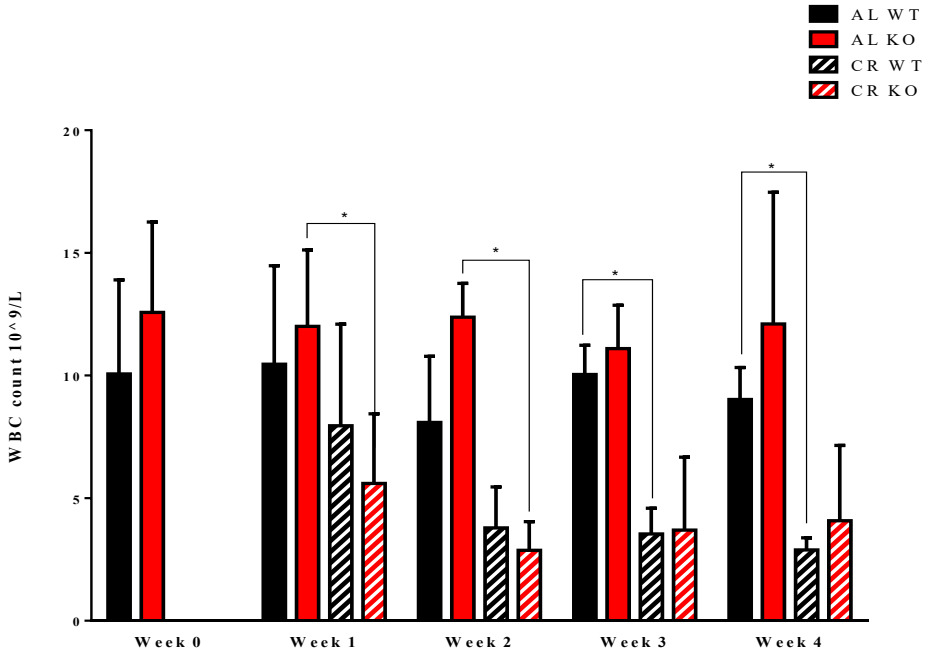

Figure 22: Peripheral white blood cells count.
Histogram shows the number of circulating WBC (expressed as 10^9 cells/L) of AL WT, AL KO, CR WT and CR KO mice (males and females data are combined) (=p<0.05).*

WBC count (10^9 cells/Liter)						
Diet	**Genotype**	**Week 0**	**Week 1**	**Week 2**	**Week 3**	**Week 4**
AL	WT	10,0 ± 3,8	10,4 ± 4,0	8,08 ± 2,6	10,0 ± 1,1	9,02 ± 1,2
AL	KO	12,5 ± 3,6	12,0 ± 3,1	12,3 ± 1,3	11,1 ± 1,7	12,1 ± 5,3
CR	WT		7,95 ± 4,1	3,78 ± 1,6	3,53 ± 1,0	2,88 ± 0,4
CR	KO		5,60 ± 2,8	2,87 ± 1,1	3,7 ± 2,9	4,07 ± 3,0

Table 10: Quantitative data of circulating WBC.
Table shows values of circulating WBC (expressed as 10^9 cells/L) in AL WT, AL KO, CR WT, CR KO mice during the CR time course. (males and females data are combined).

7. Flow cytometry analysis of Peripheral White Blood cells

Results obtained with WBC count suggested that both CR and global Adiponectin KO caused an impairment of normal haematopoieis. Therefore, circulating lymphocytes, granulocytes and monocytes were analysed by flow cytometry. The global reduction of circulating WBC, produced an increased percent of granulocytes was in CR KO mice. Specifically, statistically significant differences were observed during the first week among AL KO, CR KO, and CR WT mice. From the second week, the percentage of circulating granulocytes also increased in CR WT animals and statistically significant differences were observed only between AL KO and CR KO animals. (Figure 23, table 11). Despite the fact that it has been observed an increased percent of granulocytes in CR KO animals, the number of total circulating granulocytes per liter of blood remains still reduced in CR animals with respect to AL mice (Table 12). Notably, female mice didn't present any modulation of granulopoiesis under CR, suggesting that sex difference might influence the Adiponectin-mediated regulation of haematopoiesis.

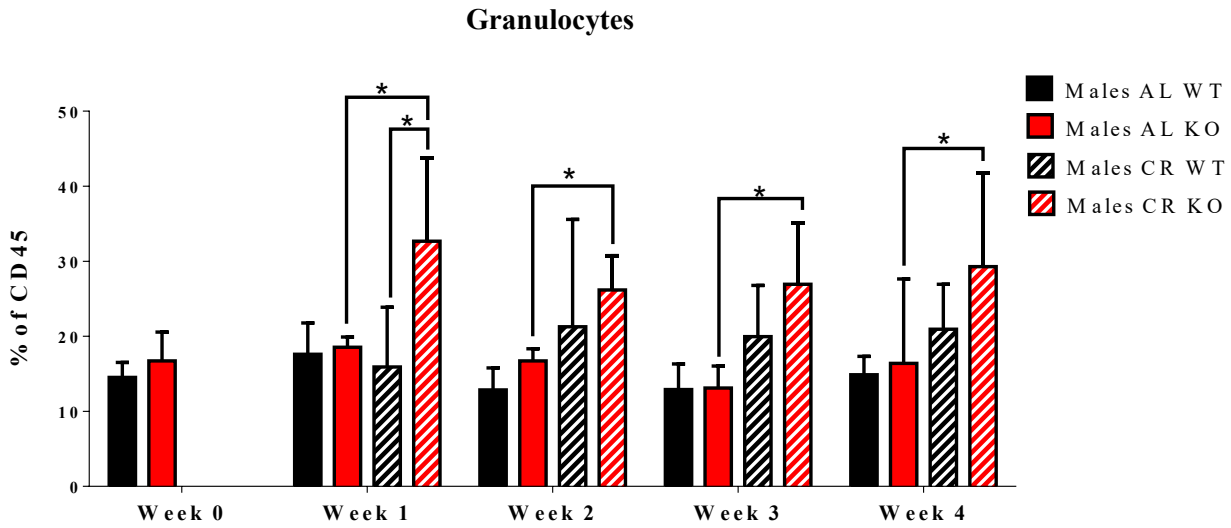

Figure 23. Flow cytometry analysis of circulating granulocytes.
Histograms show the number of circulating granulocytes (expressed as % of total CD45 cells) in male AL WT, AL KO, CR WT, CR KO mice during the CR time course. (=p<0.05).*

Granulocytes (% of total CD45 cells)							
Sex	**Diet**	**Genotype**	**Week 0**	**Week 1**	**Week 2**	**Week 3**	**Week 4**
F	AL	WT	13,6 ± 5,6	11,9 ± 1,5	12 ± 4,6	12,2 ± 3,0	16,9 ± 6,7
F	AL	KO	11,5 ± 2,2	14,5 ± 3,4	12,3 ± 1,6	13,6 ± 1,9	12,7 ± 3,4
F	CR	WT		15,8 ± 13	15,1 ± 7,8	14,0 ± 7,4	17,4 ± 10
F	CR	KO		11,7 ± 2,2	12,1 ± 1,5	12,1 ± 4,0	21,7 ± 15
M	AL	WT	14,5 ± 2,0	17,6 ± 4,1	13,8 ± 3,1	13,1 ± 3,1	14,8 ± 7,3
M	AL	KO	16,7 ± 3,8	18,5 ± 1,3	16,7 ± 2,2	12,6 ± 3,4	16,4 ± 3,6
M	CR	WT		16,6 ± 8,4	18,5 ± 12	20,8 ± 7,5	20,9 ± 6,3
M	CR	KO		32,6 ± 11	30,6 ± 4,9	25,9 ± 8,3	29,3 ± 11

Table 11: Quantitative data of circulating granulocytes.
Table shows values of circulating granulocytes (expressed as % of total CD45 cells) in females and males AL WT, AL KO, CR WT, CR KO mice during the CR time course.

Total number of granulocytes (10^9cells/L)							
Sex	**Diet**	**Genotype**	**Week 0**	**Week 1**	**Week 2**	**Week 3**	**Week 4**
F	AL	WT	1,36 ± 0,289	1,23 ± 0,074	0,96 ± 0,015	1,22 ± 0,040	1,52 ± 0,122
F	AL	KO	1,43 ± 0,113	1,74 ± 0,183	1,51 ± 0,031	1,50 ± 0,048	1,53 ± 0,276
F	CR	WT		1,25 ± 0,669	0,57 ± 0,071	0,49 ± 0,036	0,50 ± 0,020
F	CR	KO		0,65 ± 0,040	0,34 ± 0,005	0,44 ± 0,051	0,88 ± 0,397
M	AL	WT	1,45 ± 0,110	1,83 ± 0,300	1,11 ± 0,089	1,31 ± 0,044	1,33 ± 0,116
M	AL	KO	2,08 ± 0,285	2,22 ± 0,089	2,05 ± 0,058	1,39 ± 0,080	1,98 ± 0,378
M	CR	WT		1,31 ± 0,454	0,69 ± 0,134	0,73 ± 0,055	0,60 ± 0,015
M	CR	KO		1,82 ± 0,562	0,87 ± 0,047	0,95 ± 0,230	1,19 ± 0,393

Table 12: Quantitative data of total circulating granulocytes.
Table shows values of total circulating granulocytes (expressed as granulocytes/L of blood) in females and males AL WT, AL KO, CR WT, CR KO mice during the CR time course.

The granulopoiesis dysregulation also turned into an imbalanced proportion between neutrophils, increased in CR mice, and eosinophils which resulted significantly reduced (Tables 13, 14).

Neutrophils (% of Granulocytes)							
Sex	**Diet**	**Genotype**	**Week 0**	**Week 1**	**Week 2**	**Week 3**	**Week 4**
F	AL	WT	77,3 ± 8,4	70,2 ± 5,3	53,3 ± 19	63,9 ± 6,6	76,2 ± 11
F	AL	KO	74,9 ± 11	66,5 ± 7,1	66,7 ± 5,7	65,1 ± 8,2	64,6 ± 15
F	CR	WT		85,8 ± 12	78,7 ± 20	75,8 ± 13	71,7 ± 16
F	CR	KO		84,7 ± 7,4	76,2 ± 7,4	63,0 ± 18	71,0 ± 15
M	AL	WT	69,8 ± 4,7	64,9 ± 7,9	66,2 ± 3,6	71,6 ± 8,7	73,4 ± 11
M	AL	KO	74,1 ± 10	66,0 ± 4,2	74,1 ± 4,1	71,2 ± 4,5	72,7 ± 10
M	CR	WT		91,9 ± 5,6	89,5 ± 8,3	88,8 ± 6,9	79,6 ± 8,9
M	CR	KO		98,5 ± 1,3	91,5 ± 6,2	91,4 ± 3,1	86,8 ± 8,2

Table 13: Quantitative data of circulating neutrophils.
Table shows values of circulating neutrophils (expressed as % of total granulocytes) in females and males AL WT, AL KO, CR WT, CR KO mice during the 4 weeks CR time course.

Eosinophils (% of Granulocytes)							
Sex	**Diet**	**Genotype**	**Week 0**	**Week 1**	**Week 2**	**Week 3**	**Week 4**
F	AL	WT	20,4 ± 8,1	28 ± 4,8	38,6 ± 13	29,5 ± 6,3	18,6 ± 9,5
F	AL	KO	22,9 ± 11	31,3 ± 7,0	29,6 ± 4,6	31,2 ± 6,7	28,2 ± 13
F	CR	WT		12,6 ± 11	16,5 ± 15	17,1 ± 9,2	20,8 ± 13
F	CR	KO		13,7 ± 6,9	20 ± 7,4	30,1 ± 13	24,0 ± 16
M	AL	WT	28,8 ± 4,8	33,9 ± 7,6	27,6 ± 7,0	24,7 ± 10	21,3 ± 11
M	AL	KO	24,0 ± 10	32,7 ± 3,6	23 ± 2,8	24,9 ± 3,8	21,2 ± 7,9
M	CR	WT		6,72 ± 5,8	4,35 ± 4,8	7,74 ± 6,5	15,3 ± 10
M	CR	KO		0,54 ± 0,7	3,33 ± 4,9	6,56 ± 1,5	9,63 ± 7,3

Table 14: Quantitative data of circulating eosinophils.
Table shows values of circulating eosinophils (expressed as % of total granulocytes) in females and males AL WT, AL KO, CR WT, CR KO mice during the 4 weeks CR time course.

Analysis of lymphocyte populations did not reveal any changes in CD3, CD4 and CD8. Interestingly, CD19 B lymphocytes represented the population which underwent the highest modulation under CR, showing a statistically significant decrease in CR KO animals with respect to AL KO during the entire CR time course. Notably, a strong genotype effect was observed during week 1 of CR where only the KO animals showed a reduced lymphopoiesis. The discrepancy between CR WT and CR KO animals (statistically significant only in week 1 and week 3) can be observed for the entire CR time course despite WT animals also showed reduced circulating lymphocytes since week 2 of CR (Figure 24 Table 15).

B Lymphocytes

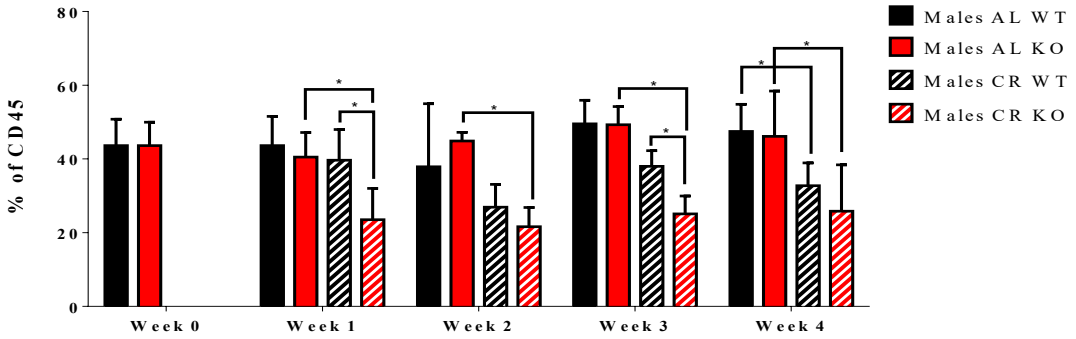

Figure 24. Flow cytometry analysis of circulating B lymphocytes.
Histograms show the number of circulating B lymphocytes (expressed as % of total CD45 cells) in males AL WT, AL KO, CR WT, CR KO mice during the CR time course (=p<0.05).*

Lymphocytes (% of CD45)							
Sex	**Diet**	**Genotype**	**Week 0**	**Week 1**	**Week 2**	**Week 3**	**Week 4**
F	AL	WT	41,1 ± 10,	36,1 ± 7,6	30,8 ± 8,3	35,5 ± 8,1	38,5 ± 7,1
F	AL	KO	38,0 ± 10,	36,1 ± 7,8	41,3 ± 6,9	42,1 ± 3,2	43,0 ± 7,4
F	CR	WT		28,1 ± 10	31,7 ± 4,8	31,8 ± 10	32,5 ± 8,6
F	CR	KO		40,4 ± 8,4	36,2 ± 5,5	39,4 ± 9,2	34,7 ± 19
M	AL	WT	43,6 ± 7,1	43,6 ± 7,9	37,8 ± 14,	49,5 ± 5,8	45,0 ± 10
M	AL	KO	43,6 ± 6,3	40,5 ± 6,6	44,6 ± 3,2	49,2 ± 5,8	51,2 ± 5,0
M	CR	WT		39,6 ± 9,1	27,1 ± 5,8	37,9 ± 6,0	33,5 ± 7,5
M	CR	KO		23,5 ± 8,4	21,2 ± 5,3	25,1 ± 5,8	24,8 ± 10

Table 15: Quantitative data of circulating B lymphocytes.
Table shows values of circulating lymphocytes (expressed as % of total eosinophils) in females and males AL WT, AL KO, CR WT, CR KO mice during the 4 weeks CR time course.

Monocytes were also analysed, but no genotype or diet effect was detected except from CR male mice (both WT and KO) that, during week 1 of CR, showed reduced circulating monocytes with respect to AL animals (AL WT: 42,6 ± 4,4; CR WT: 31,6 ± 13,6; AL KO: 43,6 ± 3.2; CR KO: 18,2 ± 12,9; data are expressed as percent of total CD45 cells).

8. Flow cytometry analysis and CFU assay of BM-MNC followig 4 weeks of CR

To test the differentiation and the proliferation capacity of HSC after 4 weeks of CR, animals were sacrificed, BM-MNC were isolated from the femurs and seeded in Methocult. After 10-12 days of incubation at 37°C, CFU were counted and examined.

No statistically significant differences were observed between CR and AL mice or between WT and KO. However, of note, in the female mice, the KO genotype tended to produce a higher number of total CFU ($p>0.05$) (Figure 25, Table 16).

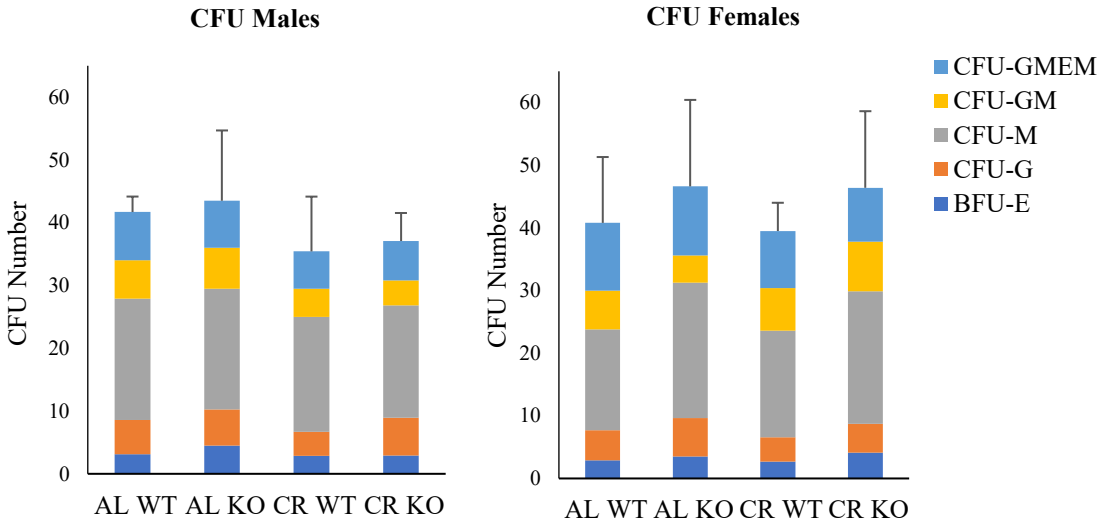

Figure 25. CFU output after 4 weeks of CR
Histograms shows the total number of CFU obtained in (A) female and (B) male mice AL WT, AL KO and in CR WT and CR KO after 4 weeks of CR. Bars represent the sum of BFU-E (blue), CFU-G (orange), CFU-M (grey), CFU-GM (yellow), CFU-GMEM (light blue).

Sex	Diet	Genotype	BFU-E	CFU-G	CFU-M	CFU-GM	CFU-GMEM	Total
F	AL	WT	2,9 ± 1,7	4,8 ± 2,9	16,1 ± 4,5	6,2 ± 1,6	10,8 ± 4,9	40,8 ± 10
F	CR	WT	2,7 ± 2,0	3,9 ± 0,8	17 ± 2,4	6,8 ± 2,5	9,1 ± 3,1	39,5 ± 4,5
F	AL	KO	3,5 ± 1,4	6,12 ± 2,7	21,6 ± 7,2	4,37 ± 1,8	11 ± 2,0	46,6 ± 13
F	CR	KO	4,1 ± 1,6	4,6 ± 1,6	21,2 ± 6,4	7,9 ± 3,1	8,6 ± 3,0	46,4 ± 12
M	AL	WT	3,1 ± 0,5	5,5 ± 0,2	19,3 ± 2,5	6,1 ± 1,8	7,7 ± 1,5	41,7 ± 2,4
M	CR	WT	2,85 ± 1,7	3,85 ± 2,2	18,2 ± 4,0	4,5 ± 3,1	5,92 ± 3,5	35,4 ± 8,7
M	AL	KO	4,5 ± 2,0	5,75 ± 3,7	19,2 ± 10,	6,5 ± 3,3	7,5 ± 1,8	43,5 ± 11
M	CR	KO	2,91 ± 1,1	6 ± 1,7	17,9 ± 2,3	4 ± 0,6	6,25 ± 1,8	37,0 ± 4,4

Table 16: Quantitative data of CFU output after 4 weeks of CR
Table shows the total number of each CFU type obtained in (A) female and (B) male mice AL WT, AL KO and in CR WT and CR KO after 4 weeks of CR.

To further analyse any potential diet or genotype induced changes in HSC, flow cytometry analysis on BM-MNC was performed. The gating strategy suggested by Oguro *et al.* (2013) has been previously used to evaluate the number and the differentiation potential of cells. In more detail, following Lineage$^-$ C-Kit$^+$ Sca-1$^+$ selection, cells were further separated in 4 different population using CD48 and CD150 markers. Serial transplantation experiments showed that CD150$^+$/CD48$^-$ fraction represent the HSC population with long-term multilineage reconstitution capacity, while CD150$^-$/CD48$^-$ cells has only transient multilineage reconstitution capacity and cannot be further transplanted in a secondary recipient. On the contrary, CD48$^+$/CD150$^-$ and CD48$^+$/CD150$^+$ fractions have restricted differentiation potential and can reconstitute the recipient with B cells, rarely with T cells but never with myeloid cells (Kiel Mj et al., 2008). Despite the differences detected in circulating WBC, flow cytometry analysis of BM-MNC did not reveal any changes in male mice. However, female AL WT mice showed an increased percent of CD150$^-$/CD48$^-$ (statistically significant) to the detriment of CD150$^-$/CD48$^+$ (not significant). (Figure 26, 27, Table 17).

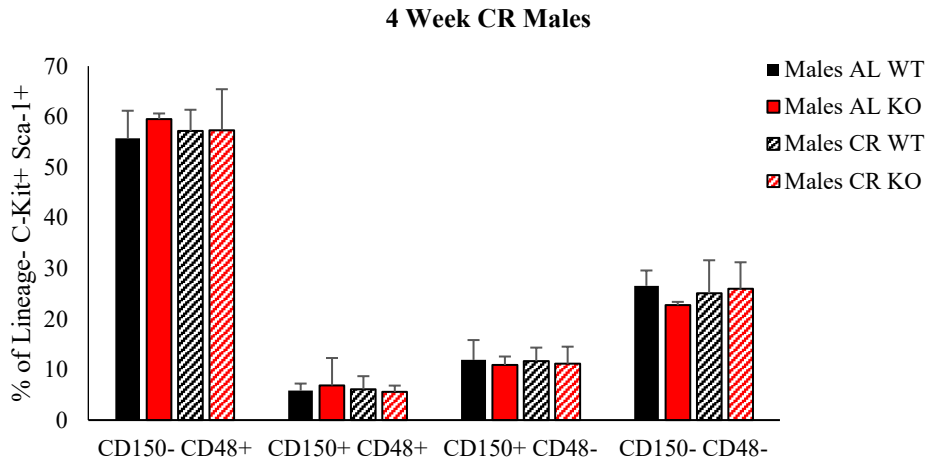

Figure 26. Flow cytometry analysis of LSK population in females.
Histograms show the number of BM CD150-/CD48+, CD150+/CD48+, CD150+/CD48-, CD150-/CD48- cells (expressed as % of total Lineage-/C-Kit+ cells) in females AL WT, AL KO and in CR WT and CR KO after 4 weeks of CR.

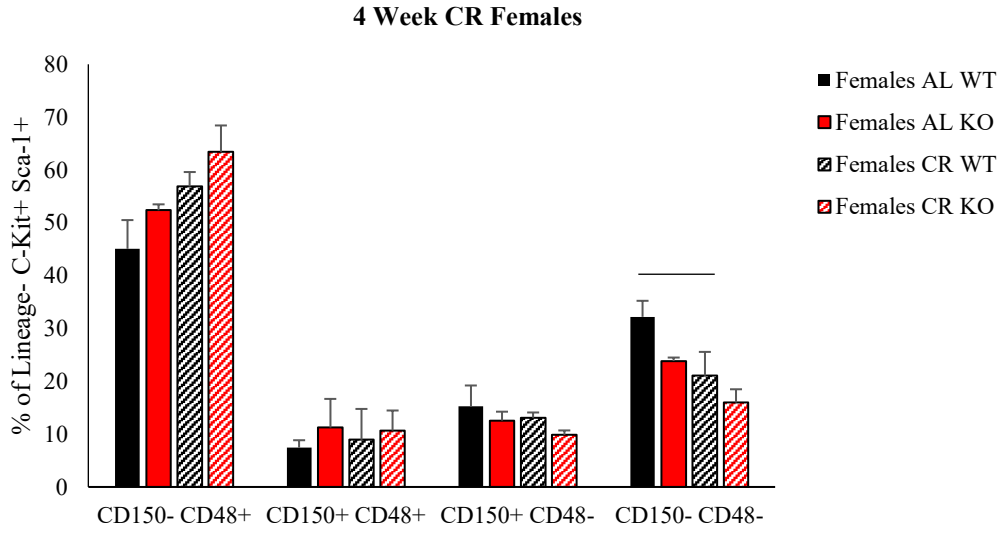

Figure 27. Flow cytometry analysis of LSK population in males.
Histograms show the number of BM CD150-/CD48+, CD150+/CD48+, CD150+/CD48-, CD150-/CD48- cells (expressed as % of total Lineage-/C-Kit+ cells) in males AL WT, AL KO and in CR WT and CR KO after 4 weeks of CR.

Sex	Diet	Genotype	CD150-CD48+	CD150+ CD48+	CD150+ CD48-	CD150- CD48-
F	AL	WT	45,0 ± 11,	7,44 ± 1,3	15,2 ± 7,7	32,2 ± 4,3
F	AL	KO	52,3 ± 9,4	11,2 ± 2,5	12,5 ± 4,6	23,8 ± 7,4
F	CR	WT	56,8 ± 5,8	8,94 ± 1,0	13,0 ± 4,4	21,0 ± 4,5
F	CR	KO	63,4 ± 4,9	10,6 ± 3,7	9,85 ± 0,8	16 ± 2,4
M	AL	WT	55,7 ± 5,4	5,82 ± 1,3	11,9 ± 3,9	26,5 ± 3,0
M	AL	KO	59,5 ± 5,4	6,86 ± 1,6	10,8 ± 0,6	22,7 ± 5,9
M	CR	WT	57,1 ± 4,2	6,08 ± 2,5	11,6 ± 2,6	25,0 ± 6,5
M	CR	KO	57,3 ± 8,1	5,56 ± 1,2	11,1 ± 3,3	25,9 ± 5,2

Table 17: Quantitative data of LSK population in males.
Table show the values of BM CD150-/CD48+, CD150+/CD48+, CD150+/CD48-, CD150-/CD48- cells (expressed as % of total Lineage-/C-Kit+ cells) in females and males AL WT, AL KO and in CR WT and CR KO after 4 weeks of CR.

Discussion

BM-A are the most abundant stromal cell population in the BM microenvironment, and the gradual replacement of the red marrow with yellow marrow happening during aging results in decreased hematopoietic activity. These findings have generated the notion that BM-A are negative regulators of hematopoiesis (Naveiras O et al., 2009; Tuljapurkar SR et al., 2011). However, their characterisation is still far from being exhaustive, both owing to the difficulty to obtain and manipulate primary human BM-A. Furthermore, the relationship between BM-A and HSC has often been explored using BM-MSC-derived adipocytes obtained by *in vitro* differentiation and the biological differences between differentiated BM-MSC and primary BM-A frequently produced contrasting results.

Varied experimental evidences seem to suggest that BM-A might actually positively support HSC (Corre J et al., 2004, 2006; Di Mascio L et al., 2007; Gainsford T et al., 1996; Laharrague P et al., 1998; Poloni A et al., 2013). In the present study, BM-A were used as stromal supporting population for HSC in an *in vitro* model and the results suggested that following a 5-week co-culture, primary human BM-A, even if not at the same level of BM-MSC, were still capable of supporting HSC maintenance, proliferation and differentiation. The LTC-IC system, which accurately reproduces HSC turnover (Eaves & Eaves, 1988), allowed establishing an *in vitro* model that mimic the BM microenvironment conditions.

Interestingly, the presence of BM-A in the co-culture led to a lower colony output in the first 4 weeks, suggesting a reduced proliferation of the more committed HPC. These results suggest that BM-A might exert an inhibitory action on the more committed HPC, but that they are able to support the survival of long-term HSC. This hypothesis is further confirmed by the results obtained with the mixed feeder layer (BM-A+BM-MSC), where

the presence of adipocytes seemed to impair HPC proliferation and differentiation, during the first 2 weeks (statistically significant only in week 1), but did not lead to a reduced final colony output. The presence of inhibitory cytokines in the cell culture supernatants is in line with an inhibitory role of BM-A exerted toward HPC particularly evident in the first 2 weeks of co-culture. However, this effect did not critically impair HSC survival and maintenance, although the number of CFU obtained in the mixed feeder layer co-cultured in the 5th week was high and not significantly different from that of the cells co-cultured only with BM-MSC. These findings suggest that BM-A do not specifically exert an inhibitory effect on hematopoiesis itself, but rather that they contribute, together with the other cells in the niche, to maintain and regulate HSC survival, protecting them against excessive proliferation and differentiation stimuli that could lead to exhaustion of the BM HSC pool. Previous authors explored the relationship between BM-A and HSC. Belaid-Choucair *et al.* (2008) developed a co-culture model using fibroblast-like fat cells (FLFC), obtained from BM-A that had lost their lipid content, as feeder layer for CD34+ cells. They found that FLFC were able to sustain macrophage but inhibit granulocyte differentiation through interaction with neuropilin-1 (NP-1). In the present study it has not been detected any granulopoiesis inhibition and microarray analysis revealed that NP-1 expression was down-regulated in BM-A compared with BM-MSC and AT-A (data not shown). Furthermore, we observed that BM-A, unlike AT-A, maintained their characteristic morphology in culture, and that very few cells differentiated into fibroblast-like cells. The discrepancy may be explained by methodological differences, indeed the BM-A used by Belaid-Choucair *et al.* (2008) were obtained from a femoral biopsy, whereas in this study cells were obtained from the whole femoral head of patients undergoing hip surgery. Results obtained in 1976 Tavassoli (1976) showed BM-A

features might differ depending on their location within BM; Scheller *et al.* (2015) recently validated these observations by describing region-specific variation in the properties BM-A and hypothesising the existence of two distinct marrow adipose tissues: "regulated marrow adipose tissue" (rMAT) made by, smaller adipocytes interspersed in active red haematopoietic marrow and "constitutive marrow adipose tissue" (cMAT) with numerous, larger adipocytes found in tissue areas with low hematopoiesis. The different results obtained here and in the study by Belaid-Choucair *et al.* (2008) could therefore rely on different subtype of isolated BM-A. In 2009, Naveiras et al (REF) studied the haematopoietic capacity of various skeletal mouse regions that differs in adiposity. The author found that HPC frequency in BM declined as a function of adipocyte number, suggesting an inverse relationship between BM-A and the haematopoietic capacity of the BM. They also developed an *in vitro* co-culture system using a mouse stromal cell line (OP9) differentiated toward the adipocyte lineage and used as a feeder layer for CD34+ cells. Results obtained are similar to those found in the present study (despite the very different experimental settings involving respectively murine differentiated BM-MSC and primary human BM-A) although they demonstrated that the adipose differentiation enabled OP9 cells to support HSC proliferation, albeit not as effectively as did untreated cells.

The functional results of the present study were further confirmed by molecular analysis, which showed closely related gene expression profiles of hematopoiesis-associated pathways in BM-A and BM-MSC. Noteworthily, cluster analysis of total gene expression profile segregated BM-A on a different branch of the dendrogram with respect to BM-MSC and AT-A, suggesting that BM-A represent a different entity compared with BM-MSC and AT-A which, on the other hand, are mesenchymal populations with strong

phenotypic and transcriptional overlap (Wagner W et al., 2005). In contrast, cluster analysis of restricted gene sets (cell-signaling pathways, hematopoietic support, etc.) showed a similar gene expression pattern in BM-A and BM-MSC. Altogether, these findings (despite they may result from tissues specific commitment (Sacchetti B et al., 2016)) confirm that BM-A play an active role in the BM niche, contributing to BM homeostasis together with other stromal cells.

The regulation of BM homeostasis is also mediated by the secretion of cytokines and growth factors, which are involved in processes such as homing, adhesion, quiescence, maintenance, self-renewal, and proliferation (Fajardo- Orduña, GR et al., 2015). Microarray analysis of cytokine gene expression showed a greater number of up-regulated genes in BM-A than in BM-MSC and AT-A. Analysis of the culture supernatant concentrations of these proteins, demonstrated similar levels of key molecules such as IL-8, CXCL12, CSF3, and LIF, in BM-A and BM-MSC, and a higher level of IL-3 in BM-A. These molecules can both induce HSC quiescence and stimulate their differentiation, therefore their presence in the culture supernatant suggested that BM-A can play both roles to meet the homeostatic requirements of the BM niche (Ilangumaran, S et al., 2016). Interestingly, all the negative hematopoiesis regulators examined in the present study showed similar levels in BM-A and BM-MSC, except TNF-α, which was higher in BM-MSC. These data suggest that BM-A, far from playing a passive role or suppressing hematopoiesis, actually participate in the regulation of BM microenvironment homeostasis (Table 2). These findings are in line with those reported by Corre et al. (2004), who demonstrated that BM-MSC-derived adipocytes are able to induce myeloid and lymphoid differentiation of HCP in the 1st days of co-culture and that BM-A are able to produce cytokines directly involved in hematopoiesis support.

Among all the adipokines secreted by BM-A, APN represented one of most intensively studied. Being one of the hormones present at the highest concentration in the blood, many studies focused on the relationship between adiponectin and obesity related diseases, however, its role in haematopoiesis regulation has not been comprehensively understood.

Cawthorn *et al.* (2014) have shown that BM-A may be a major source of circulating adiponectin, they showed that under CR regimen the number of adipocytes in the marrow is augmented and specifically contribute to increased level of circulating plasmatic APN.

Therefore, to evaluate the role of APN in haematopoiesis regulation APN KO murine model were placed under CR dietary regimen and their haematopoietic parameters were studied.

WBC count revealed that CR has strong effect on the immune system indeed both WT and KO animals showed a significantly reduced number of circulating leukocytes for the whole CR time course. Interestingly, only KO animals showed a significantly reduced number during the first two weeks of CR with respect to WT, suggesting an APN mediated regulation of haematopoiesis. To evaluate which PB cell lineage was specifically affected by genotype and dietary regimen, flow cytometry analysis was performed, and lymphocyte, granulocyte and monocyte populations were evaluated. Notably, especially during week 1 of CR, KO animals presented a statistically significant reduction of circulating B cells, while WT animals revealed impaired B lymphopoiesis with respect to AL mice only on week 4. Results obtained in WT animals are not surprising as it has already been demonstrated that, long-term CR strongly impairs HSC differentiation into lymphoid lineages inhibiting the proliferation of lymphoid progenitors

and resulting in decreased production of peripheral B lymphocytes and impaired immune function. (Tang D et al., 2016). However, the genotype effect observed at week 1 suggests that APN may play a protective role toward the adaptive immune system in an emergency condition such as food deprivation.

Flow cytometry analysis also revealed that on week 1 of CR, granulocyte number is increased in KO animals and as observed for circulating B cells only at the end of week 4 of CR, the same effect was observed in WT animals. An APN mediated effect on granulopoiesis has previously been demonstrated by several authors, however, both a stimulatory and inhibitory effect has been observed and results are still controversial. In more detail, Yokota *et al.* (Yokota T et al., 2000) showed, in accordance with data from the present study, that APN has an inhibitory effect on granulopoiesis; hypothesising that this hormone might be involved in ending the inflammatory processes in the BM microenvironment.

On the contrary, another study published by Masamoto *et al.* (2016) showed that the loss of APN causes impaired granulopoiesis and reduced antibacterial response, however this study was performed on obese mice therefore several obesity related complications such as chronic inflammatory status, insulin resistance or dyslipidemia might also have influenced the effect of APN on normal granulopoiesis.

Flow cytometry data on PB blood obtained in the present study, considering the strong genotype effect observed on week 1, suggest that APN might be involved in the regulation of B lymphopoiesis and granulopoiesis in short-term CR.

Noteworthily, these changes were observed only in male animals suggesting that sex hormones might play a synergistic role together with APN in the modulation of the response to CR.

To evaluate if changes observed in PB were the consequences of perturbation of the BM-HSCs compartment, flow cytometry analysis and CFU assay were performed on femoral BM-MNC. CFU assay reveals information about proliferation ad differentiation potential of myeloid precursor cells, therefore if CR or APN play a role in the regulation of HSC niche, variations in the number of CFU might be noticed. Similarly, Flow cytometry analysis on LSK population can reveal a potential imbalanced proportion among Long-Term HSC, multipotent progenitors and CD48+ progenitors with restricted differentiation capability. However, CFU assay and flow cytometry analysis performed at the end of the 4 weeks CR time course did not reveal any APN mediated change in the proliferation and differentiation potential of HSC suggesting that the alterations observed in PB in KO animals might be the consequence of a systemic effect rather than a specific interaction between HSC and APN.

In this study, the first co-culture system of primary human adipocytes directly isolated from BM without stressful cell manipulation or differentiation protocols has been established, to study the relationship between adipocytes and HSC. The LTC-IC system demonstrated that there is a positive interaction between BM-A and HSC, and that BM-A themselves are able to sustain HSC survival in the LTC-IC system.

This research also provides the first complete study of the transcriptome of primary human BM-A, documenting a distinct gene expression signature compared with AT-A and suggesting that BM-A are involved in BM niche homeostasis processes. The co-culture, molecular, and cytokine secretion profile data described above lend further support to the notion that BM-A play an active role in the BM niche, directly interacting with HSC and stromal cells.

Furthermore, *in vivo* data demonstrated that BM-A through APN secretion, protect the immune system from the sudden decrease of circulating white blood cells observed under condition of food deprivation, preventing in particular the impairment of adaptive immune system.

The present findings allow speculating that BM-A, which clearly are not the main HSC supporting population in BM, may at least contribute to their survival together with other stromal cells and may regulate the production of immune cells through APN secretion.

References

Adams GB, Chabner KT, Alley IR, Olson DP, Szczepiorkowski ZM, Poznansky MC Kos CH, Pollak MR, Brown EM, Scadden DT. (2006). Stem cell engraftment at the endosteal niche is specified by the calcium-sensing receptor. Nature. 439: 599–603

Adams GB, Scadden DT. (2006). The hematopoietic stem cell in its place. Nat Immunol. 7(4):333-337.

Ambrosi TH, Scialdone A, Graja A, Gohlke S, Jank AM, Bocian C, Woelk L, Fan H, Logan DW, Schürmann A, Saraiva LR, Schulz TJ. (2017). Adipocyte Accumulation in the Bone Marrow during Obesity and Aging Impairs Stem Cell-Based Hematopoietic and Bone Regeneration. Cell Stem Cell. 1;20(6):771-784.

Askmyr M, Sims NA, Martin TJ, Purton LE. (2009). What is the true nature of the osteoblastic hematopoietic stem cell niche? Trends Endocrinol Metab. 2009 20(6):303-309.

Atashi F, Modarressi A, Pepper MS. (2015). The role of reactive oxygen species in mesenchymal stem cell adipogenic and osteogenic differentiation: a review. Stem Cells Dev. 24: 1150–1163.

Augello A, De Bari C. (2010). The regulation of differentiation in mesenchymal stem cells. Hum Gene Ther. 21: 1226–1238.

Avecilla ST, Hattori K, Heissig B, Tejada R, Liao F, Shido K, Jin DK, Dias S, Zhang F, Hartman TE, Hackett NR, Crystal RG, Witte L, Hicklin DJ, Bohlen P, Eaton D, Lyden D, de Sauvage F, Rafii S. (2004). Chemokine-mediated interaction of hematopoietic progenitors with the bone marrow vascular niche is required for thrombopoiesis. Nat Med. 10(1):64-71.

Barbatelli G, Murano I, Madsen L, Hao Q, Jimenez M, Kristiansen K, Giacobino JP, De Matteis R, Cinti S. (2010). The emergence of cold-induced brown adipocytes in mouse white fat depots is determined predominantly by white to brown adipocyte transdifferentiation. Am J Physiol Endocrinol Metab. 298(6):E1244-53.

Bathija A, Davis S, S. Trubowitz S. (1978). Marrow adipose tissue: response to erythropoiesis, Am. J. Hematol. 5 (4) 315–321

Baum CM, Weissman IL, Tsukamoto AS, Buckle AM, Peault B. (1992). Isolation of a candidate human hematopoietic stem-cell population. Proc Natl Acad Sci USA. 89(7):2804-2808.

Becker AJ, McCulloch EA, Till JE. (1963). Cytological demonstration of the clonal nature of spleen colonies derived from transplanted mouse marrow cells. Nature. 197:452–4546.

Behre CJ, Gummesson A, Jernas M, Lystig TC, Fagerberg B, Carlsson B, Carlsson LM. (2007). Dissociation between adipose tissue expression and serum levels of adiponectin during and after diet-induced weight loss in obese subjects with and without the metabolic syndrome. Metabolism. 56:1022–1028.

Belaid-Choucair Z, Lepelletier Y, Poncin G, Thiry A, Humblet C, Maachi M, Beaulieu A, Schneider E, Briquet A, Mineur P, Lambert C, Mendes-Da-Cruz D, Ahui ML, Asnafi V, Dy M, Boniver J, Nusgens BV, Hermine O, Defresne MP. (2008). Human bone marrow adipocytes block granulopoiesis through neuropilin-1-induced granulocyte colony-stimulating factor inhibition. Stem Cells. 26(6):1556-1564.

Bensidhoum M, Chapel A, Francois S, Demarquay C, Mazurier C, Fouillard L, Bouchet S, Bertho JM, Gourmelon P, Aigueperse J, Charbord P, Gorin NC, Thierry D, Lopez M. (2004). Homing of in vitro expanded Stro-1- or Stro-1+ human mesenchymal stem cells into the NOD/SCID mouse and their role in supporting human CD34 cell engraftment. Blood. 103(9):3313-3319.

Berg AH, Combs TP, Du X, Brownlee M, Scherer PE. (2001). The adipocyte-secreted protein Acrp30 enhances hepatic insulin action. Nat Med. 7(8):947-953.

Bianco, P (2014). “Mesenchymal” Stem Cells. Annual Review of Cell and Developmental Biology, 30(1), 677–704.

Bonnet D. (2002). Haematopoietic stem cells. J Pathol. 197(4):430-40.

Bromberg O, Frisch BJ, Weber JM, Porter RL, Civitelli R, Calvi LM. (2012). Osteoblastic N-cadherin is not required for microenvironmental support and regulation of hematopoietic stem and progenitor cells. Blood. 120(2):303-313.

Butler JM, Nolan DJ, Vertes EL, Varnum-Finney B, Kobayashi H, Hooper AT, Seandel M, Shido K, White IA, Kobayashi M, Witte L, May C, Shawber C, Kimura Y, Kitajewski J, Rosenwaks Z, Bernstein ID, Rafii S. (2010). Endothelial cells are essential for the self-renewal and repopulation of Notch-dependent hematopoietic stem cells. Cell Stem Cell. 6(3):251-264.

Calvi LM, Adams GB, Weibrecht KW, Weber JM, Olson DP, Knight MC, Martin RP, Schipani E, Divieti P, Bringhurst FR, Milner LA, Kronenberg HM, Scadden DT. (2003). Osteoblastic cells regulate the haematopoietic stem cell niche. Nature. 425(6960):841-846.

Cao Z, Umek RM, McKnight SL. (1991). Regulated expression of three C/EBP isoforms during adipose conversion of 3T3-L1 cells. Genes Dev 5: 1538–1552.

Caplan AI. (1991). Mesenchymal stem cells. Journal of Orthopaedic Research. 9(5), 641–650.

Cawthorn WP, Scheller EL, Learman BS, Parlee SD, Simon BR, Mori H, Ning X, Bree AJ, Schell B, Broome DT, Soliman SS, Del Proposto JL, Lumeng CN, Mitra A, Pandit SV, Gallagher KA, Miller JD, Krishnan V, Hui SK, Bredella MA, Fazeli PK, Klibanski A, Horowitz MC, Rosen CJ, MacDougald OA. (2014). Bone marrow adipose tissue is an endocrine organ that contributes to increased circulating adiponectin during caloric restriction. Cell Metab. 5;20(2):368-375.

Chattopadhyay N, Vassilev PM, Brown EM. (1997). Calcium-sensing receptor: roles in and beyond systemic calcium homeostasis. Biol Chem. 378(8):759-768.

Chen Q, Shou P, Zheng C, Jiang M, Cao G, Yang Q, Cao J, Xie N, Velletri T, Zhang X, Xu C, Zhang L, Yang H, Hou J, Wang Y, Shi Y. (2016). Fate decision of mesenchymal stem cells: adipocytes or osteoblasts? Cell Death Differ. 23(7):1128-1139.

Chute JP, Muramoto GG, Fung J, Oxford C. (2004). Soluble factors elaborated by human brain endothelial cells induce the concomitant expansion of purified human BM CD34+CD38- cells and SCID-repopulating cells. Blood. 105(2):576-583.

Chute JP, Saini AA, Chute DJ, Wells MR, Clark WB, Harlan DM, Park J, Stull MK, Civin C, Davis TA. (2002). Ex vivo culture with human brain endothelial cells

increases the SCID-repopulating capacity of adult human bone marrow. Blood. 100(13):4433-4439.

Combs TP, Berg AH, Rajala MW, Klebanov S, Iyengar P, Jimenez-Chillaron JC, Patti ME, Klein SL, Weinstein RS, Scherer PE. (2003). Sexual differentiation, pregnancy, calorie restriction, and aging affect the adipocyte-specific secretory protein adiponectin. Diabetes. 52:268–276.

Corre J, Barreau C, Cousin B, Chavoin JP, Caton D, Fournial G, Penicaud L, Casteilla L, Laharrague P. (2006). Human subcutaneous adipose cells support complete differentiation but not self-renewal of hematopoietic progenitors. J Cell Physiol. 208(2):282-288.

Corre, J, Planat-Benard, V, Corberand, JX, Pénicaud, L, Casteilla, L, Laharrague, P. (2004). Human bone marrow adipocytes support complete myeloid and lymphoid differentiation from human CD34 cells. British Journal of Haematology. 127, 344–347.

Craft CS, Li Z, MacDougald OA, Scheller EL. (2018). Molecular differences between subtypes of bone marrow adipocytes. Curr Mol Biol Rep. 4(1):16-23.

Dazzi, F., Ramasamy, R., Glennie, S., Jones, S. P., & Roberts, I. (2006). The role of mesenchymal stem cells in haemopoiesis. Blood. 20(3), 161–171.

De Matteis R, Zingaretti MC, Murano I, Vitali A, Frontini A, Giannulis I, Barbatelli G, Marcucci F, Bordicchia M, Sarzani R, Raviola E, Cinti S. (2009). In vivo physiological transdifferentiation of adult adipose cells. Stem Cells. 27(11):2761-2768.

Devine SM, Bartholomew AM, Mahmud N, Nelson M, Patil S, Hardy W, Sturgeon C, Hewett T, Chung T, Stock W, Sher D, Weissman S, Ferrer K, Mosca J, Deans R, Moseley A, Hoffman R. (2001). Mesenchymal stem cells are capable of homing to the bone marrow of non-human primates following systemic infusion. Exp Hematol. 29(2):244-255.

Dexter, TM, Allen, TD, Lajtha LG. (1977). Conditions controlling the proliferation of haemopoietic stem cells in vitro. Journal of Cellular Physiology, 91, 335–344

Di Mascio L, Voermans C, Uqoezwa M, Duncan A, Lu D, Wu J, Sankar U, Reya T. (2007). Identification of adiponectin as a novel hemopoietic stem cell growth factor. J Immunol. 2007 15;178(6):3511-3520.

Di Nicola M, Carlo-Stella C, Magni M, Milanesi M, Longoni PD, Matteucci P, Grisanti S, Gianni AM. (2002). Human bone marrow stromal cells suppress T-lymphocyte proliferation induced by cellular or nonspecific mitogenic stimuli. Blood. 99(10):3838-3843.

Ding L, Morrison SJ. (2013). Haematopoietic stem cells and early lymphoid progenitors occupy distinct bone marrow niches. Nature. 14; 495(7440):231-235.

Ding L, Saunders TL, Enikolopov G, Morrison SJ. (2012). Endothelial and perivascular cells maintain haematopoietic stem cells. Nature. 481:457–462.

Dolezalova R, Lacinova Z, Dolinkova M, Kleiblova P, Haluzikova D, Housa D, Papezova H, Haluzik M. (2007). Changes of endocrine function of adipose tissue in anorexia nervosa: comparison of circulating levels versus subcutaneous mRNA expression. Clin Endocrinol (Oxf). 67:674–678.

Eastment, C., Denholm, E., Katsnelson, I., & Arnold, E. (1982). In vitro proliferation of hematopoietic stem cells in the absence of an adherent monolayer. Blood. 60, 130–135.

Eaves AC, Eaves CJ. (1988). Maintenance and proliferation control of primitive hemopoietic progenitors in long-term cultures of human marrow cells. Blood Cells. 14, 355–368.

Ellis SL, Grassinger J, Jones A, Borg J, Camenisch T, Haylock D, Bertoncello I, Nilsson SK. (2011). The relationship between bone, hemopoietic stem cells, and vasculature. Blood. 118(6):1516-1524.

Fajardo-Orduña GR, Mayani H, Montesinos JJ. (2015). Hematopoietic support capacity of mesenchymal stem cells: Biology and clinical potential. Archives of Medical Research. 46, 589–596

Fantuzzi G. (2013). Adiponectin in inflammatory and immune-mediated diseases. Cytokine. 64(1):1-10.

Friedenstein AJ, Gorskaja, JF, and Kulagina NN. (1976). Fibroblast precursors in normal and irradiated mouse hematopoietic organs. Exp. Hematol. 4, 267–274.

Friedenstein AJ, Petrakova KV, Kurolesova AI, and Frolova GP. (1968). Heterotopic of bone marrow. Analysis of precursor cells for osteogenic and hematopoietic tissues. Transplantation 6, 230–247.

Friedenstein AJ., Chailakhjan RK, and Lalykina KS. (1970). The development of fibroblast colonies in monolayer cultures of guinea-pig bone marrow and spleen cells. Cell Tissue Kinet. 3, 393–403.

Gainsford T, Willson TA, Metcalf D, Handman E, McFarlane C, Ng A, Nicola NA, Alexander WS, Hilton DJ. (1996). Leptin can induce proliferation, differentiation, and functional activation of hemopoietic cells. Proc Natl Acad Sci U S A. 10;93(25):14564-14568.

Greenbaum A, Hsu YM, Day RB, Schuettpelz LG, Christopher MJ, Borgerding JN, Nagasawa T, Link DC. (2013). CXCL12 in early mesenchymal progenitors is required for haematopoietic stem-cell maintenance. Nature. 14; 495(7440):227-230.

Hao QL, Thiemann FT, Petersen D, Smogorzewska EM, Crooks GM. (1996). Extended long-term culture reveals a highly quiescent and primitive human hematopoietic progenitor population. Blood. 88(9):3306-3313

Hardouin P, Pansini V, Cortet B. (2014). Bone marrow fat. Joint, Bone, Spine, 81, 313–319.

Hardouin P, Rharass T, Lucas S. (2016). Bone marrow adipose tissue: To be or not to Be a typical adipose tissue? Frontiers in Endocrinology. 7, 85.

Hooper AT, Butler JM, Nolan DJ, Kranz A, Iida K, Kobayashi M, Kopp HG, Shido K, Petit I, Yanger K, James D, Witte L, Zhu Z, Wu Y, Pytowski B, Rosenwaks Z, Mittal V, Sato TN, Rafii S. (2009). Engraftment and reconstitution of hematopoiesis is dependent on VEGFR2-mediated regeneration of sinusoidal endothelial cells. Cell Stem Cell. 4(3):263-274.

Hooper AT, Butler JM, Nolan DJ, Kranz A, Iida K, Kobayashi M, Kopp HG, Shido K, Petit I, Yanger K, James D, Witte L, Zhu Z, Wu Y, Pytowski B, Rosenwaks Z, Mittal V, Sato TN, Rafii S. (2009). Engraftment and reconstitution of hematopoiesis is dependent on VEGFR2-mediated regeneration of sinusoidal endothelial cells. Cell Stem Cell. 4(3):263-274.

Hosokawa K, Arai F, Yoshihara H, Iwasaki H, Hembree M, Yin T, Nakamura Y, Gomei Y, Takubo K, Shiama H, Matsuoka S, Li L, Suda T. (2009). Cadherin-based adhesion is a potential target for niche manipulation to protect hematopoietic stem cells in adult bone marrow. Cell Stem Cell. 6(3):194-198.

Hosokawa K, Arai F, Yoshihara H, Iwasaki H, Nakamura Y, Gomei Y, Suda T. (2010). Knockdown of N-cadherin suppresses the long-term engraftment of hematopoietic stem cells. Blood. 116(4):554-563.

Huang S, Terstappen LW. (1994). Lymphoid and myeloid differentiation of single human CD34+, HLA-DR+, CD38- hematopoietic stem cells. Blood. 83(6):1515-1526

Huber TL, Kouskoff V, Fehling HJ, Palis J, Keller G. (2004). Haemangioblast commitment is initiated in the primitive streak of the mouse embryo. Nature.;432(7017):625-630.

Ilangumaran S, Villalobos-Hernandez A, Bobbal, D, Ramanathan S. (2016). The hepatocyte growth factor (HGF)-MET receptor tyrosine kinase signaling pathway: Diverse roles in modulating immune cell functions. Cytokine. 82, 125–139.

In 't Anker PS, Scherjon SA, Kleijburg-van der Keur C, Noort WA, Claas FH, Willemze R, Fibbe WE, Kanhai HH. (2003). Amniotic fluid as a novel source of mesenchymal stem cells for therapeutic transplantation. Blood. 102(4):1548-1549.

Justesen J, Stenderup K, Ebbesen EN, Mosekilde L, Steiniche T, Kassem M. (2001). Adipocyte tissue volume in bone marrow is increased with aging and in patients with osteoporosis. Biogerontology. 2: 165–171.

Kiel MJ, Morrison SJ. (2008). Uncertainty in the niches that maintain haematopoietic stem cells. Nat Rev Immunol. 8: 290–301.

Kiel MJ, Radice GL, Morrison SJ. (2007). Lack of evidence that hematopoietic stem cells depends on N-cadherin-mediated adhesion to osteoblasts for their maintenance. Cell Stem Cell. 1: 204–217;

Kiel MJ, Yilmaz OH, Morrison SJ. (2008). CD150- cells are transiently reconstituting multipotent progenitors with little or no stem cell activity. Blood. 15;111(8):4413-4414.

Kim J, Ko J. (2014). A novel PPARgamma2 modulator sLZIP controls the balance between adipogenesis and osteogenesis during mesenchymal stem cell differentiation. Cell Death Differ 21: 1642–1655.

Kobayashi H, Butler JM, O'Donnell R, Kobayashi M, Ding BS, Bonner B, Chiu VK, Nolan DJ, Shido K, Benjamin L, Rafii S. (2010). Angiocrine factors from Akt-activated endothelial cells balance self-renewal and differentiation of haematopoietic stem cells. Nat Cell Biol. 12(11):1046-1056.

Koç ON, Gerson SL, Cooper BW, Dyhouse SM, Haynesworth SE, Caplan AI, Lazarus HM. (2000). Rapid hematopoietic recovery after coinfusion of autologous-blood stem cells and culture-expanded marrow mesenchymal stem cells in advanced breast cancer patients receiving high-dose chemotherapy. J Clin Oncol. 18(2):307-316.

Kopp HG, Avecilla ST, Hooper AT, Rafii S. (2005). The bone marrow vascular niche: home of HSC differentiation and mobilization. Physiology (Bethesda). 20:349-356.

Kopp HG, Avecilla ST, Hooper AT, Rafii S. (2005). The bone marrow vascular niche: home of HSC differentiation and mobilization. Physiology (Bethesda). 20:349-356.

Kovacova Z, Vitkova M, Kovacikova M, Klimcakova E, Bajzova M, Hnevkovska Z, Rossmeislova L, Stich V, Langin D, Polak J. (2009). Secretion of adiponectin multimeric complexes from adipose tissue explants is not modified by very low calory diet. Eur J Endocrinol. 160:585–592.

Kushwaha P, Khedgikar V, Gautam J, Dixit P, Chillara R, Verma A, Thakur R, Mishra DP, Singh D, Maurya R, Chattopadhyay N, Mishra PR. (2014). A novel

therapeutic approach with Caviunin-based isoflavonoid that en routes bone marrow cells to bone formation via BMP2/Wnt-beta-catenin signaling. Cell Death Differ. 5: e1422.

Laharrague P, Larrouy D, Fontanilles AM, Truel N, Campfield A, Tenenbaum R, Galitzky J, Corberand JX, Pénicaud L, Casteilla L. (1998). High expression of leptin by human bone marrow adipocytes in primary culture. FASEB J. 12(9):747-752.

Lefterova MI, Zhang Y, Steger DJ, Schupp M, Schug J, Cristancho A, Feng D, Zhuo D, Stoeckert CJ Jr, Liu XS, Lazar MA. (2008). PPARgamma and C/EBP factors orchestrate adipocyte biology via adjacent binding on a genome-wide scale. Genes Dev 22: 2941–2952.

Lévesque JP, Helwani FM, Winkler IG. (2010). The endosteal 'osteoblastic' niche and its role in hematopoietic stem cell homing and mobilization. Leukemia. 24(12):1979-1992

Li H, Ghazanfari R, Zacharaki D, Lim HC, Scheding S. (2016). Isolation and characterization of primary bone marrow mesenchymal stromal cells. Ann N Y Acad Sci. 1370(1):109-118.

Li N, Eljaafari A, Bensoussan D, Wang Y, Latger-Cannard V, Serrurier B, Boura C, Kennel A, Stoltz J, Feugier P. (2006). Human umbilical vein endothelial cells increase ex vivo expansion of human CD34(+) PBPC through IL-6 secretion. Cytotherapy. 8(4):335-342.

Lo Celso C, Fleming HE, Wu JW, Zhao CX, Miake-Lye S, Fujisaki J, Côté D, Rowe DW, Lin CP, Scadden DT. (2009). Live-animal tracking of individual haematopoietic stem/progenitor cells in their niche. Nature. 457(7225):92-96.

Lu LS, Wang SJ, Auerbach R. (1996). In vitro and in vivo differentiation into B cells, T cells, and myeloid cells of primitive yolk sac hematopoietic precursor cells expanded > 100-fold by coculture with a clonal yolk sac endothelial cell line. Proc Natl Acad Sci USA. 93: 14782–14787

Majumdar MK, Thiede MA, Haynesworth SE, Bruder SP, Gerson SL. (2000). Human marrow-derived mesenchymal stem cells (MSCs) express hematopoietic

cytokines and support long-term hematopoiesis when differentiated toward stromal and osteogenic lineages. Journal of Hematotherapy & Stem Cell Research. 9(6), 841–848.

Masamoto Y, Arai S, Sato T, Kubota N, Takamoto I, Kadowaki T, Kurokawa M. (2017). Adiponectin Enhances Quiescence Exit of Murine Hematopoietic Stem Cells and Hematopoietic Recovery Through mTORC1 Potentiation. Stem Cells. 35(7):1835-1848.

Masamoto Y, Arai S, Sato T, Yoshimi A, Kubota N, Takamoto I, Iwakura Y, Yoshimura A, Kadowaki T, Kurokawa M. (2016). Adiponectin Enhances Antibacterial Activity of Hematopoietic Cells by Suppressing Bone Marrow Inflammation. Immunity. 21;44(6):1422-1433.

Mattiucci D, Maurizi G, Izzi V, Cenci L, Ciarlantini M, Mancini S, Mensà E, Pascarella R, Vivarelli M, Olivieri A, Leoni P, Poloni A. (2018). Bone marrow adipocytes support hematopoietic stem cell survival. J Cell Physiol. 233(2):1500-1511.

Mattiucci D, Naveiras O, Poloni A. (2018). Bone Marrow “Yellow” and “Red” Adipocytes”: Good or Bad Cells? Current Molecular Biology Reports 4 (3), 117-122.

Maurizi G, Poloni A, Mattiucci D, Santi S, Maurizi A, Izzi V, Giuliani A, Mancini S, Zingaretti MC, Perugini J, Severi I, Falconi M, Vivarelli M, Rippo MR, Corvera S, Giordano A, Leoni P, Cinti S. (2017). Human White Adipocytes Convert Into "Rainbow" Adipocytes In Vitro. J Cell Physiol. 232(10):2887-2899.

Méndez-Ferrer S, Michurina TV, Ferraro F, Mazloom AR, Macarthur BD, Lira SA, Scadden DT, Ma'ayan A, Enikolopov GN, Frenette PS. (2010). Mesenchymal and haematopoietic stem cells form a unique bone marrow niche. Nature. 466(7308):829-834.

Meunier P, Aaron J, Edouard C, Vignon G. (1971). Osteoporosis and replacement of cell populations of marrow by adipose tissue - a quantitative study of 84 iliac bone biopsies. Clin Orthop Relat Res. 80: 147–154.

Miller JS, McCullar V, Punzel M, Lemischka IR, Moore KA. (1999). Single adult human CD34(+)/Lin-/CD38(-) progenitors give rise to natural killer cells, B-lineage cells, dendritic cells, and myeloid cells. Blood. 93(1):96-106.

Moerman EJ, Teng K, Lipschitz DA, Lecka-Czernik B. (2004). Aging activates adipogenic and suppresses osteogenic programs in mesenchymal marrow stroma/stem cells: the role of PPAR-gamma 2 transcription factor and TGF-beta/BMP signaling pathways. Aging Cell. 3: 379–389.

Morrison SJ, Scadden DT. (2014). The bone marrow niche for haematopoietic stem cells. Nature. 505(7483):327-334.

Morrison SJ. (2009). Hematopoietic stem cells do not depend on N-cadherin to regulate their maintenance. Cell stem cell. 4:170–179.

Morrison SJ, Weissman IL. (1994). The long-term repopulating subset of hematopoietic stem cells is deterministic and isolatable by phenotype. Immunity. 1(8): 661-673.

Naveiras O, Nardi V, Wenzel PL, Hauschka PV, Fahey F, Daley GQ. (2009). Bone-marrow adipocytes as negative regulators of the haematopoietic microenvironment. Nature. 9;460(7252):259-263.

Nilsson SK, Johnston HM, Whitty GA, Williams B, Webb RJ, Denhardt DT, Bertoncello I, Bendall LJ, Simmons PJ, Haylock DN. (2005). Osteopontin, a key component of the hematopoietic stem cell niche and regulator of primitive hematopoietic progenitor cells. Blood. 106(4):1232-1239.

Oberlin E, Tavian M, Blazsek I, Peault B. (2002). Blood-forming potential of vascular endothelium in the human embryo. Development 129: 4147–4157.

Oguro H, Ding L, Morrison SJ. (2013). SLAM family markers resolve functionally distinct subpopulations of hematopoietic stem cells and multipotent progenitors. Cell Stem Cell. 13(1):102-116.

Oguro H, Ding L, Morrison SJ. (2013). SLAM family markers resolve functionally distinct subpopulations of hematopoietic stem cells and multipotent progenitors. Cell Stem Cell. 3;13(1):102-116.

Omatsu Y, Sugiyama T, Kohara H, Kondoh G, Fujii N, Kohno K, Nagasawa T. (2010). The essential functions of adipo-osteogenic progenitors as the hematopoietic stem and progenitor cell niche. Immunity. 33(3):387-399.

Oostendorp RA, Harvey KN, Kusadasi N, de Bruijn MF, Saris C, Ploemacher RE, Medvinsky AL, Dzierzak EA. (2002). Stromal cell lines from mouse aorta-gonads-mesonephros subregions are potent supporters of hematopoietic stem cell activity. Blood. 99(4):1183-1189.

Pajvani UB, Du X, Combs TP, Berg AH, Rajala MW, Schulthess T, Engel J, Brownlee M, Scherer PE. (2003). Structure-function studies of the adipocyte-secreted hormone Acrp30/adiponectin. Implications for metabolic regulation and bioactivity. J Biol Chem. 14;278(11):9073-9085.

Pannacciulli N, Vettor R, Milan G, Granzotto M, Catucci A, Federspil G, De Giacomo P, Giorgino R, De Pergola G. (2003). Anorexia nervosa is characterized by increased adiponectin plasma levels and reduced nonoxidative glucose metabolism. J Clin Endocrinol Metab. 88:1748–1752.

Pappenheim A. (1896). Archiv f. pathol. Anat. 145: 587. Park D, Spencer JA, Koh BI, Kobayashi T, Fujisaki J, Clemens TL, Lin CP, Kronenberg HM, Scadden DT. (2012). Endogenous bone marrow MSCs are dynamic, fate-restricted participants in bone maintenance and regeneration. Cell Stem Cell. 10(3):259-272

Park D, Sykes DB, Scadden DT. (2012). The hematopoietic stem cell niche. Front Biosci (Landmark Ed). 17:30-39.

Poloni A, Maurizi G, Serrani F, Mancini S, Zingaretti MC, Frontini A, Cinti S, Olivieri A, Leoni P. (2013). Molecular and functional characterization of human bone marrow adipocytes. Exp Hematol. 41(6):558-566.

Poloni A, Maurizi G, Anastasi S, Mondini E, Mattiucci D, Discepoli G, Tiberi F, Mancini S, Partelli S, Maurizi A, Cinti S, Olivieri A, Leoni P. (2015). Plasticity of human dedifferentiated adipocytes toward endothelial cells. Exp Hematol. 43(2):137-146.

Poloni A, Maurizi G, Foia F, Mondini E, Mattiucci D, Ambrogini P, Lattanzi D, Mancini S, Falconi M, Cinti S, Olivieri A, Leoni P. (2015). Glial-like differentiation potential of human mature adipocytes. J Mol Neurosci. 55(1):91-98. B

Poloni A, Maurizi G, Leoni P, Serrani F, Mancini S, Frontini A, Zingaretti MC, Siquini W, Sarzani R, Cinti S. (2012). Human dedifferentiated adipocytes show similar properties to bone marrow-derived mesenchymal stem cells. Stem Cells. 30(5):965-974.

Pontikoglou C, Deschaseaux F, Sensebé L, Papadaki HA. (2011). Bone marrow mesenchymal stem cells: biological properties and their role in hematopoiesis and hematopoietic stem cell transplantation. Stem Cell Rev. 7(3):569-589.

Prockop DJ. (1997). Marrow stromal cells as stem cells for nonhematopoietic tissues. Science. 276(5309), 71–74.

Ramalho-Santos M, Willenbring H. (2007). On the origin of the term "stem cell". Cell Stem Cell. 1(1):35-8.

Robles H, Park S, Joens MS, Fitzpatrick JAJ, Craft CS, Scheller EL. (2018). Characterization of the bone marrow adipocyte niche with three-dimensional electron microscopy. Bone. (Epub ahead of print).

Rossi DJ, Seita J, Czechowicz A, Bhattacharya D, Bryder D, Weissman IL. (2007). Hematopoietic stem cell quiescence attenuates DNA damage response and permits DNA damage accumulation during aging. Cell Cycle. 6(19):2371–2376.

Sacchetti B, Funari A, Remoli C, Giannicola G, Kogler G, Liedtke S, Cossu G, Serafini M, Sampaolesi M, Tagliafico E, Tenedini E, Saggio I, Robey PG, Riminucci M, Bianco P. (2016). No Identical "Mesenchymal Stem Cells" at Different Times and Sites: Human Committed Progenitors of Distinct Origin and Differentiation Potential Are Incorporated as Adventitial Cells in Microvessels Stem Cell Reports. 14;6(6):897-913.

Salter AB, Meadows SK, Muramoto GG, Himburg H, Doan P, Daher P, Russell L, Chen B, Chao NJ, Chute JP. (2009). Endothelial progenitor cell infusion induces hematopoietic stem cell reconstitution in vivo. Blood. 113(9):2104-2107.

Sanchez-Gurmaches, J, Guertin DA. (2014). Adipocyte lineages: Tracing back the origins of fat. Biochimica et Biophysica Acta. 1842, 340–351.

Scheller EL, Burr AA, MacDougald OA, Cawthorn WP. (2016). Inside out: Bone marrow adipose tissue as a source of circulating adiponectin. Adipocyte. 22;5(3):251-269.

Scheller EL, Doucette CR, Learman BS, Cawthorn WP, Khandaker S, Schell B, Wu B, Ding SY, Bredella MA, Fazeli PK, Khoury B, Jepsen KJ, Pilch PF, Klibanski A, Rosen CJ, MacDougald OA. (2015). Region-specific variation in the properties of skeletal adipocytes reveals regulated and constitutive marrow adipose tissues. Nat Commun. 6;6:7808.

Schofield R. (1978). The relationship between the spleen colony-forming cell and the haemopoietic stem cell. Blood Cells. 4, 7–25

Seita J, Weissman IL. (2010). Hematopoietic stem cell: self-renewal versus differentiation. Wiley Interdiscip Rev Syst Biol Med2(6):640-653.

Shen W, Chen J, Gantz M, Punyanitya M, Heymsfield SB, Gallagher D, Albu J, Engelson E, Kotler D, Pi-Sunyer X, Gilsanz V. (2012). MRI-measured pelvic bone marrow adipose tissue is inversely related to DXA-measured bone mineral in younger and older adults. Eur J Clin Nutr. 66(9):983-988.

Siminovitch L, Till JE. (1963). The Distribution of Colony-Forming Cells among Spleen Colonies. J Cell Physiol. 62:327–336.

Spangrude GJ, Heimfeld S, Weissman IL. (1988). Purification and characterization of mouse hematopoietic stem cells. Science. 241(4861):58–62.

Spindler TJ, Tseng AW, Zhou X, Adams GB. (2014). Adipocytic cells augment the support of primitive hematopoietic cells in vitro but have no effect in the bone marrow niche under homeostatic conditions. Stem Cells Dev. 15;23(4):434-441.

Stier S, Ko Y, Forkert R, Lutz C, Neuhaus T, Grünewald E, Cheng T, Dombkowski D, Calvi LM, Rittling SR, Scadden DT. (2005). Osteopontin is a hematopoietic stem cell niche component that negatively regulates stem cell pool size. J Exp Med. 201(11):1781-1791. 8

Sugiyama T, Kohara H, Noda M, Nagasawa T. (2006). Maintenance of the hematopoietic stem cell pool by CXCL12-CXCR4 chemokine signaling in bone marrow stromal cell niches. Immunity. (6):977-988.

Sugiyama T, Kohara H, Noda M, Nagasawa T. (2006). Maintenance of the hematopoietic stem cell pool by CXCL12–CXCR4 chemokine signaling in bone marrow stromal cell niches. Immunity. 25:977–988.

Suresh S, Alvarez JC, Noguchi CT. (2017). Erythropoietin Eliminates Increased Bone Marrow Adiposity and Alters Bone Features in Obese Mice. Am Soc Hematology.

Taichman RS, Emerson SG. (1998). The role of osteoblasts in the hematopoietic microenvironment. Stem Cells 16, 7–15.

Taichman RS, Emerson SG. (1998). The role of osteoblasts in the hematopoietic microenvironment. Stem Cells. 16(1):7-15.

Taichman, RS. (2005). Blood and bone: two tissues whose fates are intertwined to create the hematopoietic stem-cell niche. Blood 105, 2631–2639.

Tang D, Tao S, Chen Z, Koliesnik IO, Calmes PG, Hoerr V, Han B, Gebert N, Zörnig M, Löffler B, Morita Y, Rudolph KL. (2016). Dietary restriction improves repopulation but impairs lymphoid differentiation capacity of hematopoietic stem cells in early aging. J Exp Med. 4;213(4):535-553.

Tavassoli M. (1976) A. Marrow adipose cells. Histochemical identification of labile and stable components. Arch Pathol Lab Med. 100(1):16-18

Tavassoli M. (1976) B. Marrow adipose cells. Histochemical identification of labile and stable components, Arch. Pathol. Lab. Med. 100 (1) 16–18;

Tavian M, Coulombel L, Luton D, Clemente HS, Dieterlen-Lievre F, Peault B. (1996). Aorta-associated CD34+ hematopoietic cells in the early human embryo. Blood 87: 67–72.

Till JE, Mc CE. (1961). A direct measurement of the radiation sensitivity of normal mouse bone marrow cells. Radiat Res. 14:213–222.

Tuljapurkar SR, McGuire TR, Brusnahan SK, Jackson JD, Garvin KL, Kessinger MA, Lane JT, O' Kane BJ, Sharp JG. (2011). Changes in human bone marrow fat content associated with changes in hematopoietic stem cell numbers and cytokine levels with aging. J Anat. 219(5):574-581.

Vande Berg BC, Malghem J, Lecouvet FE, Maldague B. (1998). Magnetic resonance imaging of normal bone marrow. Eur Radiol. 8(8):1327-1334.

Wagner W, Wein F, Seckinger A, Frankhauser M, Wirkner U, Krause U, Blake J, Schwager C, Eckstein V, Ansorge W, Ho AD. (2005). Comparative characteristics of mesenchymal stem cells from human bone marrow, adipose tissue, and umbilical cord blood. Exp Hematol. 33(11):1402-1416.

Walkley CR, Olsen GH, Dworkin S, Fabb SA, Swann J, McArthur GA, Westmoreland SV, Chambon P, Scadden DT, Purton LE. (2007). A microenvironment-induced myeloproliferative syndrome caused by retinoic acid receptor gamma deficiency. Cell. 129:1097–1110.

Wang Z, Al-Regaiey KA, Masternak MM, Bartke A. (2006). Adipocytokines and lipid levels in Ames dwarf and calorie-restricted mice. The journals of gerontology Series A, Biological sciences and medical sciences. 61:323–331.

Wang ZV, Scherer PE. (2016). Adiponectin, the past two decades. J Mol Cell Biol. 8(2):93-100.

Wei J, Shimazu J, Makinistoglu MP, Maurizi A, Kajimura D, Zong H, Takarada T, Lezaki T, Pessin JE, Hinoi E, Karsenty G. (2015). Glucose Uptake and Runx2 Synergize to Orchestrate Osteoblast Differentiation and Bone Formation. Cell. 161(7):1576-1591.

Weiss L (1976). The hematopoietic microenvironment of the bone marrow: an ultrastructural study of the stroma in rats. Anat. Rec. 186:161–184

Weiss L (1980). The haemopoietic microenvironment of bone marrow: an ultrastructural study of the interactions of blood cells, stroma and blood vessels. Ciba Found. Symp. 71:3–19

Wilson A, Murphy MJ, Oskarsson T, Kaloulis K, Bettess MD, Oser GM, Pasche AC, Knabenhans C, Macdonald HR, Trumpp A. (2004). c-Myc controls the balance between hematopoietic stem cell self-renewal and differentiation. Genes Dev. 18(22):2747-2763.

Wilson A, Trumpp A. (2006). Bone-marrow haematopoietic-stem-cell niches. Nat Rev Immunol. 6(2):93-106.

Worton RG, McCulloch EA, Till JE. (1969). Physical separation of hemopoietic stem cells differing in their capacity for self-renewal. J Exp Med. 130(1):91-103.

Wu AM, Till JE, Siminovitch L, McCulloch EA. (1968). Cytological evidence for a relationship between normal hemotopoietic colony forming cells and cells of the lymphoid system. J Exp Med. 127(3):455–464.

Xie Y, Yin T, Wiegraebe W, He XC, Miller D, Stark D, Perko K, Alexander R, Schwartz J, Grindley JC, Park J, Haug JS, Wunderlich JP, Li H, Zhang S, Johnson T, Feldman RA, Li L. (2008). Detection of functional haematopoietic stem cell niche using real-time imaging. Nature. 457(7225):97-101.

Yamauchi T, Kamon J, Waki H, Terauchi Y, Kubota N, Hara K, Mori Y, Ide T, Murakami K, Tsuboyama-Kasaoka N, Ezaki O, Akanuma Y, Gavrilova O, Vinson C, Reitman ML, Kagechika H, Shudo K, Yoda M, Nakano Y, Tobe K, Nagai R, Kimura S, Tomita M, Froguel P, Kadowaki T. (2001). The fat-derived hormone adiponectin reverses insulin resistance associated with both lipoatrophy and obesity. Nat Med. 7(8):941-946.

Ye R, Scherer PE. (2013). Adiponectin, driver or passenger on the road to insulin sensitivity? Mol Metab. 19;2(3):133-141.

Yeung DK, Griffith JF, Antonio GE, Lee FK, Woo J, Leung PC. (2005). Osteoporosis is associated with increased marrow fat content and decreased marrow fat unsaturation: a proton MR spectroscopy study. J Magn Reson Imaging. 22(2):279-85.

Yildirim S, Boehmler AM, Kanz L, Möhle R. (2005). Expansion of cord blood CD34+ hematopoietic progenitor cells in coculture with autologous umbilical vein

endothelial cells (HUVEC) is superior to cytokine-supplemented liquid culture. Bone Marrow Transplant. 36(1):71-79.

Yokota T, Meka CS, Kouro T, Medina KL, Igarashi H, Takahashi M, Oritani K, Funahashi T, Tomiyama Y, Matsuzawa Y, Kincade PW. (2003). Adiponectin, a fat cell product, influences the earliest lymphocyte precursors in bone marrow cultures by activation of the cyclooxygenase-prostaglandin pathway in stromal cells. J Immunol. 15;171(10):5091-5099.

Yokota T, Oritani K, Takahashi I, Ishikawa J, Matsuyama A, Ouchi N, Kihara S, Funahashi T, Tenner AJ, Tomiyama Y, Matsuzawa Y. (2000). Adiponectin, a new member of the family of soluble defense collagens, negatively regulates the growth of myelomonocytic progenitors and the functions of macrophages. Blood. 1;96(5):1723-1732.

Yu VW, Scadden DT. (2016). Hematopoietic Stem Cell and Its Bone Marrow Niche. Curr Top Dev Biol. 118:21-44.

Zhang J, Niu C, Ye L, Huang H, He X, Tong WG, Ross J, Haug J, Johnson T, Feng JQ, Harris S, Wiedemann LM, Mishina Y, Li L. (2003). Identification of the haematopoietic stem cell niche and control of the niche size. Nature. 425(6960):836-841.

Zhang Y, Marsboom G, Toth PT, Rehman J. (2013). Mitochondrial respiration regulates adipogenic differentiation of human mesenchymal stem cells. PLoS One. 8: e77077.

Zhou BO, Yu H, Yue R, Zhao Z, Rios JJ, Naveiras O, Morrison SJ. (2017). Bone marrow adipocytes promote the regeneration of stem cells and haematopoiesis by secreting SCF. Nat Cell Biol. 19(8):891-903.

Acknowledgements

I would like to thank the all laboratory and the clinic of haematology of Università Politecnica delle Marche. I would like to pay a very special gratitude to my supervisor, prof. Antonella Poloni and to Dr. Stefania Mancini. Thanks also to Prof. Pietro Leoni and Prof. Attilio Olivieri

I am also grateful to prof. Will Cawthorn that allowed me to develop my research in his laboratory in Edinburgh at the Queen's Medical Research Institute and to the "Scots" fellows Andrea, Ben and Karla. I would like to pay gratitude to Richard Sulston who kindly provided preliminary data that contributed to this work.

I would like to thank prof. Olaia Naveiras for having me in her laboratory in Lausanne at the École polytechnique fédérale de Lausanne.

And Thanks to the BONEAhead initiative for making all our collaborations possible.